Evaluación Sistemática del Flavonoide Rutina para Fortalecer la Resiliencia de la Abeja Africanizada (*Apis mellifera*) frente al Estrés por Plaguicidas y Patógenos.

Sergio Alejandro Mayorga

Universidad del Rosario

Escuela de Ciencias e Ingeniería

Bogotá, Colombia

2025

Evaluación Sistemática del Flavonoide Rutina para Fortalecer la Resiliencia de la Abeja Africanizada (*Apis mellifera*) frente al Estrés por Plaguicidas y Patógenos.

Estudiante

Sergio Alejandro Mayorga

Biólogo, Universidad del Rosario

Documento de tesis presentado como requisito para obtener el título de:

Magister en Ciencias Naturales

Director

Andre J Riveros, Ph.D

Director, Grupo de investigaciones CANNON

Escuela de Ciencias e Ingeniería

Universidad del Rosario

Codirectora

Carolina Ramírez Santana, Ph.D

Directora, Centro de estudio de enfermedades autoinmunes (CREA)

Escuela de Medicina y Ciencias de la Salud

Universidad del Rosario

Universidad del Rosario

Escuela de Ciencias e Ingeniería

Bogotá, Colombia

2025

Agradecimientos

Esta tesis es el producto del trabajo y el esfuerzo de muchas personas, que, con su apoyo, deseos, e incluso sonrisas lograron llevarme hasta este punto. Todos ellos contribuyeron en alguna forma a este trabajo, por lo tanto, esta tesis no es solo mía sino de cada una de las personas que aquí menciono, les doy las gracias por todo desde lo mas profundo de mi corazón.

A mi mamá Diana Patricia Mayorga Bohórquez y a mi abuela Florinda Bohórquez, quienes me encaminaron y me apoyaron a su manera, con amor, paciencia, y dedicación. A ellas no solo les debo este trabajo sino el hombre que soy, son prueba máxima de que nunca es tarde para comenzar de nuevo, de que no importa el tiempo perdido sino el tiempo que te queda por vivir. Incluyo en esta tesis a Owen, aunque jamás entenderá esto, le doy gracias por despertarme cada mañana con el amor y la emoción más genuino de todos.

Le agradezco a Juan Esteban Reyes quien por años me acompaño de forma paciente y amorosa, su apoyo no solo impacto este proyecto sino mi vida de una forma que jamás imagine, gracias por estar siempre. También agradezco a su familia Gabriela Reyes y Sandra Calderón por acogerme y resguardarme cuando más lo necesitaba.

Quiero agradecer a mi gran amigo Julián Medina quien estuvo conmigo siempre, con sus conversaciones y risas logro alegrar este difícil camino. También agradezco profundamente a mis amigos Angie Ramírez, Felipe Rodríguez, Cristian Cubillos, Alejandra González, Natalia Sanabria, Luisa Gómez, Julián Romero, y Lorena.

También le doy las gracias a mis asesores, quienes me ayudaron a encaminar mi vida no solo como científico sino como persona. El doctor Andre Riveros no solo me introdujo al mundo de las abejas, sino que abrió mi mente a un mundo donde puedo lograr cosas buenas, gracias por creer en mí. La doctora Carolina Ramírez siempre estuvo lista para apoyarme en cualquier dificultad, con alegría y entusiasmo me enseño que las únicas malas ideas son las que se desechan sin intentar.

Doy un agradecimiento especial a las doctoras Yeny Acosta y Diana Monsalve del CREA, quienes contribuyeron a mi formación como científico y la materialización de este proyecto. También, agradezco al doctor Juan David Ramírez, la doctora Marina Muñoz y la futura doctora Tatiana Cáceres por toda su contribución a la materialización de este proyecto.

A mis colegas de CANNON y el CREA quienes, con sus ideas, discusiones, métodos, y sugerencias lograron llevar el proyecto hasta aquí. Un especial agradecimiento a Lina García, Juan Pablo Hernández, Valeria Velandia, Natalia Barragán y Laura Herrera, y a Natalia Buitrago. Finalmente agradezco, a todo el personal administrativo de la Escuela de Ciencias

e Ingeniería de la Universidad del Rosario. Especialmente a Sandra Chávez, Juan Pablo Reina, Angelica Rincón, y María Martínez.

Resumen

La salud de la abeja melífera (*Apis mellifera*) se ve amenazada por la interacción sinérgica entre plaguicidas y patógenos. Las intervenciones nutricionales con fitoquímicos como los flavonoides son una estrategia prometedora para mitigar este estrés. El objetivo de esta tesis fue evaluar sistemáticamente el potencial protector del flavonoide rutina contra el estrés inducido por el plaguicida imidacloprid y por patógenos claves. Mediante bioensayos de laboratorio controlados, se expusieron abejas a imidacloprid y/o patógenos (*Varroa destructor*, *Nosema ceranae* y el Virus de las Alas Deformes) con y sin suplementación profiláctica de rutina. Los resultados iniciales demostraron que la rutina mitiga eficazmente la inmunosupresión, y el estrés oxidativo y metabólico causados por la exposición crónica a imidacloprid. Sin embargo, al evaluar su efecto frente a desafíos patogénicos, se reveló una eficacia dependiente del contexto. La suplementación con rutina aumentó la resistencia y supervivencia frente a los parásitos *V. destructor* y *N. ceranae*, pero exacerbó la mortalidad en abejas infectadas con DWV, evidenciando un "trade-off" inmunológico crítico. En conclusión, esta investigación demuestra que la rutina no es un simple inmunoestimulante, sino un complejo inmunomodulador cuyos efectos dependen de la naturaleza del estrés. Estos hallazgos subrayan que la eficacia de las intervenciones nutricionales es profundamente contexto-dependiente y sientan las bases para el desarrollo de estrategias de apicultura de precisión.

Abstract

A Systematic Evaluation of the Flavonoid Rutin for Enhancing Resilience of the Africanized Honey Bee (*Apis mellifera*) to Pesticide and Pathogen Stress.

Sergio A. Mayorga.

General Introduction

The western honey bee, *Apis mellifera*, is the world's most important managed pollinator, providing essential ecosystem services that underpin global food security and the maintenance of terrestrial biodiversity (1,2). In recent decades, alarming declines in honey bee populations have been reported globally, posing a significant threat to both agricultural economies and natural ecosystems. This decline is not attributed to a single cause but rather to a multifactorial crisis driven by a complex web of interacting stressors, including habitat loss, climate change, and, most notably, the combined pressures of agrochemical exposure and endemic diseases (3–5).

Among the most significant drivers of honey bee decline are the synergistic interactions between pesticides and pathogens. Systemic insecticides, particularly neonicotinoids like Imidacloprid, are ubiquitous in agricultural landscapes. Even at sublethal concentrations found in nectar and pollen, these neurotoxic compounds exert profound negative effects on bees, impairing their navigation, foraging, and, critically, their immune function (6–10). This pesticide-induced physiological weakening leaves colonies highly vulnerable to the array of pathogens they naturally encounter. Endemic threats such as the parasitic mite *Varroa destructor*, the gut microsporidian *Nosema ceranae*, and the Deformed Wing Iflavirus Virus (DWV) can become acutely damaging in chemically-stressed bees, creating a lethal feedback loop where pesticide exposure exacerbates disease, amplifying the effects of the pesticide (4).

In the face of this complex challenge, there is an urgent need for innovative and sustainable strategies to bolster bee resilience. One of the most promising avenues lies within the field of nutritional ecology, which explores how dietary components can enhance host health and defense. Honey bees naturally consume a variety of plant secondary metabolites, or phytochemicals, present in pollen and nectar. Among these are flavonoids, a class of polyphenolic compounds renowned for their potent antioxidant and immunomodulatory properties (11,12). Rutin (quercetin-3-O-Rutinoside), a common dietary flavonoid, has emerged as a particularly strong candidate for therapeutic and prophylactic applications in apiculture due to its protective effect against cognitive alterations induced by neonicotinoids in bumble bees (13,14).

While the theoretical benefits of such phytochemicals are clear, a comprehensive and systematic evaluation of a single compound's protective potential effects on core physiological systems in the laboratory has been largely absent from scientific literature. This thesis aims to fill that critical knowledge gap. The overarching goal was to systematically

evaluate the potential of the flavonoid Rutin as a mitigator of pesticide- and pathogen-induced stress in the Africanized honey bee *Apis mellifera*.

The Thesis format

To achieve the main goal of this thesis, the research was structured into three distinct, yet interconnected, chapters. Each chapter consists of a scientific article, including contributing authors; yet sharing a continue sequence of tables, figures, and references. **Chapter 1** establishes a physiological baseline, investigating the capacity of prophylactic administration Rutin to mitigate the direct immunosuppressive effects of chronic oral administration of Imidacloprid in a controlled laboratory setting. **Chapter 2** delves deeper into the underlying mechanisms, exploring how the administration of rutin counteracts the oxidative and metabolic stress induced by the pesticide, thus providing a more detailed picture of its protective action. Building on this mechanistic foundation, **Chapter 3** tests the functional consequences of this protection by assessing whether Rutin supplementation enhances honey bee resilience against challenge by three key pathogens: *V. destructor*, *N. ceranae*, and DWV.

Collectively, this body of work proposes and validates an innovative approach to improving pollinators' health by harnessing the protective power of natural phytochemicals found within the bees' own diet. The findings presented herein have multi-level implications, contributing novel insights to the basic science of insect toxicology and nutritional immunology, presenting the foundation for a potential new product for sustainable beekeeping practices, and, offering a promising tool to help build more resilient pollinator populations in an increasingly challenging world.

General Methods

All laboratory-based experiments (Chapters 1-3) followed the principles outlined in the OECD Test Guideline 245, "Honey Bee (*Apis mellifera*), Chronic Oral Toxicity Test", which informed the 10-day exposure period, general bee maintenance, and study validity criteria (15).

All procedures involving honey bees were conducted in strict accordance with the guidelines established by the relevant Colombian regulations. Procedures were designed to minimize bee stress; handling was limited, and the number of animals used was the minimum determined necessary for statistical validity.

Honey Bee Collection and Laboratory Maintenance

Healthy adult foragers of the Africanized honey bees (*Apis mellifera*) were collected from three healthy, queenright source colonies located at the apiary of the Universidad del Rosario in Bogotá, Colombia (4.38° N, 74.04°; RH: 82–86%; T: 24.2–26.5 °C). Colonies were confirmed to be "healthy" based on low *Varroa destructor* infestation (<1%) and the absence of symptoms of other common diseases. Bees were collected from hive entrances during peak activity (09:00–12:00 h) using a translucent acrylic trap (16). The use of forager bees was

chosen to represent the segment of the colony population most directly exposed to environmental contaminants during foraging activities.

In the laboratory, bees were briefly anesthetized by chilling on ice (<5 minutes) and transferred to experimental cages (Figure 1). Throughout the acclimatization and experimental periods, bees were housed in groups of 10-15 individuals in ventilated plastic cages inside a laboratory incubator at 34 ± 1 °C and 65 ± 5% RH. All bees were provided with *ad libitum* access to sterile water via a feeder and were fed a 50% (w/v) sucrose solution daily, separate from the treatment administration (17). Mortality was recorded daily for each cage.

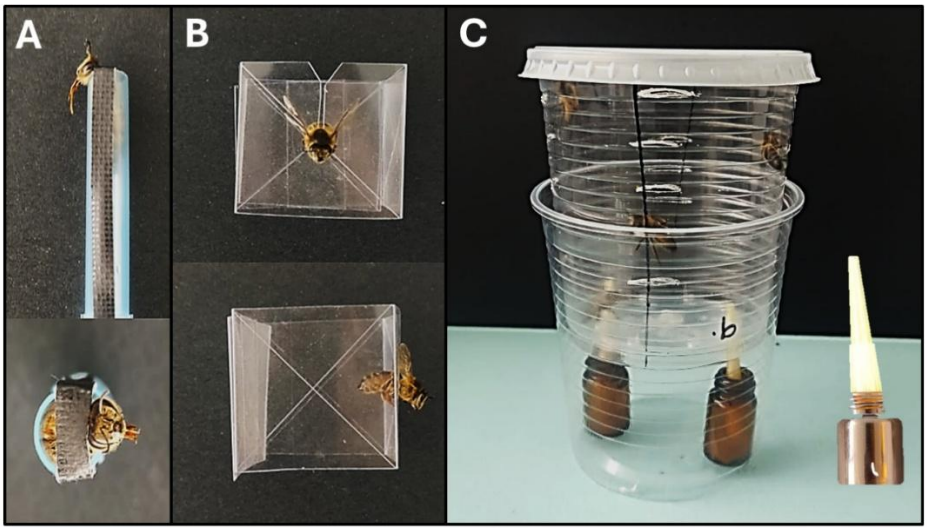

Figure 1. Experimental setups for bee housing and handling. (A) An individual bee immobilized in a restraining harness, used for precise oral administration of treatments. Top: side view; Bottom: top-down view. **(B)** A single bee restrained in an individual ventilated acrylic cube for short-term observation. **(C)** A group housing cage, constructed from modified plastic cups, used for maintaining bees throughout the 10-day survival assays.

Test Compounds and Treatment Administration

The test compounds were Imidacloprid, sourced from a commercial formulation (Confidor®, Bayer; 350 g/L), and Rutin hydrate (≥94% purity; Thermo Fisher Scientific, Cat. No. 132395000). Stock solutions were prepared in ultrapure water and subsequently diluted in a 1M sucrose solution to achieve the final treatment concentrations.

Bees were randomly assigned to one of four experimental groups (Table 1). Treatments were administered orally twice daily (9:00-17:00h). In each administration, every bee in a cage was fed 10 µL of the corresponding treatment solution. The experimental design involved a 10-day period with staggered exposure and prophylactic supplementation. Imidacloprid and rutin concentrations and dosages were based on our preliminary toxicological endpoint data (particularly the LD_{50}), empirical data generated by our research group unpublished, the

proposed Rutin concentrations for protection (14), and the reported semi-realistic field exposure Imidacloprid concentrations (8–10,18–20).

Table 1. Experimental design for chronic exposure to imidacloprid and prophylactic supplementation with rutin.

Treatment	Duration	Concentrations and dosages
Control	10 days	10 µL of a 1M sucrose solution.
Imid	3 days (Control) + 7 days (Imidacloprid)	10 µL of a 0.039 µM Imidacloprid with a 1M solution (~0.09 ng /bee / day).
Rut	7 days (Control) + 3 days (Rutin)	10 µL of a 1 µM Rutin with a 1M solution (~6.4 ng /bee / day).
Rut + Imid	3 days (Rutin) + 7 days (Imidacloprid)	Same as Rut and Imid solutions.

This staggered design was employed to test the prophylactic potential of Rutin. The Rut + Imid group received Rutin for three days prior to the introduction of Imidacloprid to assess whether pre-treatment could mitigate the subsequent pesticide-induced stress.

OECD Guideline Validation

The validity of the experimental setup was confirmed according to OECD 245 criteria (15). First, cumulative mortality in the Control group over the 10-day period did not exceed the 15% threshold. Second, a positive toxic reference group was run concurrently, wherein bees were treated with 25% dimethoate, which achieved the required >50% mortality by day 10, confirming the susceptibility of the test population. Furthermore, standard toxicological endpoints including LC_{50} and LD_{50} values for imidacloprid were determined in preliminary range-finding studies to inform dose selection (data not presented).

Hemolymph Collection

Hemolymph was collected from individual bees first anesthetized by chilling on ice. Using a sterile micro-capillary needle, the dorsal sinus of the bee was punctured at the cervical membrane (between the head and thorax). Up to 5 µL of clear hemolymph was drawn into a pre-chilled, sterile glass capillary tube. To minimize melanization and coagulation, hemolymph was immediately dispensed into a microcentrifuge tube containing 50 µL of ice-cold, sterile insect anticoagulant buffer (1X PBS containing 10 mM EDTA and 30 mM sodium citrate, pH 7.0). For assays requiring pooled samples, hemolymph from 10-15 bees was collected into the same tube and used immediately for subsequent analyses.

Chapter 1: Prophylactic Rutin Mitigates chronic Imidacloprid immunosuppression in Honey Bees (*Apis mellifera*).

Sergio A. Mayorga[a,c], Yeny Acosta[c], Diana M. Monsalve[c], Andre J. Riveros[a,b], Carolina Ramírez[c]

[a] *CANNON Research Group, Department of Biology, School of Science and Engineering, Universidad del Rosario, Bogotá, Colombia*

[b] *Department of Neuroscience, College of Science, University of Arizona. Tucson, Arizona. USA*

[c] *Center for Autoimmune Diseases Research (CREA), School of Medicine and Health Sciences, Universidad del Rosario. Bogotá. Colombia*

Introduction

The global decline of pollinator populations, particularly the western honey bee (*Apis mellifera*), represents a significant threat to ecosystem stability and global food security. As the primary managed pollinator, *A. mellifera* is essential for the reproduction of countless wild plant species and the yield of approximately 75% of globally important crops (1,2). While this decline is multifactorial, the widespread use of systemic pesticides in agriculture has been identified as a primary driver of sublethal stress that impairs honey bee health and colony viability (21). Among the most scrutinized of these agrochemicals are neonicotinoids like Imidacloprid, which are frequently detected in nectar, pollen, and water, leading to chronic exposure (22). Beyond its well-documented neurotoxic effects, Imidacloprid is a potent immunomodulator. Exposure suppresses the honey bee's innate immune system—comprising both cellular defenses (e.g., phagocytosis, encapsulation) and humoral responses (e.g., antimicrobial peptides)—leaving bees more vulnerable to endemic pathogens and creating a synergistic pathway that can accelerate colony collapse (7,23–25).

Given the profound impact of pesticides, strategies that enhance bee resilience are of paramount importance. Nutritional interventions, particularly supplementation with naturally occurring phytochemicals, have emerged as a promising avenue (26). Flavonoids, a class of plant secondary metabolites, are of particular interest due to their well-established antioxidant, anti-inflammatory, and immunomodulatory properties (12). Rutin (quercetin-3-O-Rutinoside), a ubiquitous flavonoid found in many types of pollen and nectar, has the capacity to counteract the oxidative stress induced by xenobiotics like Imidacloprid (27). However, while some studies suggest flavonoids can bolster insect immunity, the specific prophylactic potential and underlying mechanisms of Rutin against pesticide-induced immunosuppression in *A. mellifera* remain largely uncharacterized.

Here, we sought to determine whether prophylactic dietary supplementation with Rutin could mitigate the systemic immunosuppression caused by chronic exposure to a field-relevant commercial formulation of Imidacloprid (Confidor®). We hypothesized that: [1] chronic exposure to Imidacloprid would induce a state of immunosuppression, detectable across

systemic, cellular, and molecular levels; [2] administration of Rutin alone would actively modulate and enhance baseline immune parameters; and [3] prophylactic administration of Rutin would ameliorate the immunological damage caused by the pesticide. To test these hypotheses, we employed a comprehensive, multi-tiered analytical approach to provide a holistic evaluation of Rutin's protective capacity, from its effects on whole-organism immune profiles down to the expression of key regulatory genes.

Methods

1. Sample Collection

On the morning following the final day of chronic exposure, we collected bees for downstream assays. For most assays, six biological replicates (each a pool of 10 bees) were established per treatment (total N=240 bees). For assays requiring individual analysis (Sessile Hemocyte Distribution, NF-κB Activation, Apoptosis Assay), three biological replicates (each a single bee) were used per treatment (total N=12 bees).

2. Immune and Physiological Assays

Total Hemocyte Quantification: Total hemocyte concentration was determined by loading 10 µL of the hemolymph-PBS suspension into a Neubauer-improved hemocytometer (28,29). Cells were counted under 400x magnification using a light microscope, and the concentration was expressed as cells per microliter.

Hemocyte Staining and Morphology: To visualize hemocyte morphology, we adhered fresh hemolymph (10 µL) to a pre-cooled coverslips for 1.5 h (33°C, 50% RH, dark). Adhered cells were fixed with 4% paraformaldehyde (PFA) overnight at 4°C, washed three times with 1X PBS, and permeabilized with 0.3% Tween-20 in PBS for 8 min. Cells were subsequently stained for F-actin with Alexa Fluor™ 555 Phalloidin (1:200 dilution; Invitrogen, Cat# A34055) and for DNA with DAPI (0.32 µM; Invitrogen, Cat# D1306). Coverslips were mounted using ProLong™ Gold Antifade Mountant (6). Confocal micrographs were acquired using a Nikon Eclipse 80i microscope and analyzed with ImageJ software v1.52 (30).

Hemocyte Phagocytosis Assay: To measure phagocytic activity *in vivo*, we injected bees between the third and fourth abdominal tergites with 1.5 µL of a 1 µm Fluoresbrite™ carboxylate microsphere suspension (Polysciences Inc., Cat# 17154; 2×10^6 beads/µL) in 1X PBS (31). After a 5-hour incubation (32°C, 50% RH), we collected hemolymph into 50 µL of an ice-cold anticoagulant buffer (70% Grace's Insect Medium 10 µL, 1X PBS pH 7.4, 98 mM NaOH, 1.7 mM EDTA, 41 mM acetic acid pH 5.2, and 10% BSA) (32–35). Phagocytic activity was calculated as the percentage of hemocytes containing one or more engulfed microspheres, with internalization confirmed by Z-stack analysis of confocal images (36,37).

Hemolymph Antimicrobial Activity: We quantified the antimicrobial activity of hemolymph using a liquid growth inhibition assay against *Escherichia coli* (DSM 682). Briefly, a bacterial suspension (~1 × 10^5 CFU/mL) was incubated with the pooled hemolymph-PBS suspension without dilution (38). Each well contained 50 µL of pooled hemolymph, 100 µL of the *E. coli* working suspension, and 50 µL of sterile LB broth. Control wells consisted of *E. coli* suspension with LB broth (positive growth) and LB broth alone (blank). We calculated the Growth Inhibition Index (GI) based on the change in optical density (OD at 600 nm) over 24 hours (see Equation 1) (39).

Hemocyte Respiratory Burst Assay (NBT Reduction): We measured Respiratory burst activity using a Nitro Blue Tetrazolium (NBT) reduction assay. Briefly, we mixed 10 µL of pooled fresh hemolymph with an equal volume of 0.87% NH_4Cl. The resulting pellet was resuspended in RPMI 1640 medium (Sigma-Aldrich, Cat# R8758) (40). ROS production was induced with PMA (phorbol 12-myristate 13-acetate; Sigma-Aldrich, Cat# P8139), and the reduction of NBT (Invitrogen, Cat# N6495) was quantified by measuring the absorbance of the formazan product at 540 nm (41). Results were normalized to total protein content, determined via a BCA Assay Kit (ThermoFisher, USA), and expressed as nmol reduced NBT/mg protein.

Encapsulation Response Assay: We implanted bees with a sterile nylon monofilament (Ø 0.2 mm, length 2 mm). After a 4-hour incubation (35°C, 50% RH), filaments were retrieved and imaged. The extent of encapsulation was quantified in ImageJ by measuring the mean gray value of the melanized capsule, where a lower mean gray value corresponded to a stronger response (42).

Nodulation Response Assay: We induced Nodulation by injecting each bee with 1 µL of *E. coli* suspension (~1 × 10^4 CFU/µL). After 24 hours, abdominal tergites were dissected. We counted the total number of visible melanized nodules within a 2 mm^2 area centered on the dorsal midline, which served as the standardized region of interest (ROI) (43,44).

Sessile Abdomen Hemocyte Quantification: Sessile hemocyte reservoirs were visualized *in vivo* by injecting a dye mixture of Hoechst 33342 (1:200; Invitrogen™, Cat# H3570) and CM-DiI (Invitrogen™, Cat# C7000). The dorsal abdominal wall was dissected and imaged via confocal microscopy. To quantify fluorescence, we drawn custom polygonal ROIs on maximum intensity projections of abdominal tergites (34,45). The mean pixel intensity of CM-DiI fluorescence within each ROI was then measured using ImageJ software v1.52 (30). To correct for background fluorescence, the average intensity from unstained naïve samples was subtracted from the values of their corresponding experimental samples (34,35). Sessile hemocyte density was quantified by counting the number of Hoechst-stained nuclei within defined ROIs and expressed as cells per mm^2

NF-κB (Relish) in Fat Body: Bees were challenged with an *E. coli* injection. After 24 h, abdominal fat bodies were dissected, fixed, and stained for F-actin with Alexa Fluor™ 555

Phalloidin (1:200 dilution; Invitrogen, Cat# A34055). Relish was counterstained using a primary rabbit anti-Relish antibody (1:50; RayBiotech, Cat# RB-14-00004-20) and a Goat anti-rabbit-Cy5 secondary antibody (Thermo Fisher Scientific, Cat# A10523). Relish activation was quantified as proportion index of cells showing predominantly relish immunofluorescence, determined via confocal microscopy (46,47).

Apoptosis Assay in Brain Tissue related to immune regulation: We evaluated apoptosis in brain tissue, including the associated corpora cardiaca and allata, using a TUNEL assay. Brains were dissected and fixed in 10% neutral buffered formalin, processed for paraffin embedding, and sectioned at 7 µm. Early apoptosis was detected using the One-step TUNEL In Situ Apoptosis Detection Kit (Elabscience, Cat# ECKA320) per the manufacturer's instructions. Nuclei were counterstained with DAPI. The apoptosis rate was calculated as the percentage of TUNEL-positive nuclei relative to the total DAPI-stained nuclei within defined ROIs.

3. Gene Expression Analysis by RT-qPCR

Relative expression of selected genes was analyzed by reverse transcription quantitative polymerase chain reaction (RT-qPCR) in individual bees (N=6 per treatment).

RNA Isolation, Quality Control, and cDNA Synthesis: Whole bees were snap-frozen and pulverized, and total RNA was extracted using TRIZOL™ reagent (Invitrogen™, Cat# 15596026) followed by RNeasy Mini Kit purification (Qiagen, Cat# 74106). RNA integrity and purity were verified by agarose gel electrophoresis and NanoDrop™ One spectrophotometry (Thermo Fisher Scientific), respectively. First-strand cDNA was synthesized from 500 ng of total RNA using the iScript™ Advanced cDNA Synthesis Kit (Bio-Rad, Cat# 1725038).

Quantitative Real-Time PCR: qPCR was performed using a Bio-Rad CFX96 Touch Real-Time PCR Detection System. Primer pairs for target and reference genes (Table 2) were designed using Primer-BLAST. Each 15 µL reaction contained KiCqStart™ SYBR® Green qPCR ReadyMix™ (Sigma-Aldrich, Cat# KCQS02), 250 nM of each primer, and 13 ng of template cDNA. The thermal cycling protocol was 95°C for 2 min; followed by 40 cycles of 95°C for 5 sec and 60°C for 30 sec (data acquisition); followed by a melt curve analysis.

Table 2. Selected Housekeeping and immune-related genes, primers sequences, and reaction efficiencies.

Gene	Function	Accession no.	Forward primer (5' - 3')	Reverse primer (5' - 3')	Eff. (%)
Dorsal-1	Activating pathways	XM_006564031	GGCAAGGAACGAA CATATCGT	GTCTCCGTTGAGTT GTTGG	99.9
Relish	Activating pathways	NM_001011599	TGGAAACGGACGA CTCTGAC	GATCTGGTTGGTGC TGCTGT	96.3

Stat92E	Activating pathways	XM_026438755	GCAGATGAAGCGAATCAGAGC	TCGATCTTGCCCTTCTTC	98.1
Dicer-1	Activating pathways	NM_001142568	ATGCCCAAGCTATGTGGAAAAG	TTGAGCAGCGCGTAGTTA	99.4
Cactus-1	Inhibitory pathways	XM_006564032	CCAAAGACATCGACAACACGT	CCAGTCGTTTTGCTTG	95.2
Amel.CLR[3]	Inhibitory pathways	XM_006560417	GTGGAAGGATCAGCAGGAAAT	TGCCTTTGTTTCCATCTCA	96.7
Serpin-2	Inhibitory pathways	NM_001011606	TCTGGCCACCCAACTCTACT	CGTTGTAGCCGTCCAAAATA	94.9
Socs-2	Inhibitory pathways	NM_001142571	ATGTGGAAGGTGCTGTTGTTC	ACTGCACATCCACTTCACA	98.6
Nimrod-C1	Immune effectors	XM_016914561	AGCGTGGTTTCACTGTTGGTA	GTTGGCTCCGTTCTTTTGA	96.8
Defensin-1	Immune effectors	NM_001011598	GCTTGCTACTGTTCGACGACT	GCCTTCCTTCTGCTCACTT	98.2
Vago[4]	Immune effectors	XM_006565103	TCTCCCTTGGAACGAACTCTT	TCGATGAATCCGAAAACATC	97.4
Lys-1	Immune effectors	NM_001011603	TTCAACATCGGTGCGTCTAAC	TTGCACCTTGTTCACATTCCG	99.6
PPO[5]	Immune effectors	NM_001011608	GTCAAGAGCCGAAACTTCAAT	CCAGCAGTAGCACCTTCAA	100.2
Spz-6	Immune effectors	NM_001011597	ACCCAACAAGAAGCCAAGTCC	AATTGCCGTAGGTGAACTC	95.5
CCG	Endocrine activators	NM_001011586	CGTATTGCCTTCGATTTGGAT	GGTTGCTTGGTGATCTTGG	99.2
Jhamt	Endocrine activators	NM_001011579	ATGCGTTCCAACCCAGTTTCC	AGGTCCTTGATCAACACC	97.6
Phantom	Endocrine inhibitors	NM_001011584	GACTGGCTAAAGGAGGAGATT	GAAACCGCTCTGGCTGATAAT	98.9
AST-A	Endocrine inhibitors	NM_001011588	TCGTGGTTCTTTCTCTCCGTA	AAGGAGCTGCGGAACTCTT	95.7
RPS5	Reference gene	NM_001011568	AATTATTTGGTCGCTGGAATG	CTTGGACTTGCCTCTAAAT	101.0
RPS18	Reference gene	NM_001014389	ATGGACGTCGATGGATAGTGT	GAACCGGCTAGGTAGAAGG	97.4
Actin	Reference gene	NM_001177653	TGCCAACACTGTCCTTTCTGAG	AATTGACCCACCAATCCA	100.2

6. Statistical Analysis

All statistical analyses were conducted in R (v4.4.1) using the RStudio environment (48,49). We employed a three-tiered analytical strategy.

First, we performed a **multivariate analysis** to obtain an immune "profile" of bees. Z-score standardized data from six core immune variables (*Hemocyte counts, Phagocytosis, Hemolymph antimicrobial activity, Hemocytes respiratory burst, Encapsulation response,*

Nodulation response) were visualized with Principal Component Analysis (PCA). Differences were tested using PERMANOVA (9,999 permutations), followed by pairwise PERMANOVA (Holm-Bonferroni adjustment) and SIMPER analysis.

Second, we performed **univariate analyses** of all the measured immune parameters (*NF-κB Relish Fat Body, Apoptosis Assay in Brain Tissue related to immune regulation, Sessile Abdomen Hemocyte Quantification*). We assessed normality of residuals (Shapiro-Wilk test) and homogeneity of variances (Levene's test). If assumptions were met, we performed a one-way ANOVA. If violated, we used the Kruskal-Wallis test. Significant omnibus tests were followed by pairwise t-tests (for ANOVA) or Dunn's test (for Kruskal-Wallis), with p-values adjusted using the Holm-Bonferroni method. We also calculated Effect sizes (η^2, Cohen's *d*).

Third, for **gene expression analysis**, the Ct value of each target gene was normalized against the geometric mean of three stable housekeeping genes (PRS5, RPS18, and ACTIN) to obtain ΔCt values. These ΔCt values were then analyzed using the same univariate workflow. For visualization, fold-change values were calculated using the $2^{-}\Delta\Delta Ct$ method.

Results

Imidacloprid Induces a Systemic Shift in the Bee Immune Profile

To assess the systemic impact of Imidacloprid and Rutin on the bee immune system, we first performed a PCA on six core immune variables. The PCA revealed a distinct separation of treatment bees, primarily along the first principal component (PC1), which accounted for 86.9% of the total variance (Figure 2). Visually, Imid bees were clearly segregated from the Control, Rut, and Rut+Imid bees along this axis, suggesting a stronger differential impact of the pesticide. All six immune variable vectors showed strong negative loadings on PC1, aligning with the separation of Imid bees and indicating that lower values across these immune parameters characterized the pesticide-exposed bees.

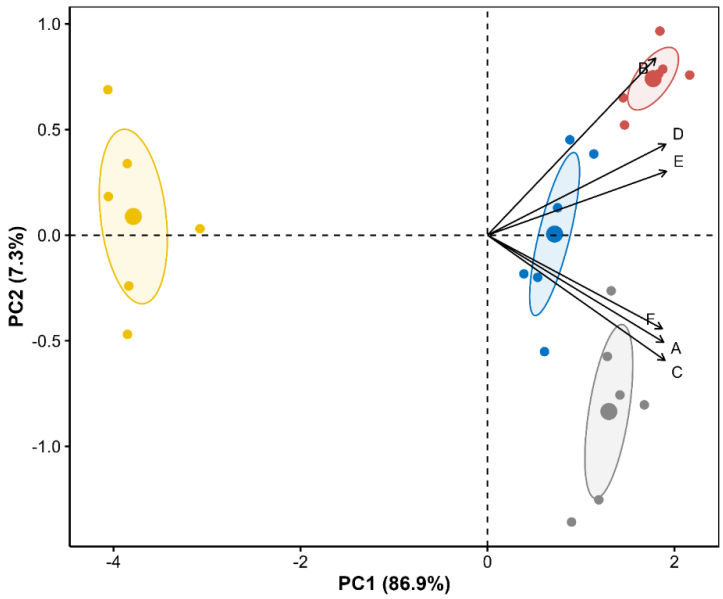

Figure 2. Principal Component Analysis (PCA) of the systemic immune response in bees across treatment groups. The plot visualizes the separation of treatment groups based on six integrated immune variables (**A.** Hemocyte counts; **B.** Phagocytosis; **C.** Hemolymph antimicrobial activity; **D.** Hemocytes respiratory burst; **E.** Encapsulation response; **F.** Nodulation response). The first two principal components (PC1 and PC2) are displayed, accounting for 86.9% and 7.3% of the total variance, respectively. Each point represents a biological replicate (n=10), with colors corresponding to the treatment groups: **Control** (blue), **Imid** (yellow), **Rut** (red), and **Rut+Imid** (grey). Ellipses represent the 95% confidence interval for each group's centroid. Vectors indicate the loading and direction of the six original immune variables. The clear separation along PC1 demonstrates a strong, systemic immunosuppressive effect of Imidacloprid and the mitigating effect of Rutin supplementation.

Our PERMANOVA confirmed a highly significant overall effect of treatment on the systemic immune profile of bees (Pseudo-$F_{(3, 20)} = 83.74$, $R^2 = 0.93$, $p < .001$). Interestingly, post-hoc pairwise comparisons revealed that the immune profiles of all bees were significantly different from one another (Pairwise PERMANOVA, all $p < .02$). To identify the specific immune parameters driving these significant pairwise differences, we performed a SIMPER analysis (Table 3).

Table 3. Contribution of immune parameters to the dissimilarity between treatment groups.

Control vs Imid		Control vs Rut		Control vs Rut+Imid		Imid vs Rut+Imid	
Nodulation	0,21	*Encapsulation*	0,21	*Hemocytes*	0,21	*Hemocytes*	0,21
Encapsulation	0,19	*Resp. burst*	0,22	*Antimicrobial*	0,38	*Nodulation*	0,20
Resp. burst	0,17	*Hemocyte counts*	0,18	*Resp. burst*	0,18	*Antimicrobial*	0,20
Antimicrobial	0,16	*Phagocytosis*	0,16	*Phagocytosis*	0,11	*Encapsulation*	0,16
Hemocytes	0,16	*Nodulation*	0,14	*Encapsulation*	0,09	*Resp. burst*	0,16
Phagocytosis	0,10	*Antimic. Activity*	0,08	*Nodulation*	0,03	*Phagocytosis*	0,07

Values represent the proportional contribution of each parameter to the average Bray-Curtis dissimilarity between pairs of treatment groups, as determined by SIMPER analysis. For each comparison, variables are listed in descending order of their contribution.

Rutin Restores Immunity and Prevents Imidacloprid-Induced Neurotoxicity

In Imid bees, we found suppressed Nodulation, Encapsulation, and Respiratory burst responses. Interestingly, Rut supplementation alone had a mixed effect on these functions: it significantly enhanced encapsulation and respiratory burst, but reduced nodulation compared to Control bees. For all three of these key cellular functions, prophylactic supplementation in Rut+Imid bees offered complete protection, restoring the responses to levels statistically indistinguishable from healthy Control bees (Table 4).

A different protective pattern, one of hyper-stimulation, was observed for other parameters. While Imidacloprid caused a severe reduction in bees' Hemocyte counts and Hemolymph antimicrobial activity, the effect of Rutin alone was to significantly elevate both immune parameters above Control bee levels. This stimulatory effect carried through to Rut+Imid bees, that presented responses that were also significantly higher than that of Control bees (Figure 3).

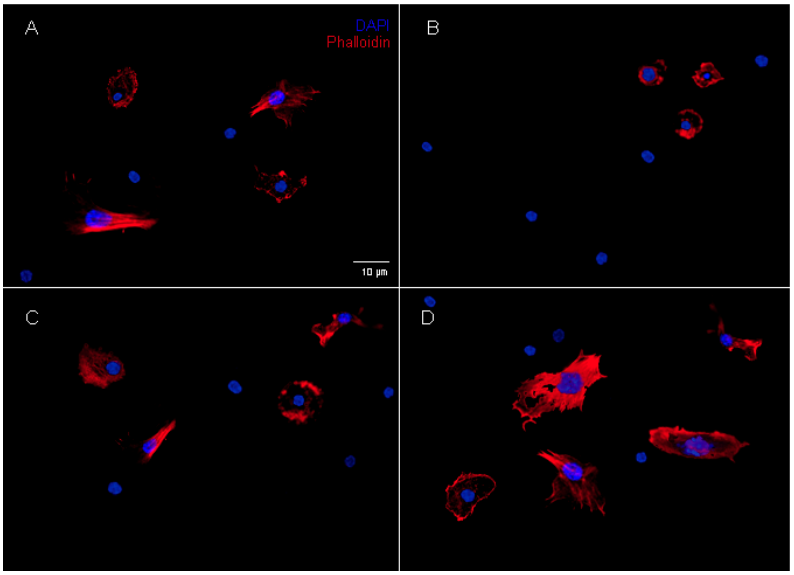

Figure 3. Representative confocal micrographs of hemocytes from treated bees. The figure shows hemocytes adhered to a coverslip from each experimental group: **(A)** Control, **(B)** Imid, **(C)** Rut, and **(D)** Rut+Imid. Cellular F-actin is stained with Alexa Fluor™ 555 Phalloidin (red), and nuclei are counterstained with DAPI (blue). The micrographs illustrate qualitative differences in hemocyte density and morphology, particularly the reduced cell numbers in Imidacloprid-exposed bees. Scale bar = 10 µm.

The Phagocytic response showed a pattern of partial recovery. We found that Imidacloprid severely suppressed phagocytosis (Cohen's d = 5.30), while Rutin alone significantly enhanced it. Despite this, Rut+Imid bees, while showing significant improvement over Imid bees, did not fully restore the function to Control bee levels (Figure 4).

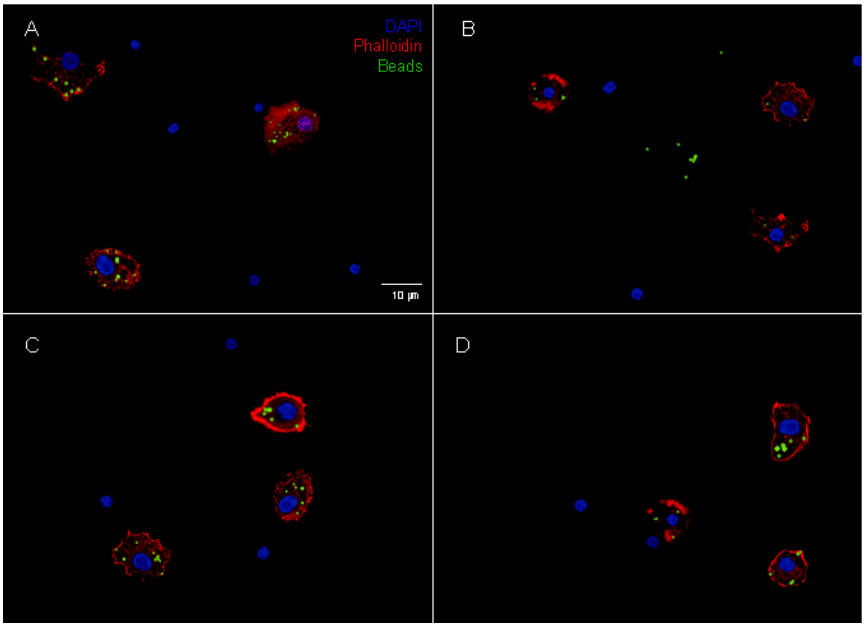

Figure 4. Representative confocal micrographs of hemocyte phagocytosis. The figure shows representative images from the in vivo phagocytosis assay for each treatment group: **(A)** Control, **(B)** Imid, **(C)** Rut, and **(D)** Rut+Imid. Fluorescent microspheres (beads) are shown in green, the F-actin cytoskeleton is stained with phalloidin (red), and cell nuclei are counterstained with DAPI (blue). The images illustrate hemocytes that have successfully engulfed one or more microspheres and highlight the apparent reduction in phagocytic activity in the Imidacloprid-treated bees. Internalization of beads was confirmed via Z-stack analysis. Scale bar = 10 µm.

Imidacloprid exposure suppressed both nodulation and encapsulation responses compared to Control bees. The protective effects of rutin manifested differently for each function. The nodulation response was most strongly enhanced in Rut+Imid bees, reaching the highest level of all treatment bees. In contrast, encapsulation activity was highest in Rut bees, while the Rut+Imid bees still maintained a robust encapsulation response that was significantly higher than controls (Figure 5).

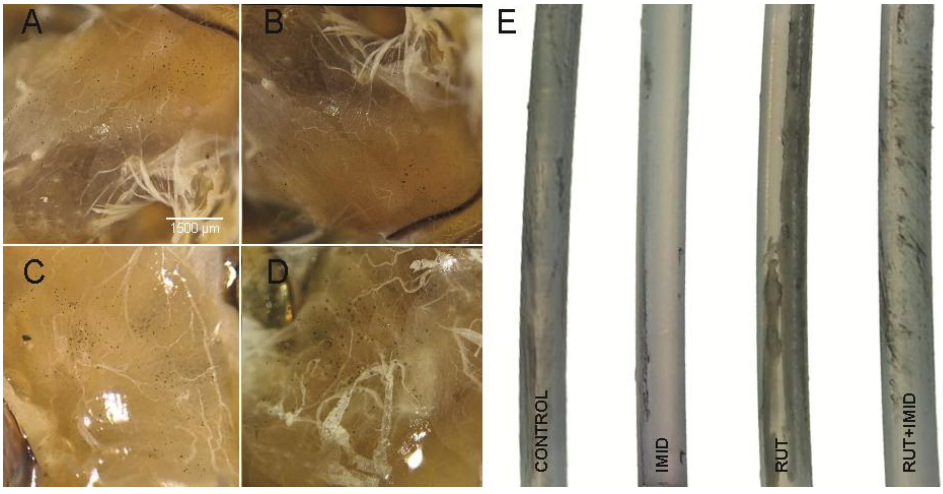

Figure 5. Nodulation and encapsulation cellular immune responses. Representative micrographs show the nodulation response (melanized nodules) on dissected abdominal tergites following an *E. coli* challenge for

each treatment group: **(A)** Control, **(B)** Imid, **(C)** Rut, and **(D)** Rut+Imid. Scale bar = 1500 µm. **(E)** Corresponding encapsulation response indicated by the degree of melanization on retrieved nylon monofilament implants for each treatment group.

Finally, we found that Imid bees presented reduced Relish (NF-κB) levels in the fat body and the population of Sessile hemocytes in the abdominal reservoir (Figure 6). Conversely, Imidacloprid also induced pathological levels of apoptosis in neuroimmune brain tissue.

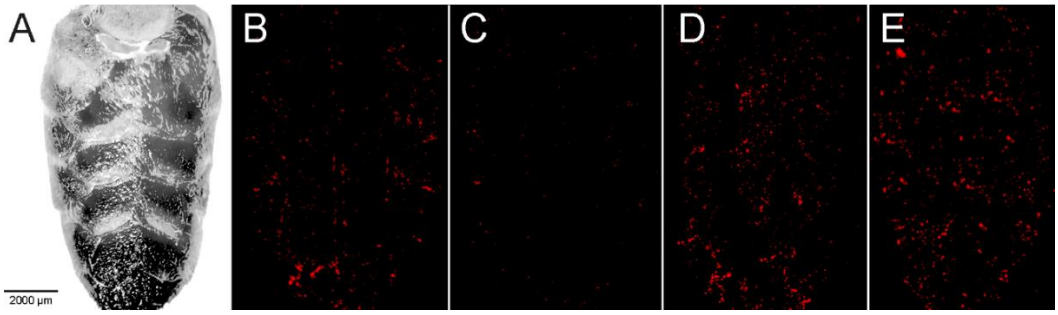

Figure 6. Sessile hemocyte reservoirs on the dorsal abdominal wall. (A) Dissected dorsal abdominal wall used for quantifying sessile hemocytes. **(B-E)** Representative confocal micrographs showing sessile hemocytes stained with CM-DiI (red) for each treatment group: **(B)** Control, **(C)** Imid, **(D)** Rutin, and **(E)** Rut+Imid. Scale bar = 2000 µm.

The effect of Rut supplementation alone was pathway-specific. It had no significant baseline effect on Relish or apoptosis rates compared to Control bees, demonstrating its innocuousness in those contexts (Figure 7). However, it acted as an immune stimulant for hemocytes, significantly increasing bees' sessile reservoir on its own.

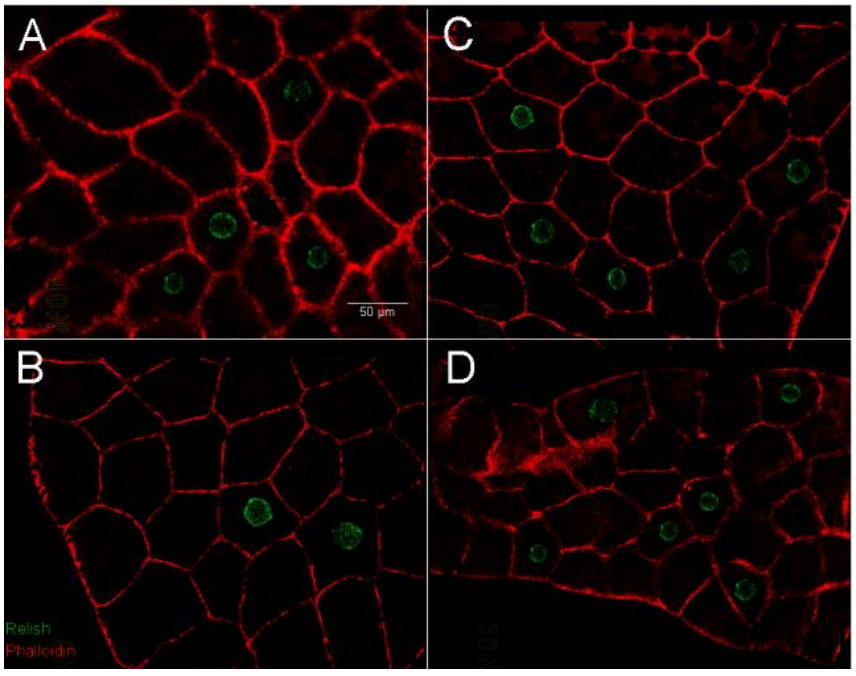

Figure 7. Relish activation in abdominal fat body tissue. Representative confocal micrographs showing Relish levels for each treatment group: **(A)** Control, **(B)** Imid, **(C)** Rut, and **(D)** Rut+Imid. The F-actin

cytoskeleton is stained with phalloidin (red) to outline the cells, and Relish immunofluorescence is shown in green. Scale bar = 50 µm.

The protective effects of Rutin were robust. For both Sessile hemocytes and Relish, bees presented a hyper-stimulatory response, elevating these responses to levels significantly higher than even the healthy Control bees. For apoptosis, however, the effect was purely restorative; Rut+Imid bees had apoptosis rates to levels indistinguishable from Control bees (Figure 8).

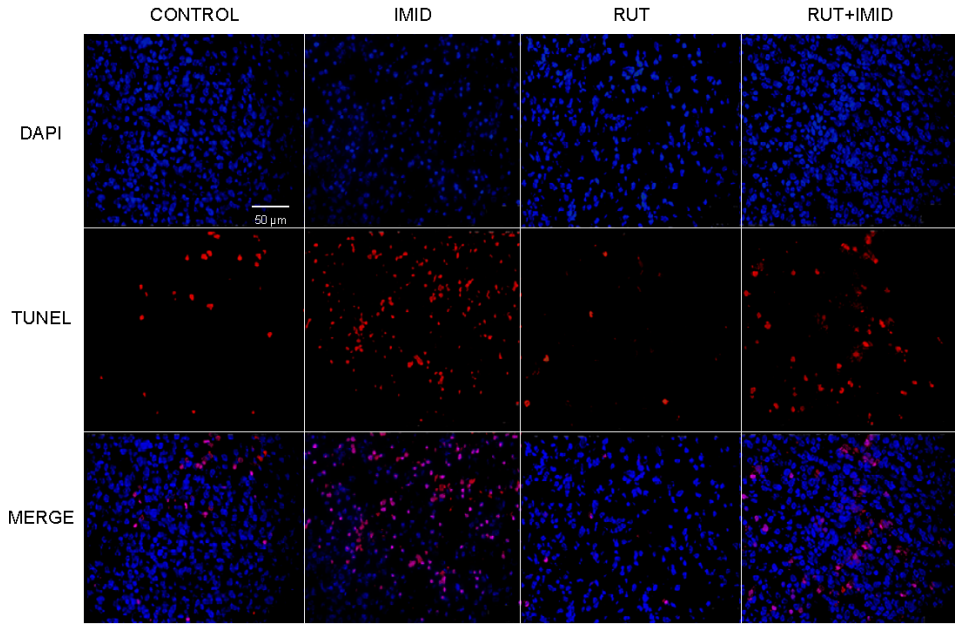

Figure 8. Rutin mitigates Imidacloprid-induced apoptosis in neuroimmune brain tissue. Representative confocal micrographs of bee brain tissue from the four treatment groups. Apoptotic cells were identified using a TUNEL assay (red fluorescence), and total cell nuclei were counterstained with DAPI (blue). The bottom row shows the merged channels.

Table 4. Effects of Imidacloprid and Rutin on Core Immune Functions.

Immune Parameter	Control	Imid	Rut	Rut+Imid	Overall ANOVA
Nodulation (%)	83.6 ± 2.58 ^{a}	31.4 ± 4.28 ^{c***}	68.9 ± 5.17 ^{b***}	85.6 ± 2.41 ^{a***}	$F(3,20) = 263.68$, $p < .001$, $\eta^2 = 0.975$
Encapsulation (%)	59.9 ± 6.31 ^{b}	27.7 ± 6.29 ^{c***}	80.7 ± 6.99 ^{a***}	63.0 ± 3.74 ^{b***}	$F(3,20) = 82.20$, $p < .001$, $\eta^2 = 0.94$
Hemocytes counts (Cells/ µL)	7402 ± 740 ^{c}	3716 ± 920 ^{d***}	9500 ± 254 ^{b***}	10572 ± 1045 ^{a***}	$F(3,20) = 86.01$, $p < .001$, $\eta^2 = 0.928$
Phagocytosis (%)	65.4 ± 6.63 ^{b}	25.1 ± 1.83 ^{d***}	84.8 ± 3.49 ^{a***}	58.7 ± 4.88 ^{c***}	$F(3,20) = 81.59$, $p < .001$, $\eta^2 = 0.925$

Antimicrobial activity (%)	53.7 ± 3.99 ^{c}	15.6 ± 2.97 ^{d***}	60.3 ± 4.96 ^{b*}	65.5 ± 2.62 ^{a***}	$F(3,20) = 104.55$, $p < .001$, $\eta^2 = 0.924$
Respiratory burst (nmol/mg)	45.1 ± 7.62 ^{b}	10.3 ± 2.89 ^{c***}	65.9 ± 4.31 ^{a**}	49.3 ± 3.48 ^{b***}	$F(3,20) = 38.42$, $p < .001$, $\eta^2 = 0.852$
Sessile hemocytes (r.a.u)	4801 ± 838 ^{c}	2172 ± 442 ^{d**}	6640 ± 684 ^{b*}	8153 ± 253 ^{a***}	$F(3,8) = 55.63$, $p < .001$, $\eta^2 = 0.954$
Relish (%)	0.96 ± 0.22 ^{b}	0.35 ± 0.13 ^{c**}	1.03 ± 0.23 ^{b}	1.45 ± 0.07 ^{a***}	$F(3,8) = 20.86$, $p < .001$, $\eta^2 = 0.887$
Apoptosis index (%)	0.45 ± 0.09 ^{a}	0.81 ± 0.09 ^{b**}	0.40 ± 0.06 ^{a}	0.52 ± 0.11 ^{a*}	$F(3,8) = 11.76$, $p = .003$, $\eta^2 = 0.815$

*Values are presented as Mean ± SD. Within a row, means not sharing a superscript letter (a, b, c, d) are significantly different based on post-hoc tests with Holm-Bonferroni correction ($p < .05$). Asterisks represent the significance level of the comparison against the Control or Imid (for Rut+Imid) group ($p < 0.05$, ** $p < 0.01$, *** $p < 0.001$).**

Rutin Restores Immune and Endocrine Gene Networks Disrupted by Imidacloprid

To understand the molecular mechanisms underlying the observed immunological changes, we quantified the relative expression of 18 genes associated with immune pathways, immune inhibitors, and endocrine immune regulators (Figure 9). The results revealed a complex landscape of immunosuppression by Imidacloprid and targeted restoration and stimulation by Rutin (Table 5).

Table 5. Effects of Imidacloprid and Rutin on Gene Expression (ΔCt Values).

Gene	Control	Imid	Rut	Rut+Imid	Overall Test
Dorsal.1	-0.42 ± 0.22 c	2.72 ± 0.87 d***	-2.59 ± 0.98 a***	0.35 ± 0.80 b***	$F(3,20) = 47.90$, $p < .001$, $\eta^2 = 0.878$
Relish	-0.09 ± 0.54 c	7.61 ± 1.29 d***	-3.07 ± 1.06 b***	-3.47 ± 1.23 a***	$F(3,20) = 138.02$, $p < .001$, $\eta^2 = 0.954$
STAT92E	-0.63 ± 0.46 b	6.25 ± 0.72 c***	-0.33 ± 0.52 b	-3.49 ± 0.54 a***	$F(3,20) = 317.07$, $p < .001$, $\eta^2 = 0.979$
Dicer.1	-0.27 ± 0.52 a	1.73 ± 2.50 a	-0.25 ± 0.33 a	-1.51 ± 1.92 a	$\chi^2(3) = 3.65$, $p = .302$, $\eta^2_H = 0.032$
Cactus.1	-0.27 ± 0.68 a	2.24 ± 2.63 a	-0.03 ± 0.69 a	-1.34 ± 1.37 a*	$\chi^2(3) = 8.62$, $p = .035$, $\eta^2_H = 0.281$
Amel.CLR	-0.50 ± 0.52 a	-3.72 ± 0.61 b***	-0.48 ± 0.68 a	-0.11 ± 0.75 a***	$F(3,20) = 41.03$, $p < .001$, $\eta^2 = 0.860$
Serpin.2	-0.08 ± 0.53 a	-3.68 ± 0.70 a	1.32 ± 2.51 a**	0.20 ± 0.16 a*	$\chi^2(3) = 14.01$, $p = .003$, $\eta^2\_H = 0.550$
SOCS2	-0.42 ± 0.53 b	-2.30 ± 0.48 c***	-0.02 ± 0.57 b	3.40 ± 1.10 a***	$F(3,20) = 66.38$, $p < .001$, $\eta^2 = 0.909$
Nimrod.C1	-0.59 ± 0.49 a	2.08 ± 1.65 b**	-0.38 ± 0.54 a	-1.47 ± 1.37 a***	$F(3,20) = 10.81$, $p < .001$, $\eta^2 = 0.619$
Defensin.1	-0.78 ± 0.39 c	2.24 ± 0.91 d***	-5.05 ± 0.67 a***	-2.91 ± 0.97 b***	$F(3,20) = 97.78$, $p < .001$, $\eta^2 = 0.936$

IFN.Y	-0.11 ± 0.41 a	3.72 ± 0.81 b***	-0.66 ± 0.76 a	-0.97 ± 0.65 a***	$F(3,20) = 62.59$, $p < .001$, $\eta^2 = 0.904$
Lys.1	-0.16 ± 0.65 c	1.86 ± 0.78 d***	-4.05 ± 0.54 a***	-1.67 ± 1.12 b***	$F(3,20) = 57.98$, $p < .001$, $\eta^2 = 0.897$
PPO3	0.11 ± 0.75 a	6.90 ± 0.78 b***	-0.19 ± 0.62 a	-0.36 ± 0.57 a***	$F(3,20) = 158.28$, $p < .001$, $\eta^2 = 0.960$
SPZ6	0.07 ± 0.54 a	5.85 ± 0.80 b***	0.03 ± 0.53 a	0.90 ± 0.96 a***	$F(3,20) = 87.19$, $p < .001$, $\eta^2 = 0.929$
CCG	-0.30 ± 0.24 b	0.12 ± 2.03 b	-0.37 ± 0.58 b	-4.64 ± 0.89 a**	$\chi^2(3) = 13.37$, $p = .004$, $\eta^2_H = 0.518$
JHAMT	-0.35 ± 0.43 b	-2.30 ± 0.70 a***	-0.48 ± 0.68 b	0.53 ± 0.66 c***	$F(3,20) = 21.62$, $p < .001$, $\eta^2 = 0.764$
AST.A	0.05 ± 0.38 b	5.87 ± 2.47 c***	-2.72 ± 1.43 a*	-0.16 ± 0.98 b***	$F(3,20) = 34.16$, $p < .001$, $\eta^2 = 0.837$
Phantom	-3.52 ± 1.52 a	1.67 ± 1.24 b***	-5.18 ± 2.17 a	-3.99 ± 1.08 a***	$F(3,20) = 22.65$, $p < .001$, $\eta^2 = 0.773$

Values are presented as Mean ± SD of ΔCt values, where a higher value indicates lower relative gene expression. Within a row, means not sharing a superscript letter (a, b, c, d) are significantly different based on post-hoc tests with Bonferroni correction (p < .05). Asterisks represent the significance level of the comparison against the Control group (for Imid and Rut columns) or against the Imid group (for the Rut+Imid column) ($p < 0.05$, ** $p < 0.01$, *** $p < 0.001$).*

Signaling Pathways: Imidacloprid broadly suppressed all three major immune signaling cascades by down-regulating the key transcription factors *Dorsal.1*, *Relish*, and *STAT92E*. This was compounded by an up-regulation of the pathway inhibitors *Amel.CLR* and *SOCS2*. Rutin alone had a stimulatory effect, significantly enhancing the expression of *Dorsal.1* and *Relish*, while being innocuous on *STAT92E* and the inhibitors. Rut+Imid bees had reversed effects; expression of activating factors was fully restored or enhanced, while the expression of inhibitors was either normalized (*Amel.CLR*) or actively suppressed (*SOCS2*).

Immune Effectors: Downstream effector genes showed two distinct recovery patterns. The expression of genes for phagocytosis (*Nimrod.C1*), melanization (*PPO3*), and signaling (*SPZ6*, *IFN.Y*) were all suppressed Imid bees, while Rut bees exhibited no significant alterations. Rut supplementation fully restored the expression of these genes to Control bee levels. In contrast, the antimicrobial peptides *Defensin.1* and *Lys.1* were not only suppressed in Imid bees but were strongly induced in Rut bees. Consequently, their expression in Rut+Imid bees was restored to levels significantly higher than even the healthy Control bees, highlighting an enhanced humoral response.

Endocrine and Other Pathways: Imidacloprid also dysregulated key endocrine axes, disrupting juvenile hormone signaling (via *JHAMT* and *AST-A*) and suppressing the ecdysteroid synthesis gene *Phantom*. Rutin alone had no effect on *JHAMT* or *Phantom* but did up-regulate the inhibitory peptide *AST-A*. Rut+Imid bees effectively restored the expression of these genes toward Control bee levels. Notably, the expression of the antiviral

gene *Dicer.1* was unaffected by any treatment, while the cyclooxygenase (COX) gene was uniquely up-regulated only in Rut+Imid bees.

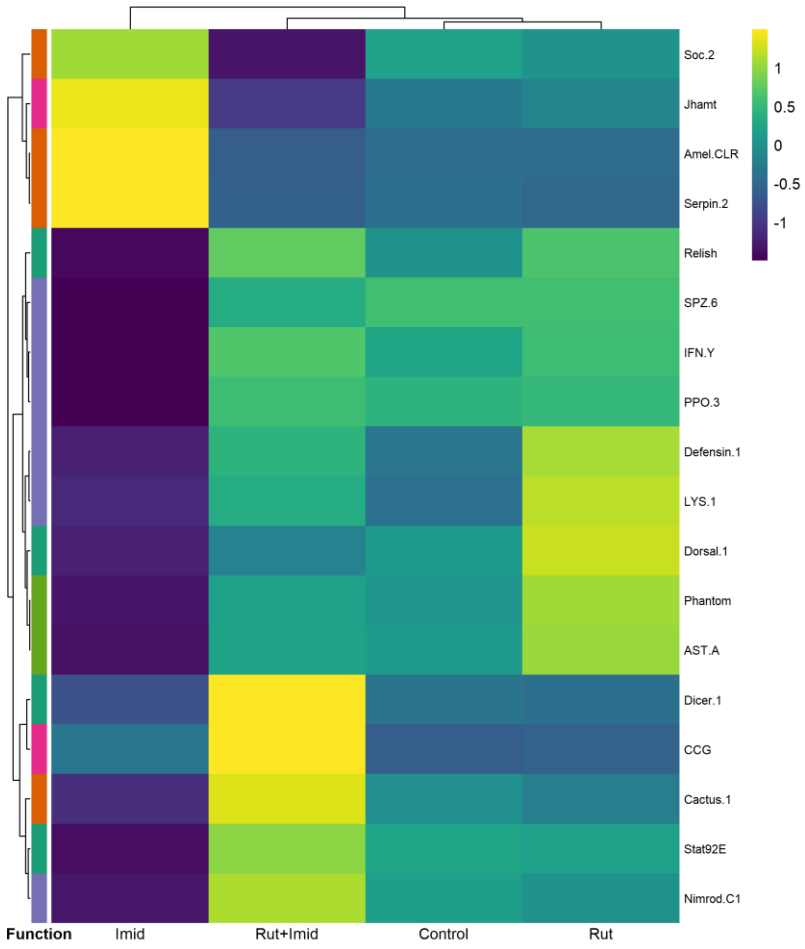

Figure 9. Heatmap of relative gene expression for immune, endocrine, and signaling pathway-related genes. The figure visually summarizes the expression patterns of 18 target genes across the four experimental groups. Both genes (rows) and treatment groups (columns) were clustered using a hierarchical algorithm based on Euclidean distance and complete linkage. The colors represent the row-scaled Z-score of the Log2(Fold Change) values, indicating how a gene's expression in a specific treatment deviates from its own average expression across all treatments. Yellow signifies higher-than-average expression, while purple signifies lower-than-average expression for that gene. The colored bar on the left indicates the functional category of each gene: **activating pathways (Dark green), inhibitory pathways (orange), immune effectors (blue), endocrine activators (pink), and endocrine inhibitors (green).** The clustering dendrograms highlight the profound and distinct impact of the Imidacloprid treatment on the overall transcriptome compared to the other groups.

Discussion

Our results provide compelling evidence that prophylactic supplementation with the flavonoid Rutin can mitigate the severe, systemic immunosuppression induced by chronic exposure to Imidacloprid in honey bees (*Apis mellifera*). Our integrated analysis demonstrates that Imidacloprid triggers a widespread collapse of bee immunity, from cellular

depletion to the dysregulation of foundational signaling pathways. Crucially, dietary Rutin not only prevented this collapse but also restored and, in some cases, enhanced key immune functions. These findings reveal clear protective mechanisms and establish Rutin as a viable, naturally-derived agent for ameliorating pesticide-induced stress in honey bees.

The Immunotoxicological Impact of Imidacloprid

The systemic immune disruption caused by Imidacloprid appears to be anchored in a direct and debilitating effect on the honey bee's cellular defenses. Our findings of severe "hemocytopenia"—a drastic reduction in both circulating and sessile immune cells—and the concomitant failure of essential functions like nodulation and encapsulation point to a primary cytotoxic or dysregulatory event. We propose this is a consequence of Imidacloprid's agonism of nicotinic acetylcholine receptors (nAChRs) expressed on bee hemocytes (Dupuis et al., 2019). This interaction may hijack an insect analogue of the mammalian cholinergic anti-inflammatory pathway, where nAChR activation normally downregulates NF-κB signaling to prevent excessive inflammation (Di Prisco et al., 2013). As a potent and persistent agonist, Imidacloprid likely forces this inhibitory switch into a chronic "on" state. This model cogently explains several of our key findings: the significant suppression of the NF-κB pathway transcription factors Dorsal and Relish at the gene expression level, the reduced levels of the Relish protein in the fat body, and the simultaneous upregulation of immunomodulators like Amel.CLR, all of which can be interpreted as molecular signatures of a deleterious, system-wide anti-inflammatory process.

This multifaceted immunosuppression is likely intensified by a state of pervasive physiological stress that alters the bee's internal environment. The induction of oxidative and energy stress is an established consequence of neonicotinoid exposure, creating a costly energy deficit that forces a trade-off against immune maintenance (Tosi et al., 2017). Our data strongly suggest such a trade-off at the endocrine level. Imidacloprid exposure generated a high-juvenile hormone (JH) and low-ecdysteroid environment, evidenced by the upregulation of the JH synthesis gene JHAMT and suppression of the ecdysteroid synthesis gene Phantom. This hormonal state is profoundly anti-inflammatory; high JH levels are classically linked to the allocation of resources away from immunity, while ecdysone is critical for promoting hemocyte proliferation (Flatt et al., 2005). By forcing the bee into a state of chronic physiological stress, Imidacloprid effectively diverts resources from the maintenance and execution of a competent immune system, providing a powerful, indirect mechanism that complements its direct attacks on immune cells and their signaling pathways.

Rutin as an Active Immunomodulator

Our initial hypothesis posited that Rutin would be innocuous, acting merely as a buffer. This was not the case. The multivariate analysis demonstrated that Rutin-supplemented bees possessed a systemic immune profile significantly distinct from Control bees, indicating that Rutin actively reshapes the bee's immunological landscape. This modulation was

predominantly stimulatory: we observed a significant increase in the total hemocyte population, an expansion of sessile reservoirs, an enhanced encapsulation response, and a potent induction of the antimicrobial peptides Defensin-1 and Lys-1. These findings align with previous reports suggesting that plant-derived flavonoids can act as immune-priming agents in insects, bolstering the standing machinery of both cellular and humoral immunity (Bors et al., 2018; Emery et al., 2021). This priming occurs without triggering a costly inflammatory state, as Rutin did not alter basal Relish levels or induce apoptosis.

While most effects were stimulatory, Rutin supplementation alone led to a significant decrease in the nodulation response. This does not necessarily imply a functional deficit. Instead, we hypothesize it reflects a strategic reallocation of immune resources. Encapsulation and nodulation rely on distinct machinery (Shrestha & Kim, 2017), and the dramatic increase in encapsulation capacity may indicate that Rutin biases cellular resources towards this defense, possibly at the expense of nodulation. This finding underscores that Rutin is a complex modulator, not a blunt instrument, that selectively sculpts a unique and resilient immune phenotype.

Immune Restoration and Resilience through Prophylactic Rutin

The most significant finding of our study was the remarkable efficacy of prophylactic Rutin in neutralizing Imidacloprid's immunotoxicity. The protective effect was comprehensive, leading to the full restoration of critical immune functions. In Rut+Imid bees, the loss of hemocytes was reversed, and the essential encapsulation and nodulation responses were restored to a capacity statistically indistinguishable from Control bees. Furthermore, Rutin completely prevented Imidacloprid-induced apoptosis in brain tissue and normalized the expression of key endocrine regulators (JHAMT, AST.A, Phantom). This suggests that the "primed" state induced by Rutin monotherapy creates a system-wide buffer against Imidacloprid's multifaceted toxicity. Delving into the molecular underpinnings, we found Rutin enabled a powerful counter-response, reversing the suppression of the immune transcription factors Dorsal, Relish, and STAT92E. This recovery was aided by active disinhibition, as the JAK/STAT pathway inhibitor SOCS2 was driven significantly below Control levels in the protected group. This combined strategy—reversing suppression and removing molecular "brakes"—creates a state of profound molecular resilience.

Finally, our results point to a novel mediator of this protective interaction. A strong upregulation of the cyclooxygenase (COX) gene was observed exclusively in Rut+Imid bees. This suggests that COX activation is not a response to either agent individually, but to the specific interaction between the flavonoid-primed immune system and the subsequent pesticide challenge. We hypothesize that the COX-prostaglandin signaling axis, a potent modulator of inflammation and homeostasis (Stanley & Kim, 2021), may be a key, yet overlooked, pathway in insect resilience to chemical stressors. This finding opens a compelling new avenue for research into the interplay between dietary flavonoids and eicosanoid signaling as a fundamental mechanism of immunoprotection in honey bees.

Conclusions, limitations, and Future Directions

Our study demonstrates that Rutin is an active immunomodulator that confers robust, multi-level protection against Imidacloprid-induced immunosuppression. Our experiments were conducted under laboratory conditions, and we did not standardize bees by age; field-level studies that account for age structure are essential to validate these findings in whole colonies. Furthermore, our study proposes mechanisms—such as the roles of the cholinergic and COX pathways—that warrant direct functional investigation. Future work should aim to causally test these hypotheses, for instance by using pharmacological inhibitors or by directly quantifying markers of oxidative stress.

Nevertheless, this study provides a powerful proof-of-concept. By priming cellular defenses, enabling a potent molecular counter-response, and engaging unique resilience pathways, Rutin supplementation emerges as a viable, naturally-derived strategy to mitigate the sublethal effects of pesticides. These findings underscore the profound potential of nutritional immunology to safeguard pollinator health and enhance the sustainability of pollination services in modern agroecosystems.

Chapter 2: Prophylactic Rutin Mitigates chronic Imidacloprid oxidative and metabolic stress in Honey Bees (*Apis mellifera*).

Sergio A. Mayorga[a,c], Yeny Acosta[c], Mónica Cala [d], Felipe Rodríguez[e], Daniel Pardo, Andre J. Riveros[a,b], Carolina Ramírez[c]

[a] *CANNON Research Group, Department of Biology, School of Science and Engineering, Universidad del Rosario, Bogotá, Colombia*

[b] *Department of Neuroscience, College of Science, University of Arizona. Tucson, Arizona. USA*

[c] *Center for Autoimmune Diseases Research (CREA), School of Medicine and Health Sciences, Universidad del Rosario. Bogotá. Colombia*

[d] *Metabolomics Core Facility-MetCore, Vicepresidency for Research, Universidad de los Andes, Bogota, Colombia*

[e] *Center for Research in Microbiology and Biotechnology – UR (CIMBIUR), School of Science and Engineering, Universidad del Rosario, Bogotá, Colombia*

Introduction

The physiological resilience of the western honey bee (*Apis mellifera*) is fundamental to its role as the world's primary managed pollinator and is under constant threat from a gauntlet of environmental stressors (3,50). While pathogens and nutritional deficits are significant contributors to colony losses, the sublethal effects of systemic agrochemicals represent a continuous challenge to bee health. These xenobiotics can disrupt organismal homeostasis, imposing a substantial energy and oxidative cost that compromises survival and colony-level performance (51). Understanding the precise mechanisms of pesticide-induced physiological stress is therefore a critical prerequisite for developing effective mitigation strategies.

Imidacloprid, a neonicotinoid insecticide, is frequently implicated in bee health decline due to its widespread use and systemic nature, which leads to chronic exposure through contaminated nectar and pollen (52). Beyond its neurotoxic mode of action, Imidacloprid is a potent disruptor of core metabolic and cellular processes. Its metabolism through detoxification pathways, can inadvertently generate an overabundance of ROS/RNS (53,54). This surge in oxidants can overwhelm the insect's endogenous antioxidant defenses leading to a state of constant oxidative stress. This imbalance results in widespread molecular damage to lipids, proteins, and nucleic acids, impairing cellular function (55).

The induction of oxidative stress is intrinsically linked to energy metabolism, as mitochondria are both the primary site of ATP production and a major source of endogenous ROS (56). Pesticide-induced mitochondrial dysfunction not only amplifies ROS production but also cripples the energy capacity of bees. An energy deficit can cascade into failures of thermoregulation, foraging, and survival, directly linking xenobiotic exposure to individual and colony fitness (57).

Nutritional supplementation with bioactive phytochemicals offers a promising approach to bolster bee resilience against such physiological challenges. Flavonoids, a class of plant-derived polyphenols, are potent antioxidants renowned for their capacity to mitigate oxidative stress (11). Rutin, a common glycosylated flavonoid, induces robust antioxidant responses and improves mitochondrial health (58–60). However, the extent to which prophylactic Rutin supplementation can specifically counteract the complex oxidative and metabolic dysregulation induced by Imidacloprid in *A. mellifera* has not been fully elucidated.

This study aimed to systematically evaluate the protective effects of prophylactic Rutin administration against Imidacloprid-induced oxidative and energy stress in honey bees. We posited that: **(1)** Chronic sublethal exposure to Imidacloprid would disrupt metabolic homeostasis, decrease survival, and induce severe oxidative stress, evidenced by elevated ROS/RNS levels, depletion of energy reserves, and impairment of mitochondrial function. **(2)** Rutin supplementation alone would enhance the basal antioxidant capacity and improve the metabolic state of the bees. **(3)** Prophylactic administration of Rutin would significantly attenuate Imidacloprid-induced mortality and physiological damage by preserving antioxidant defenses and maintaining mitochondrial and metabolic integrity. To address these hypotheses, we employed a multi-level approach, integrating analyses of survival, organism-level physiology, enzymatic activity, targeted gene expression, and metabolomics to provide a comprehensive portrait of Rutin's protective action.

Methods

1. Sample Collection

On the morning following the final day of chronic exposure, we collected bees for downstream assays. For most assays, five biological replicates (each a pool of 12 bees) were established per treatment (total N=240 bees). For metabolomics and enzymatic activity assays, three biological replicates (each a single bee) were used per treatment (total N=12 bees).

2. Physiological and Enzymatic Assays

Survival Analysis: We monitored bees following the chronic exposure period. Bees were housed in cages within an incubator at 34.5°C and 60% and were provided with 1M sucrose solution *ad libitum*. Survival was monitored daily for six days, and any dead individuals were counted and removed each day.

Body Mass Measurement: We measured the fresh body mass of each bee at the end of the treatment period using an analytical balance. Bees exhibiting body damage or excess condensation were excluded from the analysis.

Total fat body Lipids Quantification: We dissected, pooled, and lyophilized the fat bodies of bees. Total lipids were extracted using a modified Folch method and quantified

colorimetrically using the sulfo-phospho-vanillin method (61,62). Absorbance was measured at 546 nm. Lipid concentration was calculated against a standard curve using oleic acid (5-35 µg). Concentration was expressed as µg of total lipid per mg of dry fat body tissue.

Hemolymph Glucose Quantification: We quantified total glucose levels in the hemolymph using the Anthrone colorimetric assay (63). We used 10 µL of the hemolymph-PBS suspension and mixed it with freshly prepared Anthrone reagent (64). After incubation, absorbance was measured at 625 nm. Glucose concentrations were calculated against a standard curve (20-200 µg/mL).

Total Reactive Oxygen and Nitrogen Species (ROS/RNS) Quantification: We homogenized hole dry bees with a mortar and washed them in 1X PBS. Total ROS/RNS were quantified using the OxiSelect™ In Vitro ROS/RNS Assay Kit (Cell Biolabs, Inc.). Supernatants from homogenized bees were incubated with a dichlorodihydrofluorescein (DCFH) probe. Fluorescence intensity (Ex: 480 nm, Em: 530 nm) was recorded using a Varioskan™ LUX microplate reader (Thermo Fisher Scientific)., USA). Results were normalized to total protein content, determined via a BCA Assay Kit (ThermoFisher, USA), and expressed as nmol DCF/mg protein. ROS/RNS concentrations were calculated against a standard curve using H_2O_2.

Ferrous Iron (Fe^{2+}) Quantification: We quantified Ferrous iron in whole-body homogenates using a commercial Iron Assay Kit (Sigma-Aldrich, Cat# MAK025). Briefly, supernatants from homogenized bees were incubated with an Iron Probe, and absorbance was measured at 593 nm. Results were normalized to total protein content and expressed as Fe^{2+}/mg protein. Fe^{2+} concentrations were calculated against a standard curve using the provided Fe^{2+} standard (8-35 nmol/mL).

Enzymatic Activity Assays: We quantified the activity of key antioxidant, detoxification, and metabolic enzymes in specific bee tissues (Table 6). Samples were dissected, pooled, and homogenized in an appropriate ice-cold buffer (100 mM potassium phosphate, pH 7.2, with 1X protease inhibitors). The homogenate was centrifuged (10,000 x g for 15 min at 4°C) to obtain a clear supernatant (enzymatic extract), and the total protein concentration of each extract was determined using a BCA assay to normalize enzyme activity.

Table 6. Overview of enzymatic assays, their biological function, and tissue of origin.

Enzymes	Function	Sample
Catalases (CATs)	Antioxidant	Thorax
Superoxide Dismutases (SODs)	Antioxidant	Hemolymph
Glutathione S-transferase (GSTs)	Detoxification	Midgut
Cytochrome P450 Monooxygenases (CYP450s)	Detoxification	Midgut
Citrate Synthase (CS)	Metabolic	Head
Succinate Dehydrogenase (SDH)	Metabolic	Head

We measured *CATs* activity in thorax extracts by monitoring the decomposition of hydrogen peroxide (H_2O_2) at 230 nm. The reaction was initiated by adding 200 µL of 10 mM H_2O_2 to a mixture of 35 µL of the enzymatic extract and 1.8 mL of 50 mM potassium phosphate buffer (pH 7.2). Activity units (U) were expressed as nmol of H_2O_2 decomposed per minute per mg of protein.

SODs activity was measured in hemolymph samples using a SOD Activity Assay Kit (Sigma-Aldrich, Cat# CS0009) according to the manufacturer's instructions. The assay measures the inhibition of the reduction of a colorimetric probe by superoxide anions generated via xanthine oxidase, with absorbance read at 450 nm. Activity units (U) were expressed as U per mg protein.

We measured *GSTs* activity in midgut extracts using a GST Assay Kit (Sigma-Aldrich, Cat# MAK453). The assay measures the formation of a GS-CDNB conjugate via an increase in absorbance at 340 nm. Activity units (U) were expressed as mmol of product formed per minute per mg of protein.

CYP450s activity was measured in midgut extracts using a fluorometric assay adapted from (65,66). The reaction mixture contained 50 µL of enzymatic extract, 0.4 mM 7-Ethoxycoumarin (7-EC), and 1 mM β-NADPH in a sodium phosphate buffer (0.1 M, pH 7.2). After a 30-min incubation at 30°C, the reaction was stopped with 15% TCA. The fluorescence of the product, 7-hydroxycoumarin, was measured (Ex: 360 nm, Em: 460 nm). Activity units (U) were expressed as nmol of 7-hydroxycoumarin produced per minute per mg of protein.

CS activity was measured in head extracts by monitoring the reaction of Coenzyme A with DTNB, which produces TNB, causing an increase in absorbance at 412 nm (67). The reaction was initiated with oxaloacetate in the presence of the sample, acetyl-CoA, and DTNB. Activity units (U) were calculated using the molar extinction coefficient for TNB (13.6 $mM^{-1}cm^{-1}$) and expressed as U per mg protein.

SDH activity was measured in head extracts by monitoring the succinate-dependent reduction of DCPIP at 600 nm (68). The reaction was performed in the presence of rotenone and antimycin A to ensure specificity. Activity units (U) were calculated using the molar extinction coefficient for DCPIP (21 $mM^{-1}cm^{-1}$) and expressed as U per mg protein.

3. Untargeted Metabolomic and Lipidomic Analysis

Sample Preparation and Extraction: For the analysis of polar metabolites, protein precipitation was performed. A 100 µL aliquot of the previously prepared whole-bee supernatant was mixed with 300 µL of cold methanol (-20 °C), vortexed for 3 min, and incubated at -20 °C for 5 min. Samples were then centrifuged (14,000 x g for 10 min at 4°C). The resulting supernatant was collected for UPLC-MS analysis. For lipid analysis, a separate extraction was performed using a methyl-tert-butyl ether (MTBE) protocol. A 50 µL aliquot

of the whole-bee supernatant was mixed with 175 µL of cold methanol and 175 µL of MTBE. The mixture was vortexed for 5 min and centrifuged (RCF, e.g., 14,000 x g for 10 min at RT). The upper, non-polar phase containing the lipids was collected for lipidomic analysis.

Liquid Chromatography-Mass Spectrometry (LC-MS): All analyses were performed on a system composed of an Agilent 1260 Infinity UHPLC coupled to an Agilent Q-TOF-MS (Agilent Technologies, Waldbronn, Germany).

Reversed-Phase Gas (RPG) Chromatography: An aliquot (5 µL) of the polar extract was injected onto an InfinityLab Poroshell 120 EC-C18 column (2.1 × 150 mm, 2.7 µm; Agilent) maintained at 40 °C. Metabolites were separated using a gradient of mobile phase A (water with 0.1% formic acid) and B (acetonitrile with 0.1% formic acid) at a flow rate of 0.3 mL/min. The gradient ran from 25% to 95% B over 35 min. MS data was acquired from 100 to 1,100 m/z in both positive (ESI+) and negative (ESI−) ionization modes.

Hydrophilic Interaction Liquid Chromatography (HILIC): An aliquot (5 µL) of the polar extract was injected onto an AdvanceBio MS Spent Media column (2.1 × 150 mm, 2.7 µm; Agilent) at 40 °C. Separation was achieved using a gradient of mobile phase A (10 mM ammonium acetate in 50% acetonitrile) and B (10 mM ammonium acetate in 95:5 acetonitrile:water) at a flow rate of 0.5 mL/min. The gradient ran from 1% to 50% B over 15 min.

Reversed-Phase (RP) Chromatography (Lipidomics): An aliquot (5 µL) of the lipid extract was injected onto an InfinityLab Poroshell 120 EC-C8 column (2.1 × 150 mm, 2.7 µm; Agilent) at 60 °C. Lipids were separated using a gradient of mobile phase A (10 mM ammonium formate in water) and B (10 mM ammonium formate in 80:20 methanol: isopropanol) at a flow rate of 0.5 mL/min. MS data was acquired from 100 to 1,800 m/z in positive ionization mode (ESI+).

Data Processing and Metabolite Identification: Raw LC-MS data were processed using Agilent MassHunter Profinder software (vB.08.0) for feature detection, alignment, and integration. The resulting feature list was manually curated to remove background noise and unrelated ions. Features were then filtered, retaining only those present in 100% of samples in at least one experimental group and with a coefficient of variation (CV) < 20% in the Quality Control (QC) samples.

Metabolite identification was performed by searching the accurate masses of significant features against public databases (HMDB, KEGG, LIPID MAPS, METLIN) using the CEU Mass Mediator tool. Putative identifications were confirmed via LC-MS/MS analysis to match fragmentation patterns.

Quality Control and Statistical Analysis: QC samples, prepared by pooling equal volumes of each sample extract, were injected every five samples to monitor analytical stability and reproducibility.

Untargeted Profiling and Feature Selection: We performed an initial processing of the complete, untargeted dataset to identify all metabolites significantly affected by the treatments. The log-transformed and Pareto-scaled data matrix was analyzed using SIMCA and MATLAB. For preliminary statistical analysis, data were log-transformed and Pareto-scaled. We first applied an unsupervised PCA to visualize data quality and the clustering of QC samples. To identify significantly altered metabolites (Table 7), a multi-criteria approach was used, combining results from univariate and multivariate analyses performed in SIMCA and MATLAB. A metabolite was considered significant if it simultaneously met the following three criteria:

1. Univariate Test: An adjusted p-value (FDR) < 0.05 from either a Student's t-test or Mann-Whitney U test.
2. Multivariate Model: A Variable Importance in Projection (VIP) score > 2.0 from an Orthogonal Partial Least Squares-Discriminant Analysis (OPLS-DA) model.
3. Magnitude of Change: A Fold Change > 1.5 (upregulated) or < 0.67 (downregulated).

Table 7. Overview of selected targeted metabolites and their putative biological functions.

Metabolite	Function	Molecular type
13-Hydroperoxy-octadecadienoic acid (HPODE)	Oxidative damage	Fatty Acid
Oxo-hydroxy-octadecenoic acid (OXOC)	Oxidative damage	Fatty Acid
Riboflavin (VB2)	Protection against oxidative stress	Nucleotide or Nucleoside
Glutamic acid (GA)	Protection against oxidative stress	Amino Acid
Adenosine monophosphate (AMP)	Energy stress	Nucleotide or Nucleoside
Hypoxanthine (HYPX)	Energy stress	Nucleotide or Nucleoside
Inosine (INO)	Resistance to energy stress	Nucleotide or Nucleoside
Pantothenate (VB5)	Resistance to energy stress	Carboxylic Acid
Undecanoylcarnitine (UCC)	Mitochondrial function	Fatty Acid
Citric acid (CA)	Mitochondrial function	Carboxylic acids and derivatives

4. Gene Expression Analysis (RT-qPCR)

RNA Isolation, Quality Control, and cDNA Synthesis: Total RNA was extracted from individual whole bees (N=4 per treatment) using TRIZOL™ reagent (Invitrogen™, Cat# 15596026) followed by RNeasy Mini Kit purification (Qiagen, Cat# 74106). RNA integrity and purity were verified by agarose gel electrophoresis and NanoDrop™ One spectrophotometry (Thermo Fisher Scientific). First-strand cDNA was synthesized from 500 ng of total RNA using the iScript™ Advanced cDNA Synthesis Kit (Bio-Rad, Cat# 1725038).

Quantitative Real-Time PCR: qPCR was performed using a Bio-Rad CFX96 Touch Real-Time PCR Detection System. Primer pairs (Table 8) were designed using Primer-BLAST.

Primer specificity and efficiency were validated via melt curve analysis and standard curve analysis, respectively. Each 15 µL reaction contained KiCqStart™ SYBR® Green qPCR ReadyMix™ (Sigma-Aldrich, Cat# KCQS02), 250 nM of each primer, and 13 ng of template cDNA. The thermal cycling protocol was 95°C for 2 min; followed by 40 cycles of 95°C for 5 sec and 60°C for 30 sec (data acquisition); followed by a melt curve analysis.

Table 8. Selected Housekeeping and metabolic and antioxidant-related genes, primers sequences, and reaction efficiencies.

Gene	Function	Accession no.	Forward primer (5' - 3')	Reverse primer (5' - 3')	Eff. (%)
CYP9Q3	Detoxification	NM_001011590	GGCGAATGGTTCCAAAGATAAG	TTCCCATTGCCGATAGTT	99
GSTS1	Detoxification	NM_001011593	TCGGTGATTCCACTCTTGGTT	GTCTTGTTGCCCTTTTTGA	100.8
TRXR1	Antioxidant Response	NM_001177651	TGCTTGAGCGTGGTTATTGG	AACCACGATCCACCAGAAAG	97.2
Ferritin	Antioxidant Response	NM_001040283	TGGCTGAACAAAGAGACCATT	CTTTGGCGATCTTCTTCCA	95.3
AMPKα	Energy stress	NM_001190740	TGGAGCATCTTCCACGAGTAT	CCAGTTTGTTCCAGTCGTC	99.7
ILP1	Energy stress	NM_001011580	CGCGCTAAATTCGAGGAACT	TGGACGGCTGACTTTAATGG	99.3
PGC-1α	Mitochondrial Biogenesis	NM_001190741	GGAGAACGAGTTCCGAAAGG	CCGATGTTGTCGTACTTGGA	98.2
TFAM	Mitochondrial Biogenesis	NM_001177655	CAGGAGCCGAAAGAGTTTGAAG	TTTCTCCGCCATCTTCCT	97.9
ATP5A	Mitochondrial Function	NM_001011571	CACCAAGCCTATGGCTCAGTG	CTTCACCAGCCATTAGAGG	99.3
SDHA	Mitochondrial Function	NM_001011572	TGGTGGAAGGTACGCAAAATG	CTGAGCTTCACCACGATAC	96.4
RPS5	Reference gene	NM_001011568	AATTATTTGGTCGCTGGAATG	CTTGGACTTGCCTCTAAAT	101.0
RPS18	Reference gene	NM_001014389	ATGGACGTCGATGGATAGTGT	GAACCGGCTAGGTAGAAGG	97.4
Actin	Reference gene	NM_001177653	TGCCAACACTGTCCTTTCTGAG	AATTGACCCACCAATCCA	100.2

5. Statistical analyses

All statistical analyses were conducted in R (v4.4.1) using the RStudio environment (48,49). We employed a five-tiered analytical strategy (including the metabolomic analysis previously explained).

First, for the **survival analysis**, differences in bee survival were visualized using Kaplan-Meier survival curves and tested using a Log-Rank test. Significant results were followed by

pairwise Log-Rank tests with p-value adjustment using the Holm-Bonferroni method. To quantify the magnitude of the effect, a Cox Proportional Hazards (CPH) model was used to estimate the Hazard Ratios (HR) for each treatment relative to the Control group. The proportional hazards assumption of the CPH model was verified prior to analysis.

Second, we performed a **multivariate analysis** to obtain general "stress profiles". Z-score standardized data from five core variables related to oxidative and energy stress (*Body Mass Measurement, Total Lipid Quantification, Hemolymph Glucose Quantification, Total Reactive Oxygen and Nitrogen Species (ROS/RNS) Quantification, Ferrous Iron (Fe^{2+}) Quantification*) were visualized with Principal Component Analysis (PCA). Differences were tested using PERMANOVA (9,999 permutations), followed by pairwise PERMANOVA (Bonferroni adjustment) and SIMPER analysis.

Third, we performed **univariate analyses** of all the measured enzyme activities an metabolic and oxidative parameters. We assessed normality of residuals (Shapiro-Wilk test) and homogeneity of variances (Levene's test). If assumptions were met, we performed a one-way ANOVA. If violated, we used the Kruskal-Wallis test. Significant omnibus tests were followed by pairwise t-tests (for ANOVA) or Dunn's test (for Kruskal-Wallis), with p-values adjusted using the Holm-Bonferroni method. We also calculated Effect sizes (η^2, Cohen's *d*).

Fourth, we analyzed **significant metabolites data**. From the list of significant metabolites, a subset of key metabolites associated with oxidative stress and metabolism was selected for final analysis and visualization. The log-transformed abundance data for this subset was analyzed using pairwise comparisons. To be reported as significantly altered between any two groups, a metabolite was required to meet three criteria simultaneously: (1) VIP score > 1.0 from the PLS-DA model; (2) FDR-adjusted p-value < 0.05 from a Student's t-Test; and (3) Fold Change > 1.5 (upregulated) or < 0.67 (downregulated). The results were visualized using a heatmap displaying the mean Log2(Fold Change) across all groups relative to the Control. adjusted using the Holm-Bonferroni method. We also calculated Effect sizes (η^2, Cohen's *d*).

Fifth, for **gene expression analysis**, the Ct value of each target gene was normalized against the geometric mean of three stable housekeeping genes (PRS5, RPS18, and ACTIN) to obtain ΔCt values. These ΔCt values were then analyzed using the same univariate workflow. For visualization, fold-change values were calculated using the $2^{-}\Delta\Delta$Ct method.

Results

Rutin Protects Bees from Imidacloprid-Induced Mortality

Chronic exposure to the different treatments had a significant effect on honey bee survival ($\chi^2(3) = 124$, $p < .001$; Figure 10). As expected, Imidacloprid exposure was extremely detrimental, drastically reducing bee longevity and increasing the mortality risk by 8-fold compared to Control bees (HR = 8.01, $p < .001$). In contrast, prophylactic administration of

Rutin alone had a modest beneficial effect, significantly reducing the mortality risk by 40% (HR = 0.61, $p = .021$).

Most importantly, Rutin supplementation offered significant protection against the pesticide. Rut+Imid bees exhibited vastly improved survival compared to Imid bees ($p < .001$). The mortality risk for Rut+Imid bees remained unchanged relative to Control bees ($p = .122$).

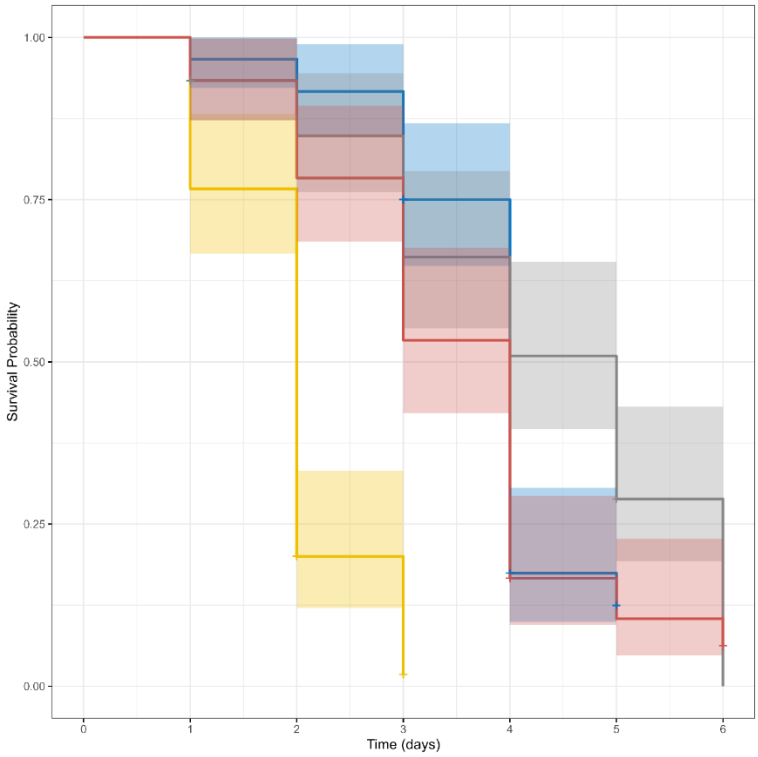

Figure 10. Kaplan-Meier survival curves of honey bees exposed to Imidacloprid and Rutin. The plot illustrates the probability of bee survival over the six-day experimental period. Lines represent the estimated survival probability for each treatment group, and the surrounding shaded areas denote the 95% confidence intervals. Each color represents a different treatment: Blue = Control, Yellow = Imid, Gray = Rut, Red = Rut+Imid. Curves were compared using a Log-rank test, which showed a significant overall effect of the treatments on bee longevity.

Imidacloprid Induces a Systemic Metabolic Stress Signature

To determine if treatments induced a systemic shift in the bees' physiological state, we performed a multivariate analysis on five core variables related to oxidative and energy stress. The PCA revealed a strong separation of treatment bees, primarily along the first principal component (PC1), which alone accounted for 83.6% of the total variance (Figure 11). Imid bees were segregated from the Control, Rut, and Rut+Imid bees, suggesting more significant effects of the pesticide on bee´s physiology. The variable loading vectors indicated this separation was primarily driven by higher levels of **ROS/RNS** and **Ferrous Iron**, which characterized Imidacloprid-exposed bees.

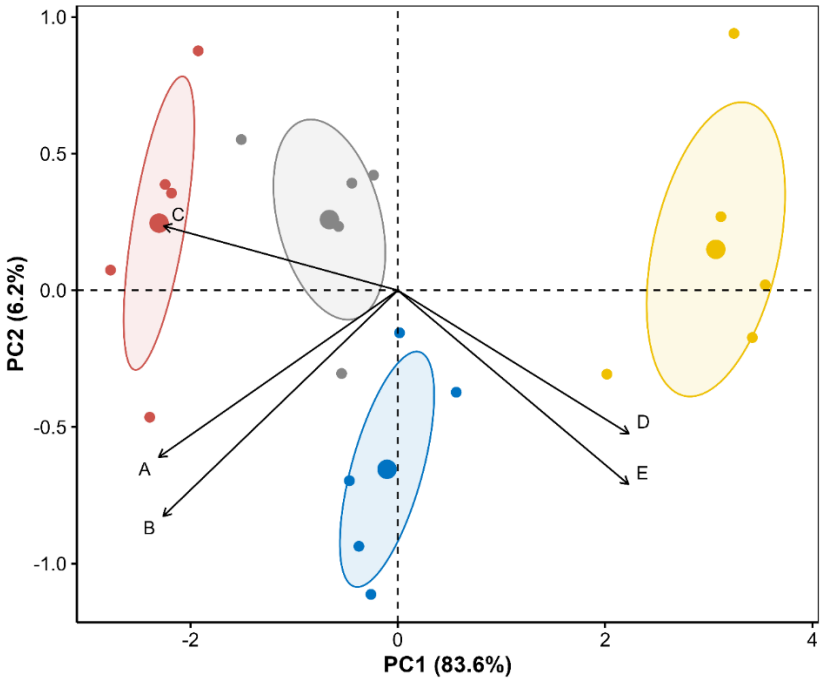

Figure 11. Principal Component Analysis (PCA) of the systemic physiological changes of bees across treatment groups. The plot visualizes the separation of treatment groups based on five core variables related to oxidative and energy stress. (**A.** Body mass; **B.** Fat body total Lipids; **C.** Hemolymph Glucose levels; **D.** Total ROS/RNS; **E.** Total Ferrous Iron). The first two principal components (PC1 and PC2) are displayed, accounting for 83.6% and 6.2% of the total variance, respectively. Each point represents a biological replicate (n=12), with colors corresponding to the treatment groups: **Control** (blue), **Imid** (yellow), **Rut** (red), and **Rut+Imid** (grey). Ellipses represent the 95% confidence interval for each group's centroid. Vectors indicate the loading and direction of the variables. The clear separation along PC1 demonstrates a strong, systemic effect of Imidacloprid and the mitigating effect of Rutin supplementation.

The PERMANOVA confirmed a significant overall effect of treatment on the bee physiological profiles ($F_{(3,16)} = 29.59$, $R^2 = 0.85$, $p < .001$). Interestingly, our post-hoc pairwise comparisons revealed that the profiles of all treatment bees were significantly different from one another (all $p = .03$). To identify the specific parameters driving these significant differences, we performed a SIMPER analysis (Table 9).

Table 9. Contribution of physiological parameters to the dissimilarity between treatment groups.

Control vs Imid		Control vs Rut		Control vs Rut+Imid		Imid vs Rut+Imid	
Total Lipids	0,29	*ROS/RNS*	0,49	*Ferrous Iron*	0,36	*ROS/RNS*	0,32
ROS/RNS	0,29	*Ferrous Iron*	0,23	*ROS/RNS*	0,31	*Ferrous Iron*	0,29
Ferrous Iron	0,19	*Total Lipids*	0,13	*Total Lipids*	0,17	*Total Lipids*	0,20
Body mass	0,14	*Hem. Glucose*	0,11	*Hem. Glucose*	0,09	*Body mass*	0,10
Hem. Glucose	0,09	*Body mass*	0,04	*Body mass*	0,06	*Hem. Glucose*	0,09

Values represent the proportional contribution of each parameter to the average Bray-Curtis dissimilarity between pairs of treatment groups, as determined by SIMPER analysis. For each comparison, variables are listed in descending order of their contribution.

Rutin Mitigates Imidacloprid-Induced Oxidative and Metabolic Stress

The treatments had significant effects on the overall metabolic and oxidative state of bees (Table 10). Imidacloprid exposure was detrimental to bees, causing a significant reduction in Body Mass, as well as a depletion of fat body Lipid reserves and hemolymph Glucose levels compared to Control bees. In contrast, Rut supplementation alone acted as a metabolic booster, significantly increasing lipid and glucose levels. Rut+Imid bees presented complete protection for these parameters, fully restoring body mass, lipid, and glucose levels to levels indistinguishable from healthy Control bees.

Furthermore, Imid bees had severe oxidative stress, evidenced by a significant increase in both ROS/RNS and systemic Ferrous Iron. Rutin demonstrated potent protective properties, acting as an antioxidant that decreased baseline ROS and as a probable chelating agent that significantly lowered ferrous iron levels. In Rut+Imid bees, Rutin's protective effects were clear. It completely normalized the ROS levels back to those of Control bees. For ferrous iron, it drastically reduced the high levels caused by Imidacloprid, bringing them down to a new baseline significantly lower than that of Control bees, mirroring the effect of Rutin alone.

Table 10. Effects of Imidacloprid and Rutin on Physiological and Metabolic Parameters.

Parameter	Control	Imid	Rut	Rut+Imid	Overall Test
Body Mass (mg)	128.01 ± 4.93 a	98.19 ± 6.77 b***	132.91 ± 7.11 a	125.26 ± 6.18 a***	$F(3,16) = 30.60$, $p < .001$, $\eta^2 = 0.852$
Lipids (µg/mg)	19.04 ± 3.33 b	10.75 ± 1.84 c***	23.48 ± 2.50 a*	17.57 ± 1.89 b**	$F(3,16) = 22.93$, $p < .001$, $\eta^2 = 0.811$
Glucose (µg/µL)	120.15 ± 11.50 b	100.73 ± 7.91 c**	143.81 ± 8.00 a**	124.74 ± 3.57 b**	$F(3,16) = 23.04$, $p < .001$, $\eta^2 = 0.812$
ROS (nmol/mg)	1.17 ± 0.17 a	2.06 ± 0.15 b***	0.51 ± 0.16 c***	0.96 ± 0.27 a***	$F(3,16) = 57.24$, $p < .001$, $\eta^2 = 0.915$
Ferrous Iron (Fe^{2+}/mg)	170.05 ± 15.27 b	248.36 ± 36.89 a***	111.99 ± 14.12 c**	121.96 ± 14.46 c***	$F(3,16) = 38.71$, $p < .001$, $\eta^2 = 0.879$

Values are presented as Mean ± SD. Within a row, means not sharing a superscript letter (a, b, c) are significantly different based on post-hoc tests with Bonferroni correction ($p < .001$). Asterisks represent the significance level of the comparison against the Control group (for Imid and Rut columns) or against the Imid group (for the Rut+Imid column) ($p < 0.05$, ** $p < 0.01$, *** $p < 0.001$).**

Rutin Boosts Detoxification and Antioxidant Enzyme Activity

We found that the treatments significantly altered the activity of core enzymatic systems involved in detoxification, antioxidant defense, and energy metabolism (Figure 12, Table 11).

Table 11. Effects of Imidacloprid and Rutin on Key Enzymatic Activities.

Enzyme	Control	Imid	Rut	Rut+Imid	Overall Test
GSTs	64.82 ± 6.81 b	27.51 ± 6.80 c**	106.30 ± 14.47 a**	85.74 ± 10.95 b***	$F(3,8) = 32.17$, $p < .001$, $\eta^2 = 0.923$
CYP450s	156.63 ± 9.24 c	104.69 ± 11.42 d*	193.12 ± 18.12 b*	239.38 ± 27.73 a***	$F(3,8) = 29.69$, $p < .001$, $\eta^2 = 0.918$
CATs	677.23 ± 47.13 b	510.83 ± 37.39 c**	672.51 ± 39.26 b	785.07 ± 50.15 a***	$F(3,8) = 19.98$, $p < .001$, $\eta^2 = 0.882$
SODs	44.17 ± 9.69 a	13.09 ± 5.71 c*	32.88 ± 8.36 b	61.82 ± 14.59 a**	$F(3,8) = 12.24$, $p = .002$, $\eta^2 = 0.821$
CS	58.38 ± 5.43 b	25.07 ± 9.36 c*	85.51 ± 15.19 a*	85.00 ± 8.90 a***	$F(3,8) = 22.94$, $p < .001$, $\eta^2 = 0.896$
SDH	82.66 ± 6.32 a	64.53 ± 15.13 a	83.65 ± 7.46 a	82.34 ± 4.32 a	$F(3,8) = 2.96$, $p = .098$, $\eta^2 = 0.526$

Values are presented as Mean ± SD. Within a row, means not sharing a superscript letter (a, b, c, d) are significantly different based on post-hoc tests with Bonferroni correction ($p < .05$). Asterisks represent the significance level of the comparison against the Control group (for Imid and Rut columns) or against the Imid group (for the Rut+Imid column) ($p < 0.05$, ** $p < 0.01$, *** $p < 0.001$).*

Detoxification System: Imidacloprid exposure suppressed the activity of both Glutathione S-transferases (GSTs) and Cytochrome P450 monooxygenases (CYP450s). In contrast, Rutin supplementation alone significantly enhanced the activity of both enzyme families. In Rut+Imid bees, this resulted in a full restoration of GST activity to Control bee levels, while CYP450 activity was stimulated to levels significantly higher than Control bees.

Antioxidant System: Imidacloprid also suppressed the primary antioxidant enzymes, Catalase (CATs) and Superoxide dismutase (SODs). Rutin alone had no significant baseline effect on the activity of these enzymes. However, in Rut+Imid bees we observed a hyper-stimulatory response in Catalase activity and a fully restored SOD activity to Control bee levels.

Energy Metabolism: The activity of the key mitochondrial enzyme Citrate Synthase (CS) was significantly suppressed in Imid bees, whereas Rutin alone boosted its activity. In Rut+Imid bees we observed a significant recovery, elevating CS activity to a level even higher than that of Control bees. In contrast, the activity of Succinate Dehydrogenase (SDH) was not significantly affected by any treatment.

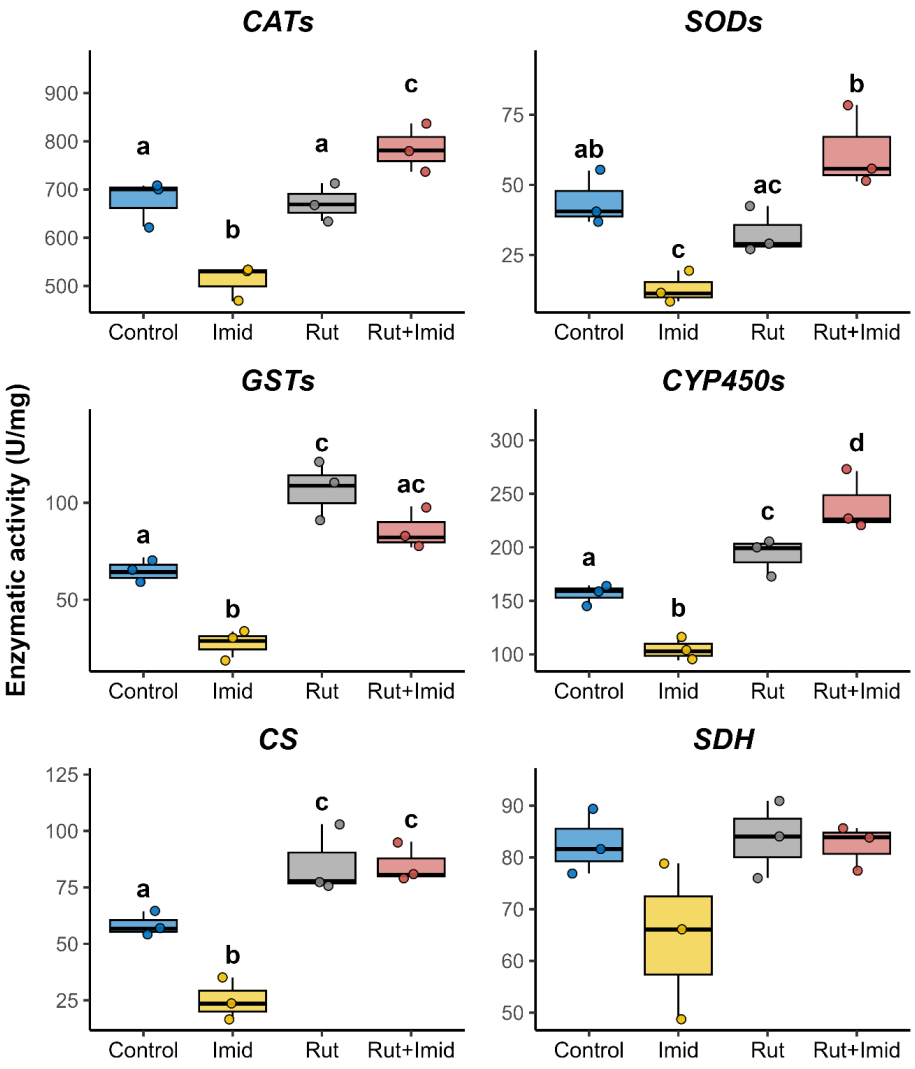

Figure 12. Effects of Imidacloprid and Rutin on Key Enzymatic Activities. The figure displays the activity (U/mg) of enzymes involved in antioxidant defense (Catalase, CATs; Superoxide Dismutase, SODs), detoxification (Glutathione S-transferases, GSTs; Cytochrome P450s, CYP450s), and energy metabolism (Citrate Synthase, CS; Succinate Dehydrogenase, SDH). Each panel shows boxplots; individual points represent biological replicates. Different letters (a, b, c, d) above the boxplots indicate statistically significant differences between groups as determined by post-hoc tests ($p < .05$).

Rutin Reverses Metabolic Signatures of Oxidative Damage and Mitochondrial Dysfunction

To investigate the metabolic underpinnings of the physiological changes observed, we analyzed a curated set of metabolites involved in oxidative stress, energy metabolism, and mitochondrial function (Table 12, Figure 13).

Table 12. Relative abundance of key metabolites between treatment groups.

Metabolite	Function / Marker	Control vs Imid	Control vs Rut	Imid vs Rut+Imid
HPODE	Oxidative Damage	**1.35** ↑**	-0.84 ↓*	**-1.46** ↓**
OXOC	Oxidative Damage	**0.94** ↑*	**-1.81** ↓**	**-0.75** ↓*
VB2	Protection against oxidative stress	-1.68 ↓**	**0.54** ↑*	0.95 ↑*
GA	Protection against oxidative stress	-0.79 ↓*	-0.29 *ns*	1.02 ↑**
AMP	Energy stress	**1.14** ↑**	-0.21 *ns*	-0.64 ↓*
HYPX	Energy stress	1.23 ↑**	-0.19 *ns*	**-0.87** ↓*
UCC	Mitochondrial function	-1.65 ↓**	**1.28** ↑**	**2.6** ↑***
CA	Mitochondrial function	**-0.65** ↓*	**1.14** ↑**	**0.79** ↑*
INO	Resistance to energy stress	**-1.38** ↓**	-0.16 *ns*	**2.11** ↑***
VB5	Resistance to energy stress	-1.31 ↓**	0.43 ↑	**0.51** ↑*

*Values are presented as Log_2 Fold-Change. Within a row, values in **bold** indicate significant VIP scores (>1). Asterisks represent significance levels (* $p < 0.05$, ** $p < 0.01$, *** $p < 0.001$). Arrows indicate overexpression (↑) or under expression (↓). "ns" indicates no significant change.*

Oxidative Stress and Protection: Imidacloprid exposure induced a clear signature of oxidative stress in bees, significantly increasing markers of lipid peroxidation (HPODE) and oxidative damage (OXOC), while depleting protective metabolites like vitamin B2 (VB2) and gallic acid (GA). Rutin alone promoted an antioxidant state in bees, decreasing OXOC and increasing VB2. Rut+Imid bees effectively reversed the oxidative damage and significantly boosted the levels of protective metabolites.

Energy Stress and Mitochondrial Function: We observed a concurrent disruption of energy metabolism. Imidacloprid increased markers of energy stress (AMP, HYPX) and depleted key metabolites for mitochondrial function (UCC, CA) and stress resistance (INO, VB5) in bees. Rutin alone enhanced metabolites associated with mitochondrial function (UCC, CA). Rut+Imid bees fully counteracted this disruption, reducing the energy stress markers and significantly restoring or enhancing the metabolites crucial for mitochondrial function and stress resistance.

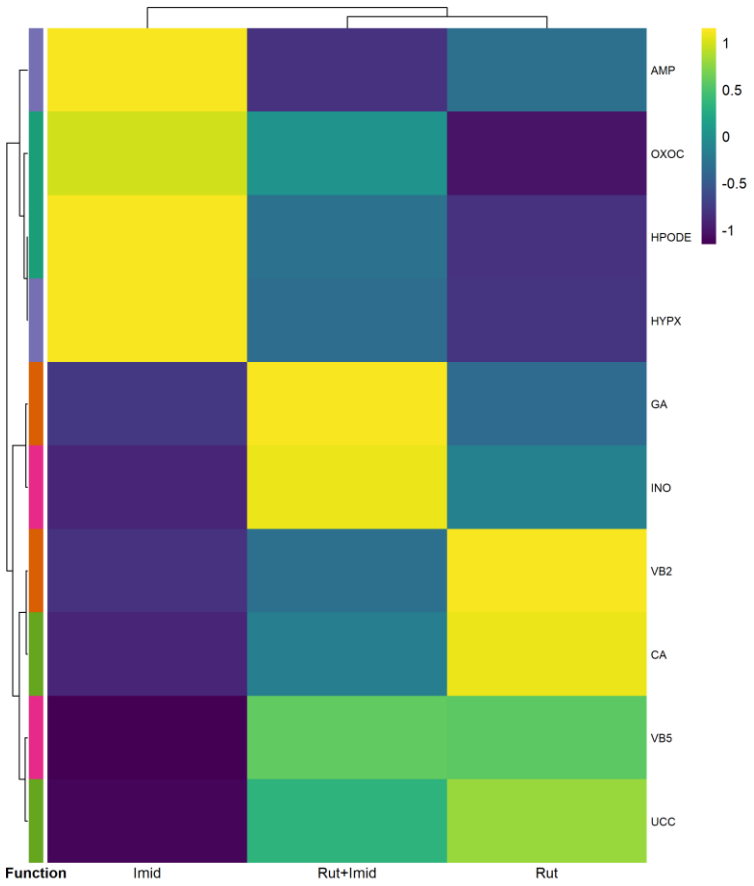

Figure 13. Heatmap of relative metabolite abundance across treatment groups. The figure visually summarizes the abundance patterns of 10 key metabolites involved in stress and metabolic pathways. Each cell represents the row-scaled Z-score of the Log2 Fold-Change for a given metabolite relative to the Control group. All were clustered using a hierarchical algorithm based on Euclidean distance and complete linkage. **Yellow** indicates a higher relative abundance compared to that metabolite's average across treatments, while **purple** indicates a lower relative abundance. The colored bar on the left indicates the functional category / associated marker of each metabolite: **Oxidative Damage (Dark green), Protection against oxidative stress (orange), Energy stress (blue), Resistance to energy stress (pink), and Mitochondrial function (green).** Clustering clearly separates the Imidacloprid treatment, characterized by an increase in oxidative and energy stress markers, from the Rutin-containing treatments, which show an opposing profile.

Rutin Restores Expression of Key Mitochondrial and Stress-Response Genes

The expression of genes related to mitochondrial function, stress response, and metabolic signaling were significantly altered by the treatments (Table 13, Figure 14).

Table 13. Effects of Imidacloprid and Rutin on Gene Expression (ΔCt Values).

Gene	Control	Imid	Rut	Rut+Imid	Overall Test
TFAM	0.46 ± 0.39 c	4.99 ± 0.71 d***	-3.52 ± 1.17 b***	-5.40 ± 1.15 a***	$F(3,12) = 101.41$, $p < .001$, $\eta^2 = 0.962$
PGC-1α	-0.01 ± 0.24 a	6.66 ± 0.68 b	-3.82 ± 1.43 c*	-2.91 ± 2.02 c*	$\chi^2(3) = 12.79$, $p = .005$, $\eta^2\_H = 0.816$

ATP5A	-0.21 ± 0.87 c	4.12 ± 0.76 d***	-3.20 ± 1.25 b**	-6.53 ± 1.14 a***	$F(3,12) = 78.03$, $p < .001$, $\eta^2 = 0.951$
SDHA	0.09 ± 1.05 b	-0.85 ± 0.59 b	-0.49 ± 0.70 b	-5.01 ± 1.56 a***	$F(3,12) = 19.80$, $p < .001$, $\eta^2 = 0.832$
GSTS1	-0.44 ± 0.46 c	2.04 ± 0.46 d***	-2.74 ± 0.68 b***	-4.82 ± 0.70 a***	$F(3,12) = 101.10$, $p < .001$, $\eta^2 = 0.962$
CYP9Q3	0.03 ± 0.37 d	-3.67 ± 0.97 c***	-1.96 ± 1.08 b*	-5.93 ± 0.68 a***	$F(3,12) = 37.97$, $p < .001$, $\eta^2 = 0.905$
TRXR1	-0.32 ± 0.97 a	-3.76 ± 1.06 b**	-1.17 ± 0.97 a*	0.02 ± 1.41 a**	$F(3,12) = 9.37$, $p = .002$, $\eta^2 = 0.701$
Ferritin	-0.01 ± 0.32 a	-7.62 ± 1.31 b***	1.89 ± 1.22 a	-0.14 ± 1.01 a***	$F(3,12) = 65.55$, $p < .001$, $\eta^2 = 0.942$
AMPKα	-0.11 ± 0.43 b	-5.86 ± 1.78 c***	3.15 ± 2.07 a*	-0.49 ± 1.25 b**	$F(3,12) = 24.18$, $p < .001$, $\eta^2 = 0.858$
ILP1	-0.29 ± 0.42 c	4.10 ± 1.05 d***	-1.89 ± 0.58 b*	-5.60 ± 1.02 a***	$F(3,12) = 97.99$, $p < .001$, $\eta^2 = 0.961$

Values are presented as Mean ± SD of ΔCt values, where a higher value indicates lower relative gene expression. Within a row, means not sharing a superscript letter (a, b, c, d) are significantly different based on post-hoc tests with Bonferroni correction (p < .05). Asterisks represent the significance level of the comparison against the Control group (for Imid and Rut columns) or against the Imid group (for the Rut+Imid column) ($p < 0.05$, ** $p < 0.01$, *** $p < 0.001$).*

Mitochondrial Biogenesis and Function: Imidacloprid exposure suppressed key markers of mitochondrial health in bees, including *TFAM* and *ATP5A*. Rutin supplementation alone generally enhanced the expression of these genes. Rut+Imid bees prompted a strong recovery, elevating the expression of these mitochondrial markers to levels significantly higher than those of the healthy Control bees, suggesting a hyper-stimulatory protective response. A similar pattern was observed for *PGC-1α*, while *SDHA* expression was uniquely and strongly up-regulated only in Rut+Imid bees.

Stress Response and Detoxification: Imidacloprid suppressed the expression of key detoxification (*GSTS1*, *CYP9Q3*) and antioxidant (*TRXR1*, *Ferritin*) genes in bees. Rutin alone had a mixed effect, enhancing the detoxification genes while having no significant baseline effect on *TRXR1* or *Ferritin*. The protective effect in Rut+Imid bees was again robust, restoring *TRXR1* and *Ferritin* to Control bee levels, while boosting the expression of *GSTS1* and *CYP9Q3* significantly above Controls.

Metabolic Signaling: The central metabolic signaling pathways involving *AMPKα* and Insulin-like Peptide 1 (*ILP1*) were also disrupted. Imidacloprid suppressed both genes, while Rutin alone enhanced their expression. Rut+Imid bees fully restored *AMPKα* expression to baseline and drove *ILP1* expression to levels exceeding those of Control bees.

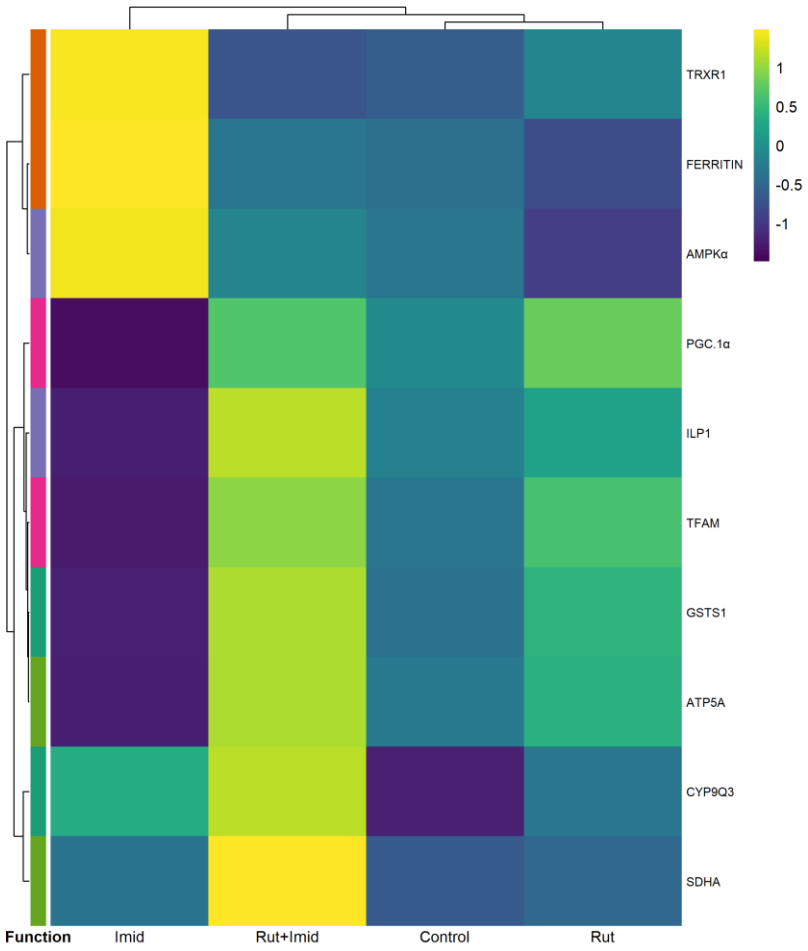

Figure 14. Heatmap of relative gene expression for mitochondrial, stress, and metabolic signaling genes. The figure visually summarizes the expression patterns of 10 target genes across the four experimental groups. The colors represent the row-scaled Z-score of the Log2(Fold Change) values, indicating how a gene's expression in a specific treatment deviates from its own average expression across all treatments. Yellow signifies higher-than-average expression, while purple signifies lower-than-average expression for that gene. The colored bar on the left indicates the functional category of each gene: **Detoxification (Dark green), Antioxidant response (orange), Energy stress response (blue), Mitochondrial biogenesis (pink), and Mitochondrial function (green).** Both genes and treatments (columns) were grouped using hierarchical clustering, which clearly separates the distinct transcriptional profile induced by Imidacloprid from the Control and Rutin-containing groups.

Discussion

Our study provides compelling evidence that prophylactic supplementation with the dietary flavonoid Rutin confers complete protection against the lethal toxicity of chronic Imidacloprid exposure in honey bees. Our multi-level analysis demonstrates that Imidacloprid induces a systemic collapse, not merely by causing stress, but by actively suppressing the bee's core metabolic, antioxidant, and detoxification machinery at both the enzymatic and transcriptional levels. In stark contrast, Rutin acts as a proactive 'metabolic conditioner,' enhancing energy reserves, mitochondrial function, and detoxification capacity

without inducing a costly baseline stress response. This conditioned state enables a potent, on-demand defensive reaction upon encountering the pesticide, completely neutralizing its toxic effects and restoring survival to the level of healthy, unexposed bees.

Imidacloprid induced Metabolic Collapse

The profound toxicity of Imidacloprid appears to be rooted in a direct and debilitating suppression of the bee's fundamental physiological machinery. A central finding of this study is that Imidacloprid exposure did not trigger a robust defensive response; instead, it actively dismantled it. We observed a significant suppression of the enzymatic activity of the primary antioxidant defenses (CAT, SOD), the core detoxification systems (GSTs, CYP450s), and the key mitochondrial pace-setting enzyme, citrate synthase. This enzymatic paralysis was mirrored at the transcriptional level, with a broad downregulation of genes essential for detoxification, antioxidant response (TRXR1, Ferritin), and mitochondrial health (TFAM, ATP5A). We hypothesize that this "suppressive toxicological footprint" is the primary mechanism of chronic Imidacloprid's action, creating a state of induced helplessness where the bee is rendered incapable of metabolizing the pesticide or mitigating its downstream consequences.

The suppression of this core machinery inevitably precipitated a systemic crisis. The failure of mitochondrial function led to a severe energy deficit, evidenced by the depletion of both lipid and glucose reserves and the loss of body mass. This energy crisis was confirmed at the metabolic level by the accumulation of energy stress markers (AMP, HYPX) and the suppression of insulin-like signaling (ILP1). This metabolic collapse, in turn, fueled runaway oxidative stress (69,70). With the antioxidant enzyme processes down, the massive increases in ROS/RNS and free Ferrous Iron went uncontrolled, leading to widespread oxidative damage, as seen in the accumulation of lipid peroxidation markers (HPODE). This cascade—from enzymatic and transcriptional suppression to metabolic failure and subsequent oxidative damage—explains the rapid decline and high mortality observed in bees.

Imidacloprid can induce mitochondrial damage and oxidative stress by Iron overload and high energy demanding detoxification responses (71–74). The suppression of CYP450 and GST activity prevents the bee from clearing the xenobiotic (probably by an oversaturated substrate inhibition), while the suppression of CAT and SOD activity prevents it from managing the resulting oxidative stress (75,76). This model of induced inhibition provides a unifying explanation for our observations, framing Imidacloprid not just as a neurotoxin but as a potent metabolic and defensive suppressant whose lethality is increased by the systematic deactivation of the bees' resilience pathways.

Rutin as a Proactive Metabolic and Detoxification Conditioner

In direct contrast to Imidacloprid, Rutin alone acted as a powerful metabolic conditioning agent, significantly improving the bee's baseline physiological state. The increase in lipid and glucose reserves above indicates an enhancement of energy storage and availability. This was

underpinned by a clear improvement in mitochondrial health, demonstrated by the boosted activity of citrate synthase and the upregulation of genes involved in mitochondrial biogenesis and function (TFAM, PGC-1α). This suggests that Rutin's primary beneficial role is to proactively upgrade the bee's metabolic engine, increasing its energy stores and functional capacity in preparation for future challenges.

This enhanced metabolic state was coupled with a proactive priming of the bee's detoxification system. Rutin supplementation alone significantly increased the baseline activity and expression of the two major detoxification enzyme families, GSTs and CYP450s. This finding is critical, Rutin might prepare the bee to metabolize and excrete a wide range of xenobiotics before they are even encountered more effectively. Rutin's aglycone - Quercetin- induces this effect in honey bees by the upregulation of multiple detoxification genes (77). This state of heightened detoxification readiness provides a plausible mechanism for its subsequent protective effects against a chemical stressor like Imidacloprid.

Rutin's conditioning effect appears to be highly efficient and targeted. While it actively boosted detoxification machinery, it had no significant baseline effect on the activity of the primary antioxidant enzymes, CAT and SOD. Yet, it still produced a potent antioxidant effect, lowering baseline ROS/RNS and ferrous iron levels. This suggests Rutin achieves its antioxidant benefits through more efficient mechanisms, such as direct radical scavenging and chelating processes (60,78–81). Therefore, Rutin might improve mitochondrial and metabolic efficiency without inducing a constitutively active and potentially costly enzymatic response (59,82).

Metabolic protection via an On-Demand Hyper-stimulatory Response

The most significant finding of our study was the remarkable efficacy of prophylactic Rutin in neutralizing Imidacloprid's detrimental effects. The alterations of the defensive machinery seen in Imid bees were completely averted. The activities of the antioxidant enzyme CAT and the detoxification enzyme CYP450 were not merely restored but were hyper-activated to levels significantly exceeding those of healthy bee Controls. This response, which the un-supplemented bees were incapable of mounting, suggests that Rutin's conditioning enables a powerful and effective reaction that may neutralize the toxin and its oxidative consequences. This robust enzymatic counter-response translated into a comprehensive and remarkably complete restoration of bee health. Rut+Imid bees showed a full recovery of body mass and a complete normalization of lipid and glucose reserves. Oxidative stress was fully Controlled, with ROS/RNS levels returning to baseline and ferrous iron being reduced to levels even lower than Control bees. This systemic recovery, driven by the hyper-stimulatory enzymatic and transcriptional response, culminated in the most critical finding: a complete restoration of survival. The mortality risk for the protected bees was indistinguishable from that of the healthy, unstressed Control bees, demonstrating a level of complete protection.

Our findings support a two-stage model of protection. First, prophylactic Rutin acts as a proactive conditioning agent, building up energy reserves and enhancing the capacity of mitochondrial and detoxification systems. Second, this enhanced capacity allows the bee to launch a reactive hyper-response upon encountering the pesticide—a response powerful enough to overcome the toxin's suppressive effects. The unique and strong upregulation of the mitochondrial gene SDHA only in Rut+Imid bees may serve as a key molecular marker for this successful state of resilience. This model, where nutritional pre-conditioning enables superior reactive defense, provides a complete explanation for the comprehensive protection observed in our study.

Conclusions, limitations, and Future Directions

While our study provides strong evidence for Rutin's protective effects, it is important to acknowledge the limitations inherent in our design. Our experiments were conducted under Controlled laboratory conditions with a simplified sucrose diet, which does not fully capture the complex nutritional, social, and environmental dynamics of a bee individual in a field colony. The use of bees of non-standardized age and the lack of pre-treatment baseline measurements introduces potential variability, while our single-endpoint design provides a static snapshot rather than a dynamic view of the physiological response over time. Furthermore, the fixed concentrations of Rutin and Imidacloprid preclude an analysis of dose-dependent effects. These limitations, however, illuminate clear avenues for future research. The most critical next step is to translate these findings into semi-field and field-level studies to determine if dietary supplementation with Rutin can improve the health, productivity, and resilience of entire colonies in real-world agricultural settings. Future laboratory work should employ time-course designs to map the temporal dynamics of the protective response. To move from correlation to causation, functional studies using techniques like RNAi to silence key hyper-activated genes (e.g., specific CYP450s or Catalase) could definitively test their role in the observed protection.

Nevertheless, this study demonstrates a powerful and complete protective mechanism. We have shown that prophylactic supplementation with the flavonoid Rutin confers comprehensive protection against the lethal metabolic toxicity of Imidacloprid. The data supports a model where Rutin acts not as a simple antioxidant, but as a potent **metabolic conditioner** that proactively enhances energy reserves, mitochondrial capacity, and detoxification systems. This priming enables a rapid, on-demand, and hyper-stimulatory counter-response that completely neutralizes the pesticide's suppressive effects, fully restoring bee health and survival. This work underscores the profound potential of nutritional immunology, suggesting that targeted dietary interventions can be a practical and effective strategy to bolster pollinator resilience against the pervasive threat of pesticides.

Chapter 3: Rutin supplementation boosts Honey Bees (*Apis mellifera*) immunity against *Varroa destructor* and *Nosema ceranae* under chronic Imidacloprid exposure.

Sergio A. Mayorga[a,c], Yeny Acosta[c], Angie Ramírez [d], Carolina Ramírez[c], Andre J. Riveros[a,b]

[a] *CANNON Research Group, Department of Biology, School of Science and Engineering, Universidad del Rosario, Bogotá, Colombia*

[b] *Department of Neuroscience, College of Science, University of Arizona. Tucson, Arizona. USA*

[c] *Center for Autoimmune Diseases Research (CREA), School of Medicine and Health Sciences, Universidad del Rosario. Bogotá. Colombia*

[d] *Center for Research in Microbiology and Biotechnology – UR (CIMBIUR), School of Science and Engineering, Universidad del Rosario, Bogotá, Colombia*

Introduction

The global decline of honey bee (*Apis mellifera*) populations is a multifactorial crisis driven by the complex and often synergistic interactions among agrochemical exposure, endemic pathogens, and nutritional deficits (21,50). While these stressors can act independently, their co-occurrence in agricultural landscapes creates a combined burden that can overwhelm bee defenses and precipitate colony collapse. A critical area of research focuses on how sublethal exposure to pesticides, such as neonicotinoids, can impair honey bee immunity, thereby increasing their susceptibility to viral, fungal, and parasitic infections that might otherwise be managed by a healthy colony (4,83).

Our previous investigations have established that chronic exposure to the neonicotinoid Imidacloprid induces a state of physiological distress in *A. mellifera*, characterized by both broad-spectrum immunosuppression and severe oxidative and energy stress. This pesticide-induced vulnerability raises a crucial ecological question: how does such compromised physiological integrity affect a bee's ability to combat pathogenic challenges? Honey bee colonies are persistently threatened by a suite of pathogens, including the ectoparasitic mite *Varroa destructor*, the gut microsporidian *Nosema ceranae*, and the viral pathogens it vectors, such as Deformed Wing Virus (DWV). *Varroa destructor* is the primary biotic threat, directly weakening bees by feeding on fat body tissue and efficiently transmitting viruses (84). Concurrently, *Nosema ceranae* compromises gut health and exacerbates energy stress, while high titers of DWV are unequivocally linked to increased morbidity and mortality (85,86). The interaction between Imidacloprid and these pathogens is therefore of paramount concern.

In parallel, nutritional interventions offer a promising strategy to bolster bee resilience. We have previously demonstrated that prophylactic supplementation with Rutin, a naturally occurring flavonoid, can significantly ameliorate the immunological and metabolic damage caused by Imidacloprid under laboratory conditions. Rutin's established antioxidant and

immunomodulatory properties suggest it may enhance a bee's capacity to resist or tolerate infection. However, whether these physiological benefits translate into tangible protection against diverse and ecologically relevant pathogens, especially in the continued presence of a chemical stressor, remains a critical unresolved question. The outcomes of such three-way interactions—host, pesticide, and pathogen—are notoriously difficult to predict, as they may be additive, synergistic, or even antagonistic depending on the specific pathogen and host defense pathways involved.

This study test the efficacy of prophylactic Rutin supplementation in mitigating the impact of pathogenic infections under conditions of chronic Imidacloprid exposure. We hypothesized that: **(1)** Imidacloprid exposure would synergize with pathogen challenge, leading to reduced survival and exacerbated disease symptoms (higher pathogen loads or tissue damage) compared to pathogen infection alone; **(2)** in the absence of pesticide stress, Rutin supplementation would enhance resilience, increasing survival and reducing pathogen-associated morbidity; and **(3)** in bees co-exposed to both stressors, Rutin would provide a degree of protection. To test these hypotheses, we challenged bees with *V. destructor*, *N. ceranae*, or DWV-A and measured a suite of pathogen-specific health endpoints to dissect the intricate outcomes of these multi-stressor interactions.

Methods

1. Sample Collection

Following the completion of the treatment period, bees from each treatment group were subdivided and subjected to one of three pathogen challenges: (1) *Varroa destructor* infestation, (2) *Nosema ceranae* infection, or (3) Deformed Wing Virus (DWV) injection. This resulted in a factorial design where each treatment subgroup was exposed to a specific pathogen. Control bees for each pathogen challenge consisted of sham-inoculated individuals (receiving a sucrose-only solution or a 1X PBS injection).

For all assays five biological replicates (each a pool of three bees) were established per treatment-pathogen group (total N=180). For each experimental replicate, healthy nurse bees were collected directly from brood frames and healthy forager bees were captured at the hive entrance during peak activity (09:00–12:00 h) using a translucent acrylic trap (16).

2. Pathogen Sourcing and Preparation

***Varroa destructor*:** Mites were sourced from colonies at a commercial apiary in Viracachá, Boyacá, Colombia (5.49° N, 73.44° W; RH: 86–92%; T: 11.5–16.3 °C) exhibiting signs of varroosis (infestation index ~3.5%) but no overt co-infections. To collect mites, ~200 nurse bees were collected and anesthetized by placing them in a sterile container on a metal rack over ice for 5-10 min (87). Mites were gently dislodged using sterile soft-tipped forceps. Mites were immediately inspected for physical integrity and motility under a stereomicroscope (88). Only active, uninjured mites were used for inoculations.

***Nosema ceranae*:** Spores were isolated from forager bees collected from the Viracachá apiary. Briefly, thirty-one midguts were dissected from foragers, pooled, and homogenized in a sterile mortar with 5 mL of nuclease-free water. The homogenate was filtered through two layers of sterile filtering paper to remove large tissue debris. To purify spores, the filtrate was washed three times by centrifuging at 5,000 x g for 5 min at 4 °C, discarding the supernatant, and resuspending the pellet in sterile water (89). Spore presence was confirmed by staining an aliquot with Giemsa stain and observing the characteristic oval spores via light microscopy (90). The final spore concentration was determined using a hemocytometer. Purity was estimated to be ~85% based on microscopic observation.

Deformed Wing Virus (DWV): A viral inoculum was prepared from bees exhibiting clear symptoms of DWV (deformed or shrunken wings) collected from the Viracachá apiary. Twenty-five heads from symptomatic bees were dissected and homogenized in 500 µL of cold, sterile 1X PBS (91,92). The homogenate was clarified by adding 100 µL of chloroform, vortexing vigorously, and centrifuging at 13,000 x g for 15 min at 4 °C (93,94). The upper aqueous phase containing the viral particles was carefully collected and stored at -80 °C until use. The presence of DWV-A in the final inoculum was confirmed via RT-PCR prior to experiments (see section 8).

3. Pathogen Inoculation Procedures

***Varroa destructor* infestation:** Healthy bees (from the experimental groups) were first anesthetized on ice. One healthy, active mite was carefully transferred onto the dorsal thorax of each anesthetized bee (95). Infestation was confirmed visually after the bee recovered. Fifteen successfully infested bees per treatment group were transferred into three replicate cages (n=5 bees per cage). Bees were maintained for six days under standard conditions with *ad libitum* 1M sucrose. Cages were monitored daily to remove dead bees and to ensure no bees carried more than one mite. Only surviving, singly-infested bees were used for downstream analyses.

***Nosema ceranae* infection:** The purified spore suspension was diluted in 1M sucrose solution to a final concentration of 1×10^6 spores/mL. Each bee was individually fed 10 µL of this solution, resulting in an inoculation dose of 1×10^4 spores per bee. This dose is established to induce sublethal infection (89,90). After inoculation, bees were transferred into three replicate cages (n=5 bees per cage) and maintained for six days under standard conditions. Dead bees were removed daily.

Deformed Wing Virus (DWV) injection: The DWV inoculum was used to challenge bees via microinjection. Prior to the main experiment, a pilot study was conducted to determine a sublethal dose (data not shown) and the standard confirmation molecular test. For the experiment, bees were anesthetized on ice, and 2 µL of the viral supernatant was injected between the third and fourth abdominal tergites (91). Fifteen bees per treatment group were

transferred into three replicate cages (n=5 bees per cage) and maintained for six days under standard conditions. Mortality was monitored daily.

4. Survival Analysis

To assess the effect of the experimental treatments on bee survival following pathogen challenge, a separate cohort of 20 bees per treatment/pathogen group was monitored for six days. Bees were housed in cages under standard conditions with mortality recorded daily.

5. *Varroa destructor* infestation outcomes

Grooming Efficacy: Each surviving bee and its cage floor were inspected under a stereomicroscope. Mite viability was assessed by observing movement or by gently prodding the mite with a fine brush (88). The outcome for each bee was classified into one of three categories: **(1)** Mite Present: The mite was found attached to the bee's body. **(2)** Mite Dislodged: The mite was found detached on the cage floor and was determined to be alive and undamaged. **(3)** Mite Damaged/Dead: The mite was found on the cage floor and was either dead or exhibited visible signs of physical damage (e.g., mutilated legs, damaged dorsal shield) (Figure 15). Data were recorded as the number of bees per cage falling into each category.

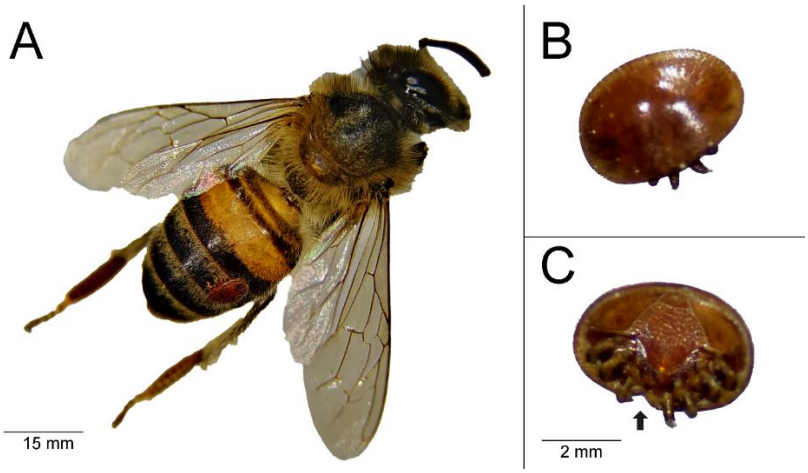

Figure 15. Outcomes of the *Varroa destructor* grooming efficacy assay. The figure illustrates the three possible outcomes for a mite following incubation with a single bee. (A) "Mite Present" outcome, where the mite remains attached to the bee's abdomen. Scale bar = 15 mm. (B) "Mite Dislodged" outcome, showing an undamaged mite recovered from the cage floor. (C) "Mite Damaged/Dead" outcome, showing a mite with visible physical damage. The arrow indicates a mutilated leg. Scale bar for (B) and (C) = 2 mm.

Total fat body lipid content: The pooled fat body samples were placed in a pre-weighed microcentrifuge tube, flash-frozen in liquid nitrogen, and lyophilized. The dry weight of the tissue was recorded. Total lipids were extracted from the dried tissue using the Folch method (62). The lipid extract was then quantified colorimetrically using the sulfo-phospho-vanillin method (61). Absorbance was measured at 546 nm. Lipid concentration was determined from

a standard curve prepared with oleic acid (5–35 µg) and expressed as µg of total lipid per mg of dry fat body tissue.

Phenoloxidase (PO) Activity: PO activity was measured colorimetrically using L-DOPA (Sigma-Aldrich, Cat. No. D9628) as a substrate. Immediately after collection, 1 µL of hemolymph was diluted in 50 µL of ultrapure water. The reaction was initiated by adding 10 µL of the diluted hemolymph to a microplate well containing 90 µL of 4 mg/mL L-DOPA solution in sterile PBS (35). The negative Control contained 10 µL of ultrapure water instead of hemolymph. The reaction kinetics were measured as the change in absorbance at 490 nm every 5 min for 30 min at 28 °C using a Varioskan™ LUX microplate reader (Thermo Fisher Scientific, Waltham, MA, USA). PO activity was calculated as the linear slope of the reaction (Vmax; mOD/min) (96).

6. *Nosema ceranae* infection outcomes

Spore Load Quantification: We employed a dual strategy to ensure accurate and sensitive quantification of *N. ceranae* spore load. First, direct spore counts were performed on a subset of samples using a hemocytometer and light microscopy to determine the concentration of mature, intact spores (89).

Second, we developed a standard curve for quantification via qPCR. A stock of purified spores was counted via hemocytometry to establish a starting concentration (1 x 10^8 spores/mL). From this stock, a ten-fold serial dilution series was prepared in sterile PBS, creating standards with known spore concentrations ranging from 1 x 10^7 to 1 x 10^2 spores/mL. Genomic DNA was extracted from a fixed volume of each dilution point. These DNA samples were then subjected to qPCR using *N. ceranae*-specific primers targeting the 16S rRNA gene (see section 8). A standard curve was generated by plotting the quantification cycle (Cq) values against the logarithm of the known spore concentration. A linear regression was applied to this curve ($R^2 > 0.98$), generating an equation that allowed for the conversion of Cq values from experimental samples directly into "spore equivalents." The final parasite load for each experimental bee was reported in spore load (number of estimated spores per bee).

Midgut Atrophy Imaging: Atrophy was assessed by quantifying tissue melanization using digital imaging. Midguts were dissected and mounted on a glass slide with the same orientation relative to the light source. Images were captured using a Leica M205 C stereomicroscope equipped with a DFC7000 T camera under fixed magnification (20x) and consistent transillumination settings. Images were converted to 8-bit grayscale in ImageJ (30). For each intestine, a standardized rectangular region of interest (ROI) was drawn over the midgut tissue, and the Mean Gray Value (MGV) was measured and used for Atrophy index (Control MGV – Treatment MGV / Control MGV).

Vitellogenin Gene Expression: As an indicator of bee physiological health and nutritional status post-infection, we quantified the relative expression of the *Vitellogenin* (*Vg*) gene (5).

Expression was measured in whole-bee homogenates at the end of the experimental period (see section 8).

7. *DWV* infection outcomes

Viral Clearance Below Detection Threshold: Given the absence of a standard for absolute viral quantification, we evaluated the capacity of the bee host to reduce viral replication to levels below a detectable threshold. This qualitative (presence/absence) approach serves as a direct proxy for the bee's ability to clear an active infection. At the end of the 6-day incubation period, total RNA was extracted from the heads of individual surviving bees. The presence of DWV RNA was then assessed via endpoint RT-PCR, using primers specific for DWV-A and DWV-B (see section 8). The outcome for each bee was recorded as binary: positive (viral RNA detected) or negative (viral RNA not detected).

Given the absence of a standard for absolute viral quantification, we evaluated the capacity of the bee host to reduce viral replication to levels below a detectable threshold. This qualitative (presence/absence) approach serves as a direct proxy for the bee's ability to clear an active infection. At the end of the 10-day incubation period, total RNA was extracted from the heads of individual surviving bees. The presence of DWV RNA was then assessed via endpoint RT-PCR in separate reactions for DWV-A and DWV-B testing (see section 8). The outcome for each bee was recorded as binary: positive (viral RNA detected) or negative (viral RNA not detected).

Inflammatory/Stress Gene Expression: To assess the level of chronic immune activation and inflammation resulting from DWV infection, we measured the relative expression of two key immune/stress pathway transcription factors: Relish and HSP70 (5,97). Gene expression was quantified in bee heads at the end of the 10-day infection period (see section 8).

8. Molecular Analyses: Nucleic Acid Extraction, Endpoint RT-PCR, *Nosema ceranae* qPCR, and Gene Expression Analysis (RT-qPCR)

RNA/DNA Extraction: For gene expression analysis and viral detection, total RNA was extracted from specific tissues as required for each assay (whole bees, or individual heads). Bee heads extraction was performed with the TRIZOL™ Reagent (Thermo Fisher, Cat. No. 15596026), the procedure was followed by a cleanup step using RNeasy Mini Kit columns (Qiagen, Cat. No. 74104) to improve RNA purity. For whole bees, RNA was extracted directly with the RNeasy Mini Kit, including an on-column DNase digestion step (Qiagen, Cat. No. 79254). Nucleic acid quality and concentration were assessed using a NanoDrop One spectrophotometer (Thermo Fisher Scientific).

Quantitative Real-Time PCR: First-strand cDNA was synthesized from 500 ng of total RNA using the iScript™ Advanced cDNA Synthesis Kit (Bio-Rad, Cat# 1725038). The qPCR was performed using a Bio-Rad CFX96 Touch Real-Time PCR Detection System. Primer pairs (Table 14) were designed using Primer-BLAST. Primer specificity and

efficiency were validated via melt curve analysis and standard curve analysis, respectively. Each 15 µL reaction contained KiCqStart™ SYBR® Green qPCR ReadyMix™ (Sigma-Aldrich, Cat# KCQS02), 250 nM of each primer, and 13 ng of template cDNA. The thermal cycling protocol was 95°C for 2 min; followed by 40 cycles of 95°C for 5 sec and 60°C for 30 sec (data acquisition); followed by a melt curve analysis.

***Nosema ceranae* Species Identification:** To confirm that infections were exclusively from *Nosema ceranae* and to screen for the presence of *Nosema apis*, we used a species-specific multiplex qPCR assay targeting the 16S rRNA gene (98). The reaction utilizes a universal forward primer common to both species and two species-specific reverse primers, one unique to *N. ceranae* and one unique to *N. apis* (Table 14). Genomic DNA extracted from spore pellets was used as the template. The presence of an amplification product from the *N. ceranae*-specific primer pair, coupled with the absence of a product from the *N. apis*-specific pair, was used to confirm monospecific infections in our source colonies. For *Nosema ceranae* quantification, each 10 µL reaction contained 5 µL of KiCqStart™ SYBR® Green qPCR ReadyMix™ (Sigma-Aldrich, Cat. No. KCQS02), 2 µL of gDNA template (~5 ng), 1 µL of the primer mixture (containing one universal forward and two species-specific reverse primers), and 2 µL of nuclease-free water. The cycling protocol was: initial denaturation at 95°C for 3 min, followed by 40 cycles of 95°C for 15 s and 60°C for 60 s. A melt curve analysis was performed to confirm product specificity. Species identity was confirmed by the amplification profile.

Screening for DWV-A and DWV-B Variants: we performed two separate endpoint RT-PCR reactions for each sample, one for DWV-A and one for DWV-B, using cDNA as the template. We used previously validated, variant-specific primer sets targeting the viral RNA-dependent RNA polymerase (RdRp) gene (99). The reaction was performed using the GoTaq® Green Master Mix (Promega, Cat. No. M7122). Each 25 µL reaction contained 12.5 µL of GoTaq Mix, 2 µL of cDNA template, 1 µL of each specific primer (10 µM forward and reverse), and 8.5 µL of nuclease-free water. The cycling protocol was: initial denaturation at 95°C for 2 min, followed by 35 cycles of 94°C for 30 s, 58°C for 45 s, and 72°C for 60 s, with a final elongation step at 72°C for 5 min. Products were visualized on a 1.5% agarose gel. The presence of a band in the respective reaction indicated infection with that variant.

Endpoint RT-PCR for DWV Detection: For qualitative detection of DWV (both in the initial inoculum screening and for the final viral clearance assessment), cDNA was first synthesized from 1 µg of total RNA using the iScript™ cDNA Synthesis Kit (Bio-Rad, Cat. No. 1708891) according to the manufacturer's instructions. The subsequent PCR reaction was performed using the GoTaq® Green Master Mix (Promega, Cat. No. M7122). Each reaction contained 12.5 µL of GoTaq Mix, 1 µL of cDNA template, 1 µL of each primer (10 µM forward and reverse; Table 14), and nuclease-free water to a final volume of 25 µL. The cycling protocol was: initial denaturation at 95°C for 2 min, followed by 35 cycles of 94°C for 30 s, 55°C for 60 s, and 72°C for 60 s, with a final elongation step at 72°C for 5 min. PCR

products were visualized on a 1.5% agarose gel stained with SYBR™ Safe DNA Gel Stain (Thermo Fisher, Cat. No. S33102). A sample was considered positive if a distinct band of the expected size was observed.

Table 14. Selected Housekeeping, Immune, Stress markers, and pathogen related genes, primers sequences, and reaction efficiencies.

Target	Organism	Function	Accession no.	Forward primer (5' - 3')	Reverse primer (5' - 3')	Eff. (%)
16S rRNA	*Nosema ceranae*	Detection	U97150	CGGATAAAAGA GTCCGTTGAG	GGTGTAGGGTATA GAATGAGTTTG	99.5
16S rRNA	*Nosema ceranae*	Detection	DQ486027	CCTTGAGAGAG AGAATTTAAGG	AATTGGTGTAGGG TATAGAATGAGTT	97.2
5' UTR	*DWV-A*	Detection	NC_00483 0.2	TGGTTTAATTTG GGTTGGTTG	AGCATGTCTTTCG TCGTCTCC	95.3
5' UTR	*DWV-B (VDV-1)*	Detection	NC_00649 4.1	ATTGCTAGGAGG GCAAGGAG	CATGTCTTTCGTC GTCTCC	100.5
Relish	*Apis mellifera*	Immunity	NM_0010 11599	TGGAAACGGAC GACTCTGAC	GATCTGGTTGGTG CTGCTGT	101.4
Vg	*Apis mellifera*	Physiology	NM_0010 11587	GCTGATGAATGG AAAGGTGAAT	CGATTCCTCATGC TCTTTGA	92.4
HSP70	*Apis mellifera*	Stress Response	NM_0010 11589	AAGCCAGAGAT TGAGGAGGA	ATCGTCGATCTCG TCGTCCTT	97.2
RPS5	*Apis mellifera*	Reference gene	NM_0010 11568	AATTATTTGGTC GCTGGAATG	CTTGGACTTGCCT CTAAAT	101.0
RPS18	*Apis mellifera*	Reference gene	NM_0010 14389	ATGGACGTCGAT GGATAGTGT	GAACCGGCTAGG TAGAAGG	97.4
Actin	*Apis mellifera*	Reference gene	NM_00117 7653	TGCCAACACTGT CCTTTCTGAG	AATTGACCCACCA ATCCA	100.2

7. Statistical Analyses

All statistical analyses were conducted in R (v4.4.1) using the RStudio environment (48,49). A significance level (α) of 0.05 was used for all tests unless otherwise stated. The analytical strategy was comprised of the following tiers:

First, for the **survival analysis,** a Cox Proportional Hazards (CPH) model was used as the primary statistical test to evaluate the effects of pre-treatment, pathogen challenge, and their interaction on bee survival. The proportional hazards assumption was verified using the Schoenfeld residuals test. Significant interaction effects were visualized using Kaplan-Meier survival curves faced by pathogen type.

Second, for **endpoint assays with categorical outcomes**, such as *Mite Fate* and *Viral Clearance*, a Chi-squared (χ^2) test of independence was used to determine if there was a significant association between the treatment group and the outcome. For significant

associations, a post-hoc analysis of standardized residuals was performed to identify which specific cells in the contingency table contributed sign.

Third, for **endpoint assays with continuous outcomes**, we assessed differences among the four treatment groups within each pathogen challenge were assessed using a consistent univariate workflow. Data was first tested for normality of residuals (Shapiro-Wilk test) and homogeneity of variances (Levene's test). If assumptions were met, a one-way ANOVA was performed. If assumptions were violated, a non-parametric Kruskal-Wallis test was used. Appropriate data transformations (e.g., logarithmic) were applied to skewed data to better meet parametric test assumptions. All significant overall tests were followed by post-hoc pairwise comparisons with a Holm-Bonferroni p-value adjustment. Effect sizes (e.g., Eta-squared, Cohen's d) were calculated for significant findings.

Fourth, for **gene expression analysis**, the Ct value of each target gene was normalized against the geometric mean of three stable housekeeping genes (PRS5, RPS18, and ACTIN) to obtain ΔCt values. These ΔCt values were then analyzed using the same univariate workflow. For visualization, fold-change values were calculated using the $2^{-}\Delta\Delta Ct$ method.

Results

1. Survival analysis

Prophylactic supplementation with Rutin and Imidacloprid exposure significantly influenced bee survival, but its effects depended on the specific pathogen challenge (Figure 16). The model revealed a significant interaction between our pre-treatments and the subsequent pathogen exposure.

Across all challenge conditions, Imidacloprid exposure was detrimental to bees, increasing the overall mortality compared to Control bees (HR = 5.10, $p < .001$). On the other hand, Rut bees exhibited a reduced overall mortality across all challenge conditions compared to Control bees (HR = 0.42, $p = .006$). Interestingly, we observed a mix effect in Rut+Imid bees (HR = 2.11, $p < .001$). When challenged against *Varroa destructor* (HR = 0.64, $p < .001$) and *Nosema ceranae* (HR = 0.21, $p = .002$), mortality decreased but when challenged against *DWV* mortality increased (Table 15).

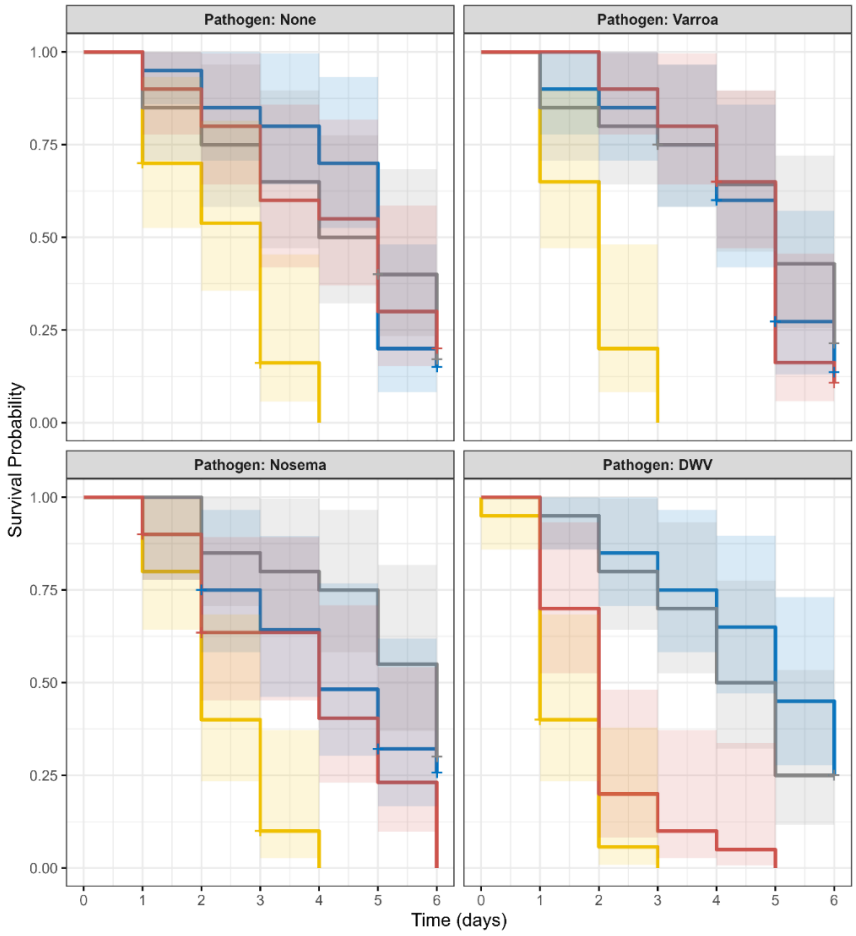

Figure 16. Kaplan-Meier survival curves for pre-treated bees under different pathogen challenges. The plot shows the probability of bee survival over time, faced by four pathogen exposure groups: None, *Varroa destructor*, *Nosema ceranae*, and DWV. Within each panel, lines represent the estimated survival probability, and shaded areas indicate the 95% confidence intervals. Colors correspond to the pre-treatment group: **Yellow** = Imid, **Blue** = Control, **Red** = Rut+Imid, and **Gray** = Rut. The data were analyzed with a Cox Proportional Hazards model, which revealed a significant interaction between pre-treatment and pathogen, indicating that the protective effects of the treatments varied depending on the specific challenge.

Table 15. Cox Proportional Hazards Model of Bee Survival.

Predictor	Hazard Ratio (HR)	95% CI	z-statistic	Adj. p
Imid	5.10	[2.45, 10.61]	7.57	< .001
Rut+Imid	2.11	[1.67, 3.46]	5.74	< .001
Rut	0.42	[1.07, 1.85]	0.59	0.006
Nosema ceranae	1.24	[0.58, 2.65]	0.58	0.016
Varroa destructor	1.35	[0.68, 2.68]	0.83	0.004
DWV	1.14	[0.93, 1.92]	0.72	0.002
Imid :Nosema ceranae	1.32	[0.52, 3.37]	-2.27	0.001
Rut+Imid: Nosema ceranae	0.21	[0.39, 2.79]	-1.46	0.002
Rut: Nosema ceranae	0.54	[0.19, 1.51]	-1.18	0.024

Imid: Varroa destructor	1.46	[0.59, 3.61]	-1.61	< .001
Rut+Imid: Varroa destructor	0.64	[0.24, 1.70]	-3.97	< .001
Rut: Varroa destructor	0.89	[0.32, 2.45]	-0.83	0.004
Imid: DWV	1.28	[0.43, 3.82]	-1.26	0.018
Rut+Imid: DWV	1.20	[0.54, 2.65]	-1.39	< .001
Rut: DWV	0.95	[0.42, 2.18]	-1.02	0.124

Table shows the Hazard Ratios (HR) and 95% Confidence Intervals (CI) from the Cox Proportional Hazards model. An HR > 1 indicates increased mortality risk, while an HR < 1 indicates decreased mortality risk relative to the reference group.

2. Outcomes of *Varroa destructor* Infestation

The Grooming Efficacy was significantly dependent on the bee's pre-treatment (Chi-squared: $\chi^2(6) = 15.78$, $p = .015$). An analysis of the residuals revealed that Imid bees were less effective at grooming, having significantly more mites still present and alive at the end of the assay. In stark contrast, Rut and Rut+Imid bees were significantly more likely to have damaged or dead mites (Figure 17).

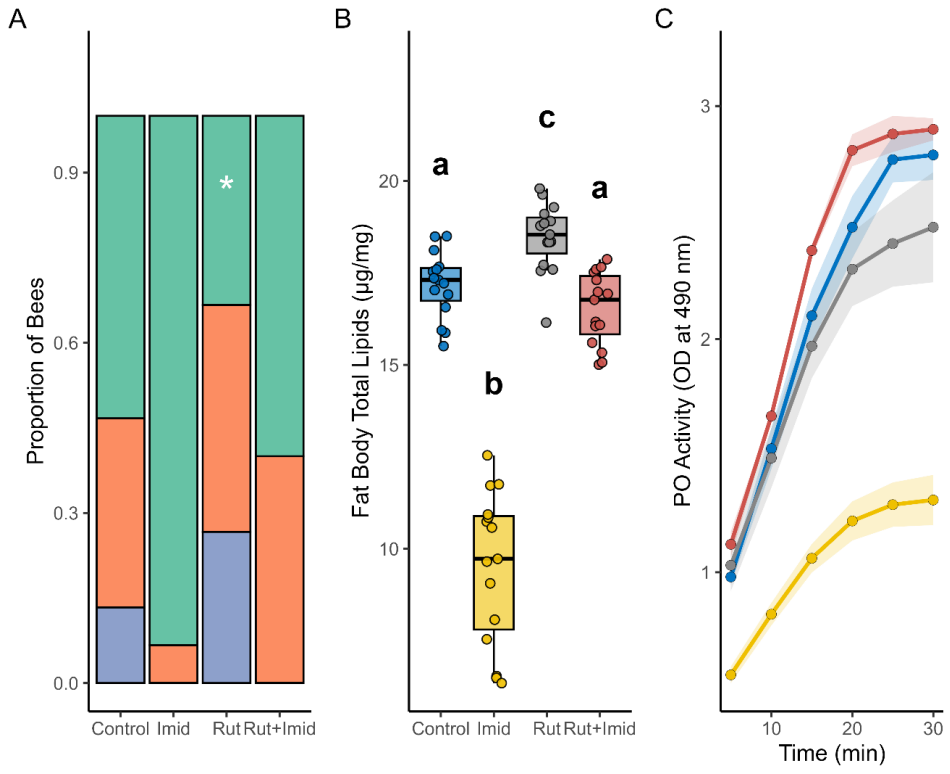

Figure 17. Behavioral, physiological, and immune outcomes following *Varroa destructor* challenge. (A) Proportional "fate" of *Varroa destructor* mites after the incubation period. Colors indicate whether the mite was found alive on the bee (green), was dislodged (orange), or was damaged/killed by the bee (blue). The overall distribution of outcomes was significantly dependent on treatment (Chi-squared test, $p < .05$); the asterisk (*) indicates a significant deviation from the expected frequency for that category as determined by standardized residual analysis. **(B)** Fat body total lipid content of bees post-infestation. Boxplots show the median and

interquartile range, with individual points representing biological replicates. Different letters (a, b, c) indicate statistically significant differences between groups ($p < .05$). **(C)** Kinetics of hemolymph Phenoloxidase (PO) activity measured as the change in optical density (OD at 490 nm) over 30 minutes. Each line represents the mean activity for a treatment group, with shaded areas indicating the 95% confidence interval. Colors correspond to the treatment groups: **Blue (Control), Yellow (Imid), Gray (Rut), Red (Rut+Imid).**

Post-infestation, Imid bees suffered from severe depletion of fat body lipids and a suppression of Phenoloxidase (PO) activity (Table 16). On the other hand, Rut bees exhibited increased fat body lipids while having no decrease effect on PO activity compared to Control bees. Rut+Imid bees effectively mitigated Imidacloprid's impact; it restored lipid levels to a state indistinguishable from the challenged Control bees and prompted a powerful, hyper-stimulatory PO response that was significantly higher than all other bee groups.

Table 16. Physiological and immune outcomes following *Varroa destructor* Infestation.

Parameter	Control	Imid	Rut	Rut+Imid	Overall Test
Fat body lipids (µg/mg)	17.20 ± 0.90 b	9.50 ± 2.06 c***	18.50 ± 0.93 a*	16.50 ± 0.98 b**	$F(3,16) = 44.54$, $p < .001$, $\eta^2\_H = 0.742$
PO activity (OD/min)	0.071 ± 0.006 a	0.032 ± 0.002 c***	0.066 ± 0.006 a	0.054 ± 0.004 b***	$F(3,16) = 63.61$, $p < .001$, $\eta^2 = 0.923$

Values are presented as Mean ± SD. Within a row, means not sharing a superscript letter (a, b, c) are significantly different based on post-hoc tests with Bonferroni correction ($p < .05$). Asterisks represent the significance level of the comparison against the Control group (for Imid and Rut columns) or against the Imid group (for the Rut+Imid column) ($p < 0.05$, ** $p < 0.01$, *** $p < 0.001$).**

3. Outcomes of *Nosema ceranae* infection

Compared to challenged Control bees, Imid bees exhibited a higher *Nosema ceranae* spore load, more severe midgut atrophy, and a potent suppression of the key health and immunity biomarker, Vitellogenin (Vg) (Table 17).

Table 17. Pathological Outcomes of *Nosema ceranae* Infection.

Parameter	Control	Imid	Rut	Rut+Imid	Overall Test
Spore Load (spores/bee)	22400 ± 3266 b	42861 ± 2790 a*	6486 ± 2028 c***	8828 ± 2255 c***	$\chi^2(3) = 51.40$, $p < .001$, $\eta^2_H = 0.85$
Midgut Atrophy Index (%)	67.5 ± 7.21 b	81.4 ± 5.56 a***	30.6 ± 4.98 d***	54.0 ± 6.95 c***	$F(3,56) = 132.29$, $p < .001$, $\eta^2 = 0.876$
Vg Expression (ΔCt)	0.09 ± 0.35 c	6.44 ± 1.44 d***	-5.20 ± 1.01 a***	-1.42 ± 1.00 b***	$F(3,16) = 111.69$, $p < .001$, $\eta^2 = 0.954$

Values are presented as Mean ± SD. For Vg Expression, data are ΔCt values where a higher value indicates lower relative gene expression. Within a row, means not sharing a superscript letter (a, b, c, d) are significantly different based on post-hoc tests ($p < .05$). Asterisks represent the significance level of the comparison against the Control group (for Imid and Rut columns) or against the Imid group (for the Rut+Imid column) ($p < 0.05$, ** $p < 0.01$, *** $p < 0.001$).*

In contrast, Rut bees had significantly lower spore loads, less gut tissue damage, and substantially higher Vitellogenin expression than even the challenged Control bees (Figure

18). For all three parameters, Rut+Imid bees exhibited a strong recovery compared to Imid bees. This effect was so robust that Rut+Imid bees were significantly healthier than the challenged Control bees, with lower spore loads, reduced midgut atrophy, and enhanced Vitellogenin expression (Figure 19).

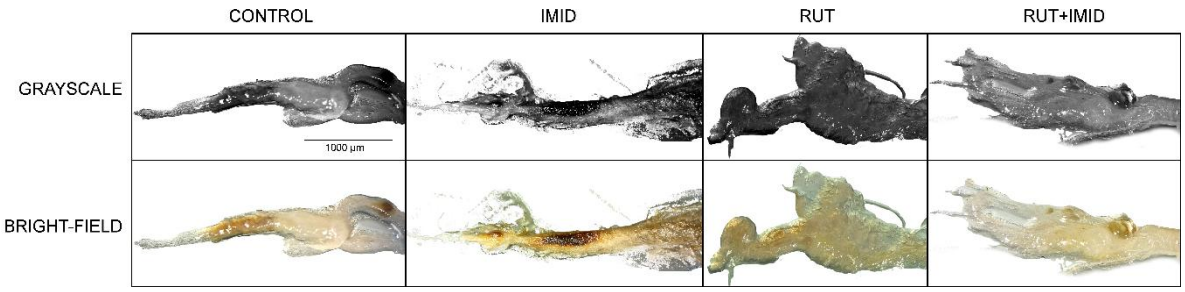

Figure 18. Midgut atrophy. Representative images of dissected midguts from *Nosema ceranae* infected bees in each of the four treatment groups. The top row shows grayscale micrographs, and the bottom row shows the corresponding bright-field images. Scale bar = 1000 µm.

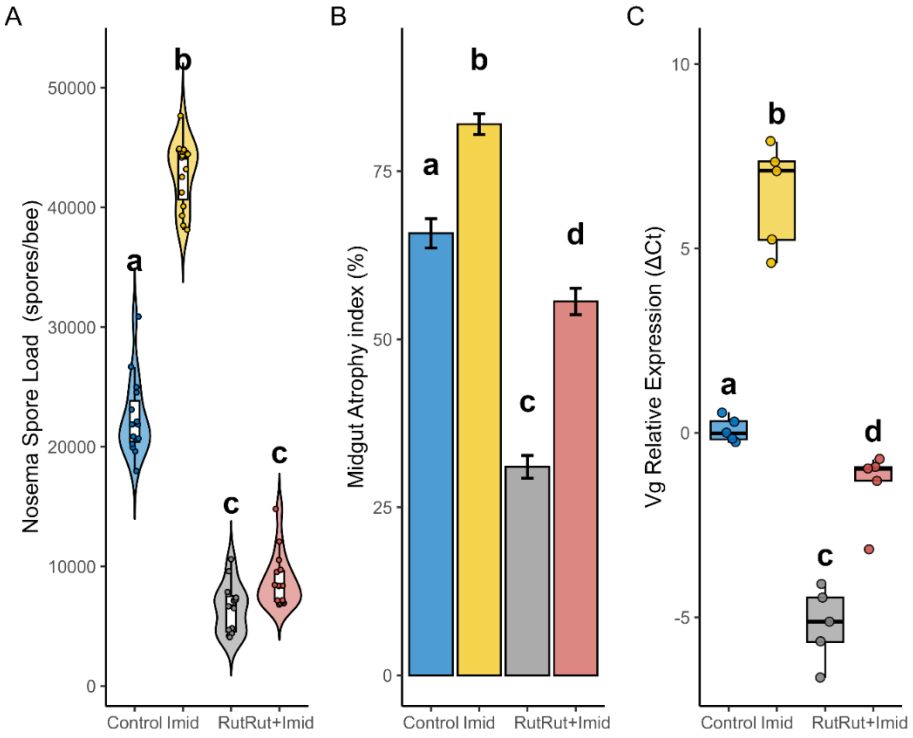

Figure 19. Pathological and molecular outcomes of *Nosema ceranae* infection. (A) *Nosema ceranae* spore load per bee at the end of the experiment. Violin plots illustrate the data distribution, with internal boxplots showing the median and interquartile range. **(B)** Midgut atrophy index (%). Bars represent the mean value for each treatment group, with error bars indicating the standard error of the mean. **(C)** Relative expression of Vitellogenin (Vg), presented as ΔCt values where a higher value indicates lower relative gene expression. Boxplots show the median and interquartile range. In all panels, different letters (a, b, c, d) above the plots indicate statistically significant differences between treatment groups as determined by post-hoc tests ($p < .05$).

4. Outcomes of *DWV* infection

The proportion of bees testing positive for DWV was significantly dependent on the pre-treatment (Chi-squared: $\chi^2(3) = 11.67$, $p = .009$). An analysis of the residuals revealed that Rut bees were less likely to have a detectable viral infection, suggesting a direct antiviral or resistance--boosting effect of Rutin. Conversely, Imid bees exhibited a trend towards higher rates of virus detection. Interestingly, Rut+Imid bees did not exhibit significant changes relative Control or Imid bees (Figure 20).

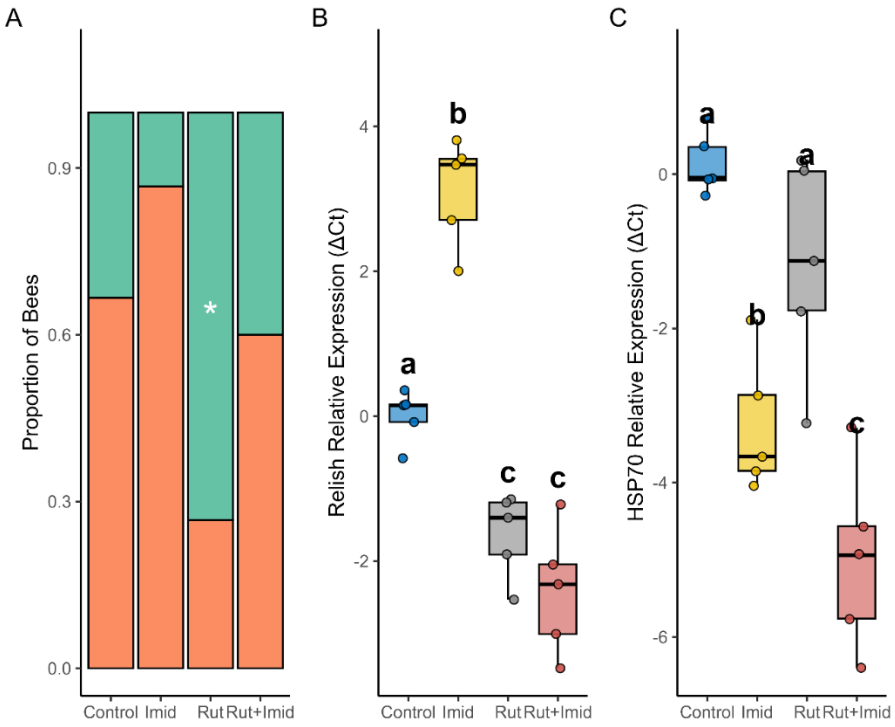

Figure 20. Outcomes of Deformed Wing Virus (DWV) infection. (A) Proportion of bees testing positive (orange) or negative (green) for DWV by the end of the experiment. The asterisk (*) indicates that the observed frequency for that category is significantly different from the expected frequency (Chi-squared test, $p < .05$). **(B)** Relative expression of the immune gene Relish. **(C)** Relative expression of the stress marker gene HSP70. For panels B and C, boxplots show the median and interquartile range of ΔCt values, where a higher value indicates lower relative gene expression. Individual points represent biological replicates. Different letters (a, b, c) above the boxplots indicate statistically significant differences between groups ($p < .001$).

These findings were supported by the expression of key genes. The expression of *Relish*, a crucial transcription factor in immune response, was potently suppressed in Imid bees. In contrast, Rut bees had enhanced *Relish* expression. This effect was boosted in Rut+Imid bees to levels higher even the healthy Control bees. The cellular stress marker *HSP70* was also affected. Imid bees showed an increase in *HSP70* expression, while Rut bees did not present altered expression compared to Control bees. Interestingly, Rut+Imid bees exhibited an even stronger up-regulation of *HSP70* (Table 18).

Table 18. Effects of Imidacloprid and Rutin on Gene Expression of DWV infected bees (ΔCt Values).

Parameter	Control	Imid	Rut	Rut+Imid	Overall Test
Relish (ΔCt)	0.00 ± 0.36 b	3.11 ± 0.74 a***	-1.64 ± 0.59 c**	-2.41 ± 0.88 c***	$F(3,16) = 66.90$, $p < .001$, $\eta^2 = 0.926$
HSP70 (ΔCt)	0.13 ± 0.41 a	-3.26 ± 0.89 c***	-1.18 ± 1.41 b	-4.99 ± 1.19 d*	$F(3,16) = 23.49$, $p < .001$, $\eta^2 = 0.815$

Values are presented as Mean ± SD of ΔCt values, where a higher value indicates lower relative gene expression. Within a row, means not sharing a superscript letter (a, b, c, d) are significantly different based on post-hoc tests with Bonferroni correction (p < .05). Asterisks represent the significance level of the comparison against the Control group (for Imid and Rut columns) or against the Imid group (for the Rut+Imid column) ($p < 0.05$, ** $p < 0.01$, *** $p < 0.001$).

Discussion

This study reveals the complex and context-dependent nature of nutritional immunology in honey bees facing a bipartite stress of pesticides and pathogens. We demonstrate that while the dietary flavonoid Rutin can provide broad-spectrum protection against diverse pathogens when acting alone, its ability to mitigate the synergistic impact of Imidacloprid and infection is highly contingent on the pathogen's biology. Our results show that prophylactic Rutin confers robust protection against the ectoparasite *Varroa destructor* and the microsporidian *Nosema ceranae* even in pesticide-stressed bees. However, this same intervention becomes deleterious when bees are challenged with the Deformed Wing Virus (*DWV*), uncovering a critical trade-off where an over-stimulated immune response can lead to immunopathology and increased mortality.

Imidacloprid synergy with bee pathogens

Our findings confirm that Imidacloprid acts as a potent stress synergist, universally increasing mortality and exacerbating disease outcomes regardless of the pathogen type. Its primary mechanism appears to be the targeted compromising of pathogen-specific host defenses. Against *Varroa destructor*, Imidacloprid impaired behavioral immunity, reducing grooming efficacy, and suppressed the key enzymatic defense, Phenoloxidase (PO). Against *Nosema ceranae*, it compromised gut integrity and suppressed the expression of Vitellogenin (Vg), a biomarker crucial for both individual bee health and social immunity (100). Against DWV, it directly suppressed the IMD immune signaling pathway, evidenced by the potent downregulation of its transcription factor, Relish (101). This demonstrates that Imidacloprid creates a state of broad immunological incompetence, weakening the specific processes required to neutralize different pathogens.

This targeted suppression logically translated into more severe disease progression. For bees challenged with *Nosema ceranae*, Imidacloprid exposure led to significantly higher spore loads and more severe midgut atrophy. For bees challenged with DWV, it induced a significant cellular stress response, indicated by the upregulation of HSP70, likely because

of uncontrolled viral replication in an immunologically weakened host (102). By lowering the threshold for successful infection and crippling the subsequent immune response, Imidacloprid allows pathogens to proliferate more effectively, leading to greater tissue damage, higher physiological stress, and ultimately, increased mortality.

Across three distinct pathogen types—an ectoparasite, a gut pathogen, and a systemic virus—Imidacloprid consistently worsened the outcome. This supports a unifying model of "induced immunological incompetence." The pesticide does not simply add a generic layer of stress; it actively immunocompromises the bee, creating vulnerabilities that diverse pathogens can exploit. This finding has profound ecological implications, suggesting that sublethal pesticide exposure in the field is a key driver that can transform minor, endemic infections into severe, colony-threatening epizootics.

Rutin as a Broad-Spectrum Resilience Enhancer

In the absence of pesticide stress, Rutin supplementation acted as a powerful, broad-spectrum resilience-enhancing agent. It bolstered behavioral defenses against *Varroa destructor*, leading to more effective grooming and mite damage. It significantly improved gut health and resistance to *Nosema ceranae*, drastically reducing spore loads and tissue atrophy. Furthermore, it appeared to confer antiviral properties, reducing the likelihood of detectable DWV infection and enhancing the expression of the antiviral transcription factor Relish. This indicates that Rutin's benefits are not limited to a single immune pathway but rather enhance multiple, disparate arms of the bee's defensive arsenal.

This enhancement of specific defenses translated into superior physiological condition and health. Rut bees maintained higher lipid reserves after a *Varroa destructor* challenge and exhibited substantially higher levels of the crucial health biomarker Vg during a *Nosema* ceranae infection (102). The ability of Rutin to improve the host's underlying physiological state—its nutritional reserves and protein synthesis capacity—is likely a key mechanism through which it promotes pathogen resistance.

Rutin appears to function as a general "priming" agent that improves the bee's overall condition, making it more robust against a range of biological threats. By enhancing behavioral, physiological, and innate immune defenses simultaneously, Rutin prepares the bee to better withstand infection. Its efficacy against three fundamentally different pathogens suggests its mode of action is to elevate the host's global state of health and defensive readiness, rather than targeting a single pathogen-specific pathway.

The Pathogen-Dependent Efficacy of Rutin-Mediated Protection

The protective effect of Rutin in pesticide-exposed bees was clearest and most complete against the ectoparasite *Varroa destructor*. Rutin supplementation fully restored the bees' grooming efficacy and rescued their depleted lipid reserves. Crucially, it enabled a powerful, on-demand, hyper-stimulatory activation of Phenoloxidase (PO), the key enzyme for

melanizing and sclerotizing mite wounds (103). This is particularly noteworthy given that *Varroa destructor* mites have evolved their own molecular mechanisms to suppress host PO activity, meaning Rutin supplementation enabled the bees to overcome the dual immunosuppressive pressure from both the parasite and the pesticide. This combination of restored behavioral defense and a potent enzymatic counter-attack provides a clear and effective mechanism for protection against a large, external parasite.

Protection against *Nosema ceranae* was similarly robust, with Rut+Imid bees exhibiting health outcomes that were even superior to the challenged Control bees. We propose that Rutin's known benefits to gut epithelial integrity, combined with its potent upregulation of Vitellogenin (Vg), created a highly resilient gut environment. Vg is critical for immune function and stress resistance, and its strong expression likely allowed the protected bees to effectively Control *Nosema ceranae* proliferation and mitigate tissue damage, even while under the physiological strain of pesticide exposure. Furthermore, it is worth noting the potential role of the gut microbiome in this interaction. It is plausible that Rutin or its metabolites beneficially modulated the gut microbial community, creating an environment that directly inhibits or is less permissive to *Nosema ceranae* colonization (104). This highlights a successful interaction where nutritional support directly counteracts the specific pathologies induced by both stressors.

In stark contrast, the interaction between Rutin, Imidacloprid, and DWV was detrimental, leading to worse survival outcomes. This paradoxical finding reveals a critical trade-off. While Rut+Imid bees showed a massive upregulation of the antiviral factor Relish, they also exhibited the highest levels of the cellular stress marker HSP70. We hypothesize that this reflects a state of deleterious immunopathology. The combination of pesticide-induced stress and Rutin-mediated immune priming may have led to an overzealous, hyper-inflammatory response to the virus. This uncontrolled immune activation, while intended to clear the pathogen, likely inflicted severe collateral damage on the host's own tissues, a phenomenon analogous to a "cytokine storm" in vertebrates. This suggests that in a host already weakened by a pesticide, indiscriminately boosting the immune system can be more harmful than the infection itself, providing a crucial cautionary lesson on the context-dependent nature of immunonutrition.

Limitations, Future Directions, and Conclusion

While this study reveals critical insights into multi-stressor interactions, it is important to acknowledge its limitations. Our experiments were conducted under controlled laboratory conditions, which cannot capture the complex social immunity dynamics of a full colony. The use of pathogens and host bees from different apiaries introduces genetic and environmental variability, and our single-endpoint measurements on surviving bees are subject to survivorship bias, potentially underestimating the true severity of the pathological outcomes. Furthermore, the lack of age standardization, the use of a simplified sucrose diet, and the fixed concentrations of all stressors limit the generalizability of our findings.

Methodologically, the absence of quantitative viral load data for DWV and a global transcriptomic analysis means our mechanistic insights, while strongly supported, are not exhaustive. These limitations, however, illuminate clear avenues for future research. Field-level studies are imperative to determine how these interactions manifest at the colony level, where social immunity plays a key role. Future work must incorporate quantitative virology (e.g., RT-qPCR for DWV titers) to directly correlate viral replication with the host's immune response and test our immunopathology hypothesis. To causally validate this hypothesis, functional genomics approaches like RNAi could be used to silence genes like Relish or HSP70 in the co-stressed bees. Moreover, as noted, the role of the gut microbiome is a crucial unexplored variable; incorporating 16S rRNA sequencing would clarify whether Rutin's potent effects against *Nosema ceranae* are mediated by beneficial shifts in the gut microbial community.

In conclusion, this study demonstrates that the outcomes of nutritional interventions in honey bees are profoundly context-dependent. We have shown that while a dietary flavonoid like Rutin can confer robust protection against parasitic and microsporidian threats, it can become deleterious in the face of a viral challenge when combined with pesticide-induced stress. Our findings support a model where an over-stimulated immune system can lead to fatal immunopathology, revealing a critical trade-off in honey bee health. This work underscores the danger of studying stressors in isolation and cautions against the assumption that "boosting" the immune system is a universally beneficial strategy. Ultimately, effective solutions for pollinator health must be holistic, accounting for the complex and often non-additive interactions between nutrition, chemicals, and the diverse pathogen landscape that bees navigate in the real world.

General Conclusion

The research presented in this thesis systematically investigated the potential of the dietary flavonoid Rutin to mitigate the complex health challenges faced by honey bees. Initial laboratory studies established Rutin as a potent protective agent, capable of effectively neutralizing the discrete immunological damage (Chapter 1) and the systemic metabolic and oxidative stress (Chapter 2) induced by the neonicotinoid Imidacloprid. However, this initial promise of broad protection was fundamentally challenged when the research incorporated pathogenic stressors, revealing the central thesis of this work: the efficacy of nutritional supplementation is profoundly context-dependent and governed by critical physiological trade-offs. The same immune-stimulating properties that conferred robust protection against the parasites *Varroa destructor* and *Nosema ceranae* proved detrimental in the face of Deformed Wing Virus (DWV), leading to a state of fatal immunopathology, a finding validated in lab settings (Chapter 3).

The implications of these findings are significant and span several fields. For bee biology, this work provides a clear, field-validated example of immunological trade-offs and the

intimate link between metabolism and immunity in an invertebrate model. For ecotoxicology, it champions the necessity of multi-stressor approaches, proving that the impact of a pesticide cannot be understood in isolation from a host's nutritional and disease status. Most practically, for apiculture, these results support a move towards **"**precision apiculture**",** where interventions like Rutin supplementation could be strategically deployed based on a colony's specific health profile, particularly its dominant pathogen load, to maximize benefits and avoid unintended harm.

In conclusion, this thesis demonstrates that nutritional interventions are not a panacea, but powerful biological modulators whose effects are dictated by the bee context. The findings presented herein underscore that the future of effective pollinator health management lies not in a search for a single solution, but in a deeper understanding of these complex interactions. This knowledge will enable the development of targeted, intelligent support strategies that help honey bee colonies successfully navigate the multifaceted challenges of the modern world.

References

1. Klein AM, Vaissière BE, Cane JH, Steffan-Dewenter I, Cunningham SA, Kremen C, et al. Importance of pollinators in changing landscapes for world crops. Vol. 274, Proceedings of the Royal Society B: Biological Sciences. Royal Society; 2007. p. 303–13.

2. Potts S, Imperatriz-Fonseca V, Ngo H et al. Safeguarding pollinators and their values to human well-being. Nature. 2016 Nov 28;540(1):220–9.

3. Havard T, Laurent M, Chauzat MP. Impact of Stressors on Honey Bees (Apis mellifera; Hymenoptera: Apidae): Some Guidance for Research Emerge from a Meta-Analysis. Diversity (Basel). 2019 Dec 20;12(1):7.

4. Doublet V, Labarussias M, de Miranda JR, Moritz RFA, Paxton RJ. Bees under stress: sublethal doses of a neonicotinoid pesticide and pathogens interact to elevate honey bee mortality across the life cycle. Environ Microbiol. 2015 Apr 11;17(4):969–83.

5. Kunc M, Dobeš P, Hurychová J, Vojtek L, Poiani S, Danihlík J, et al. The Year of the Honey Bee (Apis mellifera L.) with Respect to Its Physiology and Immunity: A Search for Biochemical Markers of Longevity. Insects. 2019 Aug 7;10(8):244.

6. Brandt A, Grikscheit K, Siede R, Grosse R, Meixner MD, Büchler R. Immunosuppression in Honeybee Queens by the Neonicotinoids Thiacloprid and Clothianidin. Sci Rep. 2017 Jul 5;7(1):4673.

7. Brandt A, Gorenflo A, Siede R, Meixner M, Büchler R. The neonicotinoids thiacloprid, imidacloprid, and clothianidin affect the immunocompetence of honey bees (Apis mellifera L.). J Insect Physiol. 2016 Mar;86:40–7.

8. National Pesticide Information Center. Imidacloprid (Technical Fact Sheet) [Internet]. Corvallis: NPIC; 2011 [cited 2025 Jun 30]. Available from: https://npic.orst.edu/factsheets/archive/imidacloprid.html

9. Bonmatin JM, Moineau I, Charvet R, Colin ME, Fleche C, Bengsch ER. Behaviour of Imidacloprid in Fields. Toxicity for Honey Bees. In: Environmental Chemistry. 1st ed. Berlin/Heidelberg: Springer-Verlag; 2005. p. 483–94.

10. Dively GP, Embrey MS, Kamel A, Hawthorne DJ, Pettis JS. Assessment of Chronic Sublethal Effects of Imidacloprid on Honey Bee Colony Health. PLoS One. 2015 Mar 18;10(3):e0118748.

11. Pietta PG. Flavonoids as Antioxidants. J Nat Prod. 2000 Jul 1;63(7):1035–42.

12. Bíliková K, Popelová P, Šimúth J. Plant flavonoids as natural compounds in honey bee nutrition and health. . Chemické Listy. 2015;109(9):682–9.

13. García LM, Caicedo-Garzón V, Riveros AJ. Oral administration of phytochemicals protects honey bees against cognitive and motor impairments induced by the insecticide fipronil. PLoS One. 2024 Mar 25;19(3):e0300899.

14. Riveros AJ, Gronenberg W. The flavonoid rutin protects the bumble bee Bombus impatiens against cognitive impairment by imidacloprid and fipronil. Journal of Experimental Biology. 2022 Sep 1;225(17).

15. OECD. Test No. 245: Honey Bee (Apis Mellifera L.), Chronic Oral Toxicity Test (10-Day Feeding). In: OECD Guidelines for the Testing of Chemicals. 1st ed. Paris: OECD Publishing; 2017. p. 1–9.

16. Matsumoto Y, Menzel R, Sandoz JC, Giurfa M. Revisiting olfactory classical conditioning of the proboscis extension response in honey bees: A step toward standardized procedures. J Neurosci Methods. 2012 Oct;211(1):159–67.

17. Hernandez J, Mesa F, Dussan A, Riveros A. Electrical characteristics of the extracellular fluid in the body segments of Apis mellifera bees. PeerJ. 2025 Jul 17;13.

18. Carreck NL, Ratnieks FLW. The dose makes the poison: have “field realistic” rates of exposure of bees to neonicotinoid insecticides been overestimated in laboratory studies? J Apic Res. 2014 Jan 2;53(5):607–14.

19. Alburaki M, Madella S, Cook SC. Non-optimal ambient temperatures aggravate insecticide toxicity and affect honey bees Apis mellifera L. gene regulation. Sci Rep. 2023 Dec 1;13(1).

20. Rondeau G, Sánchez-Bayo F, Tennekes HA, Decourtye A, Ramírez-Romero R, Desneux N. Delayed and time-cumulative toxicity of imidacloprid in bees, ants and termites. Sci Rep. 2014 Jul 4;4.

21. Sánchez-Bayo F, Goulson D, Pennacchio F, Nazzi F, Goka K, Desneux N. Are bee diseases linked to pesticides? — A brief review. Environ Int. 2016 May;89(1):7–11.

22. Woodcock BA, Bullock JM, Shore RF, Heard M, et al. Country-specific effects of neonicotinoid pesticides on honey bees and wild bees. Science (1979). 2017;356(6345):1393–5.

23. Chmiel J, Daisley B, Siede R, Meixner M, Büchler R. Understanding the effects of sublethal neonicotinoid exposure on honey bee and bumble bee health. J Insect Physiol. 2017;100(1):77–86.

24. Alaux C, Brunet J, Dussaubat C, Mondet F, Tchamitchan S, Cousin M, et al. Interactions between Nosema microspores and a neonicotinoid weaken honeybees (Apis mellifera). . Environ Microbiol. 2010;12(3):774–82.

25. Tison L, Hahn M, Holtz S, Rößner a, Greggers U, Menzel R. The neonicotinoid imidacloprid impairs memory and brain processing in the honeybee (Apis mellifera L.). . Journal of Experimental Biology. 2016;219(18):2845–53.

26. Drescher N, Wallace H, Katouli M, Massaro C, Leonhardt S. The effect of nutritional supplementation on the colony health and gut microbiota of European honey bees, Apis mellifera. . Apidologie. 2017;48(6):757–71.

27. Wang Y, Cao C, Wang D. Physiological Responses of the Firefly Pyrocoelia analis (Coleoptera: Lampyridae) to an Environmental Residue From Chemical Pesticide Imidacloprid. Front Physiol. 2022;13(1).

28. Burritt NL, Foss NJ, Neeno-Eckwall EC, Church JO, Hilger AM, Hildebrand JA, et al. Sepsis and Hemocyte Loss in Honey Bees (Apis mellifera) Infected with Serratia marcescens Strain Sicaria. PLoS One. 2016 Dec 21;11(12):e0167752.

29. Richardson RT, Ballinger MN, Qian F, Christman JW, Johnson RM. Morphological and functional characterization of honey bee, Apis mellifera, hemocyte cell communities. Apidologie. 2018 Jun 1;49(3):397–410.

30. Schneider CA, Rasband WS, Eliceiri KW. NIH Image to ImageJ: 25 years of image analysis. Nat Methods. 2012 Jul 28;9(7):671–5.

31. Adolfsson K, Abariute L, Dabkowska AP, Schneider M, Häcker U, Prinz CN. Direct comparison between in vivo and in vitro microsized particle phagocytosis assays in Drosophila melanogaster. Toxicology in Vitro. 2018 Feb;46:213–8.

32. Hystad EM, Salmela H, Amdam GV, Münch D. Hemocyte-mediated phagocytosis differs between honey bee (Apis mellifera) worker castes. PLoS One. 2017 Sep 1;12(9).

33. Loy JD, Harris DLH. Evaluation of in vivo Hemocyte Phagocytosis of Microsphere Beads in Litopenaeus vannamei Utilizing Flow Cytometry Following Administration of Bacterial Lipopolysaccharides [Internet]. 2010 Jan. Available from: https://www.iastatedigitalpress.com/air/article/id/6941/

34. League GP, Hillyer JF. Functional integration of the circulatory, immune, and respiratory systems in mosquito larvae: Pathogen killing in the hemocyte-rich tracheal tufts. BMC Biol. 2016 Sep 19;14(1).

35. League GP, Estévez-Lao TY, Yan Y, Garcia-Lopez VA, Hillyer JF. Anopheles gambiae larvae mount stronger immune responses against bacterial infection than adults: Evidence of adaptive decoupling in mosquitoes. Parasit Vectors. 2017 Aug 1;10(1).

36. Pawley J. Confocal Z-series. In: Handbook of Biological Confocal Microscopy. 3rd ed. Springer; 2006. p. 491–505.

37. Walderdorff L, Laval-Gilly P, Wechtler L, Bonnefoy A, Falla-Angel J. Phagocytic activity of human macrophages and Drosophila hemocytes after exposure to the neonicotinoid imidacloprid. Pestic Biochem Physiol. 2019 Oct;160:95–101.

38. Randolt K, Gimple O, Geissendörfer J, Reinders J, Prusko C, Mueller MJ, et al. Immune-related proteins induced in the hemolymph after aseptic and septic injury differ in honey bee worker larvae and adults. Arch Insect Biochem Physiol. 2008 Dec 31;69(4):155–67.

39. Campbell J. High-Throughput Assessment of Bacterial Growth Inhibition by Optical Density Measurements. Curr Protoc Chem Biol. 2010 Oct;2(4):195–208.

40. Vera-Jimenez NI, Pietretti D, Wiegertjes GF, Nielsen ME. Comparative study of β-glucan induced respiratory burst measured by nitroblue tetrazolium assay and real-time luminol-enhanced chemiluminescence assay in common carp (Cyprinus carpio L.). Fish Shellfish Immunol. 2013 May;34(5):1216–22.

41. Akinbo DB, Ajayi OI, Eluji OM, Olatunji I, Okoroloko TM. Impaired phagocytosis and oxidative respiratory burst activity in sickle cell anemia leukocytes. J Taibah Univ Med Sci. 2024 Aug;19(4):867–76.

42. Annoscia D, Di Prisco G, Becchimanzi A, Caprio E, Frizzera D, Linguadoca A, et al. Neonicotinoid Clothianidin reduces honey bee immune response and contributes to Varroa mite proliferation. Nat Commun. 2020 Nov 18;11(1):5887.

43. Gätschenberger H, Azzami K, Tautz J, Beier H. Antibacterial Immune Competence of Honey Bees (Apis mellifera) Is Adapted to Different Life Stages and Environmental Risks. PLoS One. 2013 Jun 17;8(6):e66415.

44. Jin G, Hrithik TH, Mandal E, Kil EJ, Jung C, Kim Y. Phospholipase A2 activity is required for immune defense of European (Apis mellifera) and Asian (Apis cerana) honeybees against American foulbrood pathogen, Paenibacillus larvae. PLoS One. 2024 Feb 1;19(2 February).

45. King JG, Hillyer JF. Spatial and temporal in vivo analysis of circulating and sessile immune cells in mosquitoes: hemocyte mitosis following infection [Internet]. 2013. Available from: http://www.biomedcentral.com/1741-7007/11/55

46. Chen K, Luan X, Liu Q, Wang J, Chang X, Snijders AM, et al. Drosophila Histone Demethylase KDM5 Regulates Social Behavior through Immune Control and Gut Microbiota Maintenance. Cell Host Microbe. 2019 Apr;25(4):537-552.e8.

47. Maitra U, Scaglione MN, Chtarbanova S, O'Donnell JM. Innate immune responses to paraquat exposure in a Drosophila model of Parkinson's disease. Sci Rep. 2019 Sep 3;9(1):12714.

48. Posit team. RStudio: Integrated Development Environment for R. Boston: Posit Software; 2025.

49. R Core Team. R: A Language and Environment for Statistical Computing. Vienna, Austria.: R Foundation for Statistical Computing; 2024.

50. Goulson D, Nicholls E, Botías C, Rotheray EL. Bee declines driven by combined stress from parasites, pesticides, and lack of flowers. Science (1979). 2015 Mar 27;347(6229).

51. Zhu YC, Yao J, Adamczyk J, Luttrell R. Feeding toxicity and impact of imidacloprid formulation and mixtures with six representative pesticides at residue concentrations on honey bee physiology (Apis mellifera). PLoS One. 2017 Jun 7;12(6):e0178421.

52. Zhang C, Wang X, Kaur P, Gan J. A critical review on the accumulation of neonicotinoid insecticides in pollen and nectar: Influencing factors and implications for pollinator exposure. Science of The Total Environment. 2023 Nov;899:165670.

53. Magesh V, Zhu Z, Tang T, Chen S, Li L, Wang L, et al. Toxicity of Neonicotinoids to Honey Bees and Detoxification Mechanism in Honey Bees. IOSR J Environ Sci Toxicol Food Technol. 2017 Apr;11(04):102–10.

54. Gong Y, Diao Q. Current knowledge of detoxification mechanisms of xenobiotic in honey bees. Ecotoxicology. 2017 Jan 7;26(1):1–12.

55. Ghosh N, Das A, Chaffee S, Roy S, Sen CK. Reactive Oxygen Species, Oxidative Damage and Cell Death. In: Immunity and Inflammation in Health and Disease. Elsevier; 2018. p. 45–55.

56. Zorov DB, Juhaszova M, Sollott SJ. Mitochondrial Reactive Oxygen Species (ROS) and ROS-Induced ROS Release. Physiol Rev. 2014 Jul;94(3):909–50.

57. Fischer N, Costa CP, Hur M, Kirkwood JS, Woodard SH. Impacts of neonicotinoid insecticides on bumble bee energy metabolism are revealed under nectar starvation. Science of The Total Environment. 2024 Feb;912:169388.

58. Seo S, Lee MS, Chang E, Shin Y, Oh S, Kim IH, et al. Rutin Increases Muscle Mitochondrial Biogenesis with AMPK Activation in High-Fat Diet-Induced Obese Rats. Nutrients. 2015 Sep 22;7(9):8152–69.

59. Takahashi L, Sert MA, Kelmer-Bracht AM, Bracht A, Ishii-Iwamoto EL. Effects of rutin and quercetin on mitochondrial metabolism and on ATP levels in germinating tissues of Glycine max. Plant Physiology and Biochemistry. 1998 Jul;36(7):495–501.

60. Yang J, Guo J, Yuan J. In vitro antioxidant properties of rutin. LWT - Food Science and Technology. 2008 Jul;41(6):1060–6.

61. Knight JA, Anderson S, Rawle JM. Chemical Basis of the Sulfo-phospho-vanillin Reaction for Estimating Total Serum Lipids. Clin Chem. 1972 Mar 1;18(3):199–202.

62. Folch J, Lees M, Sloane GH. A simple method for the isolation and purification of total lipides from animal tissues. J Biol Chem. 1957 May;226(1):497–509.

63. Roe JH. THE DETERMINATION OF DEXTRAN IN BLOOD AND URINE WITH ANTHRONE REAGENT. Journal of Biological Chemistry. 1954 Jun;208(2):889–96.

64. Laurentin A, Edwards CA. A microtiter modification of the anthrone-sulfuric acid colorimetric assay for glucose-based carbohydrates. Anal Biochem. 2003 Apr 1;315(1):143–5.

65. Edwards AM, Glistak ML, Lucas CM, Wilson PA. 7-ethoxycoumarin deethylase activity as a convenient measure of liver drug metabolizing enzymes: Regulation in cultured rat hepatocytes. Biochem Pharmacol. 1984 May;33(9):1537–46.

66. Buters JTM, Schiller CD, Chou RC. A highly sensitive tool for the assay of cytochrome P450 enzyme activity in rat, dog and man. Biochem Pharmacol. 1993 Nov;46(9):1577–84.

67. Srere PA. [1] Citrate synthase. In: Methods in Enzymology. 1st ed. 1969. p. 3–11.

68. Jones AJY, Hirst J. A spectrophotometric coupled enzyme assay to measure the activity of succinate dehydrogenase. Anal Biochem. 2013 Nov;442(1):19–23.

69. Preiser J. Oxidative Stress. Journal of Parenteral and Enteral Nutrition. 2012 Mar;36(2):147–54.

70. Singh Bais Lecturer S. An Overview on Imidacloprid Pesticide Inducing Oxidative Stress. International Journal of Research and Analytical Reviews [Internet]. 2019; Available from: www.ijrar.org

71. Zhang D, Wu C, Ba D, Wang N, Wang Y, Li X, et al. Ferroptosis contribute to neonicotinoid imidacloprid-evoked pyroptosis by activating the HMGB1-RAGE/TLR4-NF-κB signaling pathway. Ecotoxicol Environ Saf. 2023 Mar;253:114655.

72. Nicodemo D, Maioli MA, Medeiros HCD, Guelfi M, Balieira KVB, De Jong D, et al. Fipronil and imidacloprid reduce honeybee mitochondrial activity. Environ Toxicol Chem. 2014 Sep 1;33(9):2070–5.

73. Paleolog J, Wilde J, Gancarz M, Strachecka A. Imidacloprid decreases energy production in the hemolymph and fat body of western honeybees even though, in sublethal doses, it increased the values of six of the nine compounds in the respiratory and citric cycle. PLoS One. 2025 Jul 1;20(7):e0320168.

74. He B, Liu Z, Wang Y, Cheng L, Qing Q, Duan J, et al. Imidacloprid activates ROS and causes mortality in honey bees (Apis mellifera) by inducing iron overload. Ecotoxicol Environ Saf. 2021 Dec;228:112709.

75. Ma X, Deng D, Chen W. Inhibitors and Activators of SOD, GSH-Px, and CAT. In: Enzyme inhibitors and activators. 1st ed. 2017. p. 207–24.

76. Miró A, Hernandez MT, Costas MJ, Cameselle J. Enzyme saturation and inhibition kinetics studied from multiple progress curves recorded

spectrophotometrically from single reaction mixtures for ADP-ribose pyrophosphatase. J Biochem Biophys Methods. 1991 Feb;22(2):177–84.

77. Mao W, Schuler MA, Berenbaum MR. Honey constituents up-regulate detoxification and immunity genes in the western honey bee Apis mellifera. Proceedings of the National Academy of Sciences. 2013 May 28;110(22):8842–6.

78. Abdullah H, Moawed F, Ahmed E, Abdel F, Haroun R. Iron chelating, antioxidant and anti-apoptotic activities of hesperidin and/or rutin against induced-ferroptosis in heart tissue of rats. Int J Immunopathol Pharmacol. 2025;39(1).

79. Afanas'ev IB, Dcrozhko AI, Brodskii A V., Kostyuk VA, Potapovitch AI. Chelating and free radical scavenging mechanisms of inhibitory action of rutin and quercetin in lipid peroxidation. Biochem Pharmacol. 1989 Jun;38(11):1763–9.

80. Nowak D, Kuźniar A, Kopacz M. Solid complexes of iron(II) and iron(III) with rutin. Struct Chem. 2010 Apr 14;21(2):323–30.

81. Enogieru AB, Haylett W, Hiss DC, Bardien S, Ekpo OE. Rutin as a Potent Antioxidant: Implications for Neurodegenerative Disorders. Oxid Med Cell Longev. 2018 Jan 27;2018(1).

82. Gong G, Qin Y, Huang W, Zhou S, Yang X, Li D. Rutin inhibits hydrogen peroxide-induced apoptosis through regulating reactive oxygen species mediated mitochondrial dysfunction pathway in human umbilical vein endothelial cells. Eur J Pharmacol. 2010 Feb;628(1–3):27–35.

83. Lundin O, Rundlöf M, Smith HG, Fries I, Bommarco R. Neonicotinoid Insecticides and Their Impacts on Bees: A Systematic Review of Research Approaches and Identification of Knowledge Gaps. PLoS One. 2015 Aug 27;10(8):e0136928.

84. Ramsey SD, Ochoa R, Bauchan G, Gulbronson C, Mowery JD, Cohen A, et al. Varroa destructor feeds primarily on honey bee fat body tissue and not hemolymph. Proc Natl Acad Sci U S A. 2019 Jan 29;116(5):1792–801.

85. Martín-Hernández R, Botías C, Barrios L, Martínez-Salvador A, Meana A, Mayack C, et al. Comparison of the energetic stress associated with experimental Nosema ceranae and Nosema apis infection of honeybees (Apis mellifera). Parasitol Res. 2011 Sep 1;109(3):605–12.

86. Martin SJ, Highfield AC, Brettell L, Villalobos EM, Budge GE, Powell M, et al. Global Honey Bee Viral Landscape Altered by a Parasitic Mite. Science (1979). 2012 Jun 8;336(6086):1304–6.

87. Dietemann V, Nazzi F, Martin SJ, Anderson DL, Locke B, Delaplane KS, et al. Standard methods for varroa research. J Apic Res. 2013 Jan 2;52(1):1–54.

88. Noble NII, Stuhl C, Nesbit M, Woods R, Ellis JD. A Comparison of Varroa destructor (Acari: Varroidae) Collection Methods and Survivability in in Vitro Rearing Systems. Florida Entomologist. 2021 May 31;104(1).

89. Fries I, Chauzat MP, Chen YP, Doublet V, Genersch E, Gisder S, et al. Standard methods for Nosema research. J Apic Res. 2013 Jan 2;52(1):1–28.

90. Mazur ED, Gajda AM. Nosemosis in Honeybees: A Review Guide on Biology and Diagnostic Methods. Applied Sciences. 2022 Jun 9;12(12):5890.

91. Desai SD, Eu Y -J., Whyard S, Currie RW. Reduction in deformed wing virus infection in larval and adult honey bees (Apis mellifera L.) by double-stranded RNA ingestion. Insect Mol Biol. 2012 Aug 12;21(4):446–55.

92. Mockel N, Gisder S, Genersch E. Horizontal transmission of deformed wing virus: pathological consequences in adult bees (Apis mellifera) depend on the transmission route. Journal of General Virology. 2011 Feb 1;92(2):370–7.

93. Koziy R V, Wood Sarah C, Kozii I V, van Rensburg Claire Janse, Moshynskyy Igor, Dvylyuk Ihor, et al. Deformed Wing Virus Infection in Honey Bees (Apis mellifera L.). Vet Pathol [Internet]. 2019 Mar 11;56(4):636–41. Available from: https://doi.org/10.1177/0300985819834617

94. Zioni N, Soroker V, Chejanovsky N. Replication of Varroa destructor virus 1 (VDV-1) and a Varroa destructor virus 1–deformed wing virus recombinant (VDV-1–DWV) in the head of the honey bee. Virology. 2011 Aug;417(1):106–12.

95. di Prisco G, Zhang X, Pennacchio F, Caprio E, Li J, Evans JD, et al. Dynamics of persistent and acute deformed wing virus infections in honey bees, apis mellifera. Viruses. 2011 Dec;3(12):2425–41.

96. Adamo SA. Estimating disease resistance in insects: phenoloxidase and lysozyme-like activity and disease resistance in the cricket Gryllus texensis. J Insect Physiol. 2004 Feb;50(2–3):209–16.

97. Brutscher LM, Daughenbaugh KF, Flenniken ML. Antiviral defense mechanisms in honey bees. Curr Opin Insect Sci. 2015 Aug;10:71–82.

98. Gisder S, Genersch E. Molecular differentiation of Nosema apis and Nosema ceranae based on species–specific sequence differences in a protein coding gene. J Invertebr Pathol. 2013 May;113(1):1–6.

99. Mordecai GJ, Wilfert L, Martin SJ, Jones IM, Schroeder DC. Diversity in a honey bee pathogen: first report of a third master variant of the Deformed Wing Virus quasispecies. ISME J. 2016 May 1;10(5):1264–73.

100. Salmena H, Sundstrom L. Vitellogenin in inflammation and immunity in social insects. Inflamm Cell Signal. 2017 May 3;5(1).

101. McMenamin AJ, Daughenbaugh KF, Parekh F, Pizzorno MC, Flenniken ML. Honey Bee and Bumble Bee Antiviral Defense. Viruses. 2018 Jul 27;10(8):395.

102. Sarioğlu-Bozkurt A, Topal E, Güneş N, Üçeş E, Cornea-Cipcigan M, Coşkun İ, et al. Changes in Vitellogenin (Vg) and Stress Protein (HSP 70) in Honey Bee (Apis mellifera anatoliaca) Groups under Different Diets Linked with Physico-Chemical, Antioxidant and Fatty and Amino Acid Profiles. Insects. 2022 Oct 26;13(11):985.

103. Koleoglu G, Goodwin PH, Reyes-Quintana M, Hamiduzzaman MMd, Guzman-Novoa E. Varroa destructor parasitism reduces hemocyte concentrations and prophenol oxidase gene expression in bees from two populations. Parasitol Res. 2018 Apr 12;117(4):1175–83.

104. Wu Y, Zheng Y, Chen Y, Chen G, Zheng H, Hu F. Apis cerana gut microbiota contribute to host health though stimulating host immune system and strengthening host resistance to Nosema ceranae. R Soc Open Sci. 2020 May 20;7(5):192100.